Spherical Single-Roll Dynamos at Large Magnetic Reynolds Numbers

David Ivers and Henrik Latter

14 October, 2007

Abstract

The asymptotic theory of Gilbert & Ponty (2000) for axisymmetric spherical single roll flow dynamos at large magnetic Reynolds R_m numbers is compared to the numerical eigen-solutions of the exact dynamo problem for two flows in a spherical electrically conducting fluid with insulating exterior. The flows are the $s_1^0 t_1^0$ of Dudley & James (1989) and an $s_1^0 t_1^0 t_3^0$ modification of it. The numerical method uses a compact vector spherical harmonic technique in angle and fourth-order finite-differences in radius. Excellent agreement is obtained in the asymptotic regime $R_\mathrm{m} > 10,000$ for both the growth rate and the angular frequency, and good agreement for the magnetic field in $R_\mathrm{m} > 100,000$. The asymptotic theory is extended to $\mathcal{O}(R_\mathrm{m}^{-1})$ for the growth rate and angular frequency, and to $\mathcal{O}(R_\mathrm{m}^{-1/2})$ for the magnetic field.

1 Introduction

We consider a class of self-exciting kinematic dynamos in which the magnetic field $\mathbf{B}$ is generated by the steady helical motion $\mathbf{v}$ of a homogeneous, incompressible, electrically conducting fluid. The magnetic field in the fluid is governed by the non-dimensionalised magnetic induction equation,

$$\partial_\tau \mathbf{B} = \nabla^2 \mathbf{B} + R_\mathrm{m} \nabla \times (\mathbf{v} \times \mathbf{B}) \tag{1.1}$$

where the magnetic Reynolds number $R_\mathrm{m} := \mathcal{V}\mathcal{L}/\eta$ is defined in terms of a typical velocity $\mathcal{V}$ and length $\mathcal{L}$, and the uniform magnetic diffusivity η. The time τ is scaled on the magnetic diffusion time $\mathcal{L}^2/\eta$. The magnetic field $\mathbf{B}$ is solenoidal everywhere,

$$\nabla \cdot \mathbf{B} = 0\,, \tag{1.2}$$

and, since the fluid is incompressible, $\nabla \cdot \mathbf{v} = \mathbf{0}$.

The simplest helical flow dynamo is the Ponomarenko (1973) dynamo, which consists of a rigid electrically-conducting cylinder of finite radius rotating with constant angular velocity Ω and moving with a constant axial velocity V, surrounded by a rigid electrical conductor at rest. In cylindrical polar coordinates (s, ϕ, z) the velocity of the cylinder is

$$\mathbf{v} = s\Omega \mathbf{1}_\phi + V \mathbf{1}_z \tag{1.3}$$

Dynamo action in this case arises from the reciprocal generation of azimuthal magnetic field from radial magnetic field by the discontinuity in the rotation, and radial field from azimuthal field by magnetic diffusion. The additional longitudinal shearing component in the helical flow is crucial for field growth as it draws apart oppositely directed field lines and prevents flux expulsion. Ponomarenko (1973) determined the magnetic field in this case analytically, showing that the field is concentrated at the velocity discontinuity on the cylinder boundary. Cylindrical helical flow dynamos with non-uniform V and Ω, such as in an electrically conducting fluid, are more difficult to solve. Nevertheless, Lortz (1968) showed that a suitable ansatz for both the magnetic field $\mathbf{B}$ and the flow $\mathbf{v}$ gives exact analytic steady solutions for such helical flows. An explicit steady solution was subsequently given by Chen and Milovich (1984). Lortz (1972) has also given a stationary asymptotic solution for a toroidal helical dynamo with circular meridional cross section of large aspect ratio, i.e. as the torus approaches a circular loop.

For helical flows in spherical geometries, however, numerical techniques are generally required to solve (1.1). If the flow is steady the magnetic field can be expressed as a linear combination of time-separable solutions of the form

$$\mathbf{B}(\mathbf{r}, \tau) = \mathbf{B}(\mathbf{r}) e^{\lambda \tau}\,. \tag{1.4}$$

This leads to an eigenvalue problem for the (complex) growth rate λ and the associated eigenfunction, which can be approximated numerically by a large-scale algebraic eigenvalue problem. For a given flow $\mathbf{v}$, the growth rate λ is a function of the magnetic Reynolds number R_m. The flow acts as a dynamo, i.e. the non-magnetic state $\mathbf{B}=\mathbf{0}$ is unstable to magnetic perturbations, if $\mathrm{Re}\,\lambda>0$ for sufficiently large R_m. Dudley & James (1989) have given examples of single and double helical roll flows in an electrically conducting sphere with an insulating exterior, which act as self-exciting dynamos for $R_\mathrm{m}\gtrsim 100$. In this case, in addition to the magnetic induction equation (1.1) and the solenoidal condition (1.2), the magnetic field $\mathbf{B}$ is governed by

$$[\mathbf{B}]_\Sigma=\mathbf{0}\,,\qquad \nabla\times\mathbf{B}=\mathbf{0}\quad\text{in }\widehat{V},\qquad \mathbf{B}\to\mathbf{0}\quad\text{as } r\to\infty, \tag{1.5}$$

where Σ is the surface of the sphere. In spherical polar coordinates (r,θ,ϕ), the Dudley & James (1989) single roll flow has the toroidal-poloidal representation,

$$\mathbf{v}=\nabla\times t\mathbf{r}+\nabla\times\nabla\times s\mathbf{r}\,, \tag{1.6}$$

with potentials $t=\sin\pi r\cos\theta$ and $s=\sigma\sin\pi r\cos\theta$. The parameter σ is a constant and $\mathbf{r}$ is the radius vector. Flows with this angular dependence may be the simplest spherical flows capable of supporting dynamo action. Similar roll flows with values of the critical magnetic Reynolds number R_m^c even smaller than those computed by Dudley & James (1989) are possible: e.g. Forest et al (2002) achieve $R_\mathrm{m}^c\approx 72$ compared to $R_\mathrm{m}^c\approx 150$ for the flow (1.6). This shows additionally that helical dynamos are efficient generators of magnetic field, in the sense that R_m^c is relatively small, which is why they are favoured by experimentalists (see Gailitis & Freiburg 1980, Forest et al 2002, for example).

Asymptotic estimates at large R_m have been given by Ruzmaikin, Sokoloff, & Shukurov (1988) for cylindrical helical flow dynamos (1.3) with non-uniform V and Ω. They show that the importance of diffusion in magnetic self-excitation means the dynamo is slow with $\mathrm{Re}\,\lambda=\mathcal{O}(R_\mathrm{m}^{1/2})$. Also, since the typical diffusion scale shrinks as R_m becomes large, a growing magnetic mode must possess a radial gradient on sufficiently short length scales, of order $R_\mathrm{m}^{-1/4}$, so that diffusion of helical magnetic field may effectively replenish radial magnetic field. This small-scale magnetic structure spatially localises on a 'resonant' stream surface at which diffusion is optimal. In the Ponomarenko dynamo the resonant stream surface is the surface of velocity discontinuity. In addition, for a field of the form $\mathbf{B}=[B_s(s)\mathbf{1}_s+B_\phi(s)\mathbf{1}_\phi+B_z(s)\mathbf{1}_z]e^{im\phi+ikz+\lambda\tau}$, there exists the following scaling,

$$\mathrm{Re}\,\lambda=\mathcal{O}(R_\mathrm{m}^{1/2})\,,\quad R_\mathrm{m}^{1/2}B_s\sim B_\phi\sim B_z\,,\quad m,k=\mathcal{O}(1). \tag{1.7}$$

Thus the field is spatially localized about the resonant stream surface to a region of width $\mathcal{O}(R_\mathrm{m}^{-1/4})$. Gilbert (1988) has presented an alternative scaling,

$$\mathrm{Re}\,\lambda=\mathcal{O}(R_\mathrm{m}^{2/3})\,,\qquad m,k=\mathcal{O}(R_\mathrm{m}^{1/3})\,, \tag{1.8}$$

where the magnetic field is localised to a region of width $\mathcal{O}(R_\mathrm{m}^{-1/3})$ about the resonant stream surface. He argues that these estimates capture the fastest growing modes at large R_m.

Gilbert & Ponty (2000) generalised these asymptotic solutions to helical dynamos in cylinders of general cross-section and in spherical geometries. In spherical dynamos the helical flow is axisymmetric and may be represented by

$$\mathbf{v}=\mathbf{v}_\mathrm{m}+W(r,\theta)r\sin\theta\mathbf{1}_\phi\,, \tag{1.9}$$

where $\mathbf{v}_\mathrm{m}$ is the meridional velocity and W is the local azimuthal angular velocity. The meridional flow $\mathbf{v}_\mathrm{m}$ is given in terms of a stream function ψ by

$$\mathbf{v}_\mathrm{m}=-\frac{\partial_\theta\psi}{r^2\sin\theta}\mathbf{1}_r+\frac{\partial_r\psi}{r\sin\theta}\mathbf{1}_\theta=\nabla\phi\times\nabla\psi=-\nabla\times\frac{\psi}{r\sin\theta}\mathbf{1}_\phi\,. \tag{1.10}$$

The streamlines of $\mathbf{v}_\mathrm{m}$ in a meridional plane are the level contours of ψ and circle a local minimum (maximum) of ψ in the clockwise (counter-clockwise) direction. A spherical single-roll helical dynamo can be pictured as a cylindrical helical flow bent into a torus and then deformed to fill the spherical shape. The representations (1.6) and (1.9) are related by $\psi=r\sin\theta\,\partial_\theta s$ and $\partial_\theta t=-Wr\sin\theta$. The Gilbert & Ponty (2000) theory predicts that the dominant mechanism of field generation is of Ponomarenko type and the scalings (2.17) coincide with those of the circular cylindrical case (1.8). The predicted eigenfunction and growth rate to dominant order are given below in (2.60), (2.62) and (2.63).

We test the asymptotic formulas (2.60), (2.62) and (2.63) on two single roll flows in a sphere,

$$\mathbf{v}_1 = \sigma \mathbf{V}_{\rm m} + r^2 \sin \pi r \, \sin^3 \theta \, \mathbf{1}_\phi \,, \qquad \mathbf{v}_2 = \sigma \mathbf{V}_{\rm m} + \sin \pi r \, \sin \theta \, \mathbf{1}_\phi \,. \tag{1.11}$$

The meridional parts contain an adjustable parameter σ, which fixes the meridional speed relative to the azimuthal speed and is used below as a tuning parameter. Thus $\mathbf{v}_{\rm m} = \sigma \mathbf{V}_{\rm m}$ and $\psi = \sigma \Psi$, where the meridional stream function Ψ is given by

$$\Psi(r, \theta) = -r \sin \pi r \sin^2 \theta \,. \tag{1.12}$$

The flows differ significantly only in their azimuthal components, which are of the restricted form $W = W(\psi)$ and the general form $W = W(r, \theta)$, respectively. The restricted form of the local angular velocity simplifies the asymptotic theory substantially and facilitates the asymptotic calculations.

The local angular velocity of the flow $\mathbf{v}_1$ is $W = -\Psi$. In terms of the fields, $\mathbf{t}_n^m := \nabla \times (t_n^m Y_n^m \mathbf{r})$ and $\mathbf{s}_n^m := \nabla \times \nabla \times (s_n^m Y_n^m \mathbf{r})$, where the spherical harmonic Y_n^m is defined by (4.2) below, this flow has the poloidal-toroidal spectral form, $\mathbf{v}_1 = \sigma \, \mathbf{s}_1^0 + \mathbf{t}_1^0 + \mathbf{t}_3^0$, in which the radial functions are

$$s_1^0 = \frac{\sin \pi r}{\sqrt{3}} \,, \qquad t_1^0 = -\frac{4}{5\sqrt{3}} \, r^2 \sin \pi r \,, \qquad t_3^0 = \frac{2}{15\sqrt{7}} \, r^2 \sin \pi r \,, \tag{1.13}$$

and the spherical harmonics are $Y_1^0 = \sqrt{3} \, \cos \theta$ and $Y_3^0 = \frac{1}{2}\sqrt{7} \, \cos \theta (5 \cos^2 \theta - 3)$.

The second flow $\mathbf{v}_2$ is the single roll flow of Dudley & James (1989). Our results extend their work to the large $R_{\rm m}$ regime. This flow has the poloidal-toroidal spectral form, $\mathbf{v}_2 = \sigma \, \mathbf{s}_1^0 + \mathbf{t}_1^0$, where

$$s_1^0 = \frac{\sin \pi r}{\sqrt{3}} \,, \qquad t_1^0 = \sin \pi r \,. \tag{1.14}$$

The local angular velocity of $\mathbf{v}_2$ is $W = (\sin \pi r)/r$, which is of general form. Note that although $\mathbf{v}_1$ has the simpler restricted form of the local angular velocity, its spherical harmonic representation is actually more complicated.

In section 2 the asymptotic theory is briefly described for the growth rate to $\mathcal{O}(R_{\rm m}^{-1/2})$ and the magnetic field to leading order. The numerical evaluation of the asymptotic formulas for the growth rate and the magnetic field is described in section 3. The numerical solution of the exact spherical dynamo eigenproblem is presented in section 4. The results of the asymptotic formulas are compared with the numerical solution of the dynamo problem in section 5. In section 6 the asymptotic theory for the growth rate is completed to $\mathcal{O}(R_{\rm m}^{-1})$ and the magnetic field to $\mathcal{O}(R_{\rm m}^{-1/2})$. Concluding remarks are given in section 7.

2 Asymptotic Theory

The asymptotic theory of Gilbert & Ponty (2000) for $R_{\rm m} \gg 1$ is described and extended in this section. Expressions for the real and imaginary parts of the growth rate are given to $\mathcal{O}(R_{\rm m}^{-1/2})$ in terms of geometric properties of the spherical single-roll flow. In addition, we derive expressions describing the spatial structure of the magnetic field modes fully to leading order and up to functions of ψ at $\mathcal{O}(R_{\rm m}^{-1/2})$. We also verify that the asymptotic formula for the magnetic field is solenoidal to leading order. The results here are needed to extend the asymptotic theory for the growth rate to $\mathcal{O}(R_{\rm m}^{-1})$ and to complete the determination of the magnetic field to $\mathcal{O}(R_{\rm m}^{-1/2})$ in Section 6.

2.1 Toroidal Co-ordinates for Axisymmetric Helical Flows

The structure of the flow (1.9), i.e. the topology of its streamlines and its differential rotation, can be exploited by a toroidal coordinate system to simplify the advection operator. The first two coordinates are determined by the meridional flow. The stream function ψ is one coordinate. The second is an angle coordinate ϑ defined as follows: if T is the period for a fluid particle to traverse the closed $\mathbf{v}_{\rm m}$-streamline $\psi = \psi_o$ once, then $T = T(\psi)$ and

$$d\vartheta = \frac{2\pi}{T} dt = \Omega \frac{d\ell}{q} = \Omega \frac{\mathbf{v}_{\rm m} \cdot d\mathbf{r}}{q^2} = \Omega \frac{r d\theta}{v_\theta} = \Omega \frac{dr}{v_r} \,, \tag{2.1}$$

where $\Omega = 2\pi/T$ is the angular frequency, $d\ell$ is the element of arc-length travelled in a time dt, $q = |\mathbf{v}_\mathrm{m}|$ and there is no stagnation point on the streamline. Thus $d\vartheta/dt = \Omega$ is constant on streamlines. For the two flows we consider we fix $\vartheta = 0$ on the s-axis ($\theta = \pi/2$), since the stagnation points of their meridional parts occur there. Clearly ϑ changes by 2π in one full traversal of the closed streamline. The azimuthal angle ϕ is replaced by the third coordinate ζ defined by

$$\zeta(\psi, \vartheta, \phi) := \phi - Z(\psi, \vartheta)\,, \qquad Z := \frac{1}{\Omega(\psi)} \int_0^\vartheta \widetilde{W}(\psi, \vartheta^*)\, d\vartheta^*\,. \tag{2.2}$$

The level surfaces of ζ are distorted azimuthal planes

The asymptotic theory is developed herein for the general case $W = W(\psi, \vartheta)$, in which the azimuthal velocity W depends on both ψ and ϑ. The substantial simplifications, which occur if $W = W(\psi)$, i.e. W is independent of ϑ, are indicated later. An overbar or pair of angle brackets denotes the average around the $\mathbf{v}_\mathrm{m}$-streamline $\psi = \psi_o$, defined by

$$\overline{f} \equiv \langle f \rangle := \frac{1}{2\pi} \oint_{\psi=\psi_o} f d\vartheta\,,$$

where f is a function of the meridional coordinates and the integration is around the streamline $\psi = \psi_o$. Clearly, the mean component of W is independent of ϑ, i.e. $\overline{W} = \overline{W}(\psi)$, and we can define the fluctuating component of W by $\widetilde{W}(\psi, \vartheta) := W(\psi, \vartheta) - \overline{W}$.

The coordinate system (ψ, ϑ, ζ) naturally gives rise to the two right-handed vector bases, $(\nabla\psi, \nabla\vartheta, \nabla\zeta)$ and $(\mathbf{f}_\psi, \mathbf{f}_\vartheta, \mathbf{f}_\zeta)$, where $\mathbf{f}_\psi := \partial\mathbf{r}/\partial\psi$, $\mathbf{f}_\vartheta := \partial\mathbf{r}/\partial\vartheta$, $\mathbf{f}_\zeta := \partial\mathbf{r}/\partial\zeta$ and $\mathbf{r}$ is the position vector. It is a useful shorthand to also denote the coordinates by ψ^i with indices $i = 1, 2, 3$, and the two bases by $\nabla\psi^i$ and $\mathbf{f}_i$. The bases are reciprocal, $\mathbf{f}_i \cdot \nabla\psi^j = \delta_i^j$, and related by

$$\mathbf{f}_\psi = J\nabla\vartheta \times \nabla\zeta\,, \quad \mathbf{f}_\vartheta = J\nabla\zeta \times \nabla\psi\,, \quad \mathbf{f}_\zeta = J\nabla\psi \times \nabla\vartheta\,, \tag{2.3}$$

where the Jacobian J of the transformation to (ψ, ϑ, ζ) is given by

$$J := \mathbf{f}_\psi \times \mathbf{f}_\vartheta \cdot \mathbf{f}_\zeta = (\nabla\psi \times \nabla\vartheta \cdot \nabla\zeta)^{-1} = \Omega^{-1}. \tag{2.4}$$

Using the properties of the flux function, equations (2.4) may be simplified to

$$\mathbf{f}_\psi = \Omega^{-1}\nabla\vartheta \times \nabla\phi + \mathbf{f}_\zeta\partial_\psi Z\,, \quad \mathbf{f}_\vartheta = \Omega^{-1}\nabla\phi \times \nabla\psi + \mathbf{f}_\zeta\partial_\vartheta Z\,, \quad \mathbf{f}_\zeta = r\sin\theta\mathbf{1}_\phi\,. \tag{2.5}$$

Using the properties of reciprocal bases the velocity and the magnetic field may be written as

$$\mathbf{v} = \Omega(\psi)\mathbf{f}_\vartheta + \overline{W}(\psi)\mathbf{f}_\zeta\,, \qquad \mathbf{B} = B_\psi\mathbf{f}_\psi + B_\vartheta\mathbf{f}_\vartheta + B_\zeta\mathbf{f}_\zeta\,. \tag{2.6}$$

The advection operator can hence be written as

$$D_t = \partial_t + \Omega(\psi)\partial_\vartheta + \overline{W}(\psi)\partial_\zeta\,. \tag{2.7}$$

Its dependence only on ψ is essential in what follows.

Using the summation convention the magnetic field can be written as $\mathbf{B} = B^i\mathbf{f}_i$, the gradient operator as $\nabla = (\nabla\psi^i)\partial_i$, where $\partial_i := \partial_{\psi^i}$, and the diffusion term in the magnetic induction equation as $\nabla^2\mathbf{B} = (\nabla^2 B^j)\mathbf{f}_j + 2\nabla B^j \cdot \nabla\mathbf{f}_j + B^j\nabla^2\mathbf{f}_j$. Thus, since $\nabla B^j = (\partial_k B^j)\nabla\psi^k$,

$$\nabla\psi^i \cdot \nabla^2\mathbf{B} = (\nabla^2 B^i) + 2(\partial_k B^j)\nabla\psi^k \cdot \nabla\mathbf{f}_j \cdot \nabla\psi^i + B^j\nabla\psi^i \cdot \nabla^2\mathbf{f}_j\,.$$

Four of the 27 terms $\nabla\psi^k \cdot \nabla\mathbf{f}_j \cdot \nabla\psi^i$ and three of the 9 terms $\nabla\psi^i \cdot \nabla^2\mathbf{f}_j$ vanish identically. Since $\nabla\mathbf{f}_\zeta = \mathbf{1}_s\mathbf{1}_\phi - \mathbf{1}_\phi\mathbf{1}_s$, $\mathbf{a} \cdot (\nabla\mathbf{f}_\zeta) \cdot \mathbf{b} = 0$ for any meridional vectors $\mathbf{a}$, $\mathbf{b}$, and hence

$$\nabla\psi \cdot (\nabla\psi \cdot \nabla\mathbf{f}_\zeta) = \nabla\psi \cdot (\nabla\vartheta \cdot \nabla\mathbf{f}_\zeta) = \nabla\vartheta \cdot (\nabla\psi \cdot \nabla\mathbf{f}_\zeta) = \nabla\vartheta \cdot (\nabla\vartheta \cdot \nabla\mathbf{f}_\zeta) = 0\,.$$

Also $\nabla^2\mathbf{f}_\zeta = \mathbf{0}$ implies $\nabla\psi \cdot \nabla^2\mathbf{f}_\zeta = \nabla\vartheta \cdot \nabla^2\mathbf{f}_\zeta = \nabla\zeta \cdot \nabla^2\mathbf{f}_\zeta = 0$.

Keeping only terms which appear later in the asymptotic analysis and suppressing the others with dots, the relevant diffusion terms are

$$\nabla\psi \cdot \nabla^2\mathbf{B} = (\nabla^2 + 2\mu_i\partial_\psi + 2\mu_j\partial_\vartheta + 2\mu_k\partial_\zeta + \mu_l)B_\psi + (2\mu_a\partial_\psi + 2\mu_b\partial_\vartheta + 2\mu_c\partial_\zeta + \mu_d)B_\vartheta + 2\mu_g\partial_\zeta B_\zeta \tag{2.8}$$

$$\nabla\vartheta \cdot \nabla^2\mathbf{B} = (\nabla^2 + 2\lambda_a\partial_\psi + 2\lambda_b\partial_\vartheta + 2\lambda_c\partial_\zeta + \lambda_d)B_\vartheta + 2\lambda_g\partial_\zeta B_\zeta + \ldots \tag{2.9}$$

$$\nabla\zeta\cdot\nabla^2\mathbf{B}=2\rho_a\partial_\psi B_\vartheta+(\nabla^2+2\rho_b\partial_\psi)B_\zeta+\dots\,, \tag{2.10}$$

where the coefficients are defined by

$$\begin{aligned}
&\mu_a:=\nabla\psi\cdot(\nabla\psi\cdot\nabla\mathbf{f}_\vartheta) && \mu_b:=\nabla\psi\cdot(\nabla\vartheta\cdot\nabla\mathbf{f}_\vartheta) && \mu_c:=\nabla\psi\cdot(\nabla\zeta\cdot\nabla\mathbf{f}_\vartheta) && \mu_d:=\nabla\psi\cdot\nabla^2\mathbf{f}_\vartheta\\
&\mu_g:=\nabla\psi\cdot(\nabla\zeta\cdot\nabla\mathbf{f}_\zeta) && \mu_i:=\nabla\psi\cdot(\nabla\psi\cdot\nabla\mathbf{f}_\psi) && \mu_j:=\nabla\psi\cdot(\nabla\vartheta\cdot\nabla\mathbf{f}_\psi) && \mu_k:=\nabla\psi\cdot(\nabla\zeta\cdot\nabla\mathbf{f}_\psi)\\
&\mu_l:=\nabla\psi\cdot\nabla^2\mathbf{f}_\psi && \lambda_a:=\nabla\vartheta\cdot(\nabla\psi\cdot\nabla\mathbf{f}_\vartheta) && \lambda_b:=\nabla\vartheta\cdot(\nabla\vartheta\cdot\nabla\mathbf{f}_\vartheta) && \lambda_c:=\nabla\vartheta\cdot(\nabla\zeta\cdot\nabla\mathbf{f}_\vartheta)\\
&\lambda_d:=\nabla\vartheta\cdot\nabla^2\mathbf{f}_\vartheta && \lambda_g:=\nabla\vartheta\cdot(\nabla\zeta\cdot\nabla\mathbf{f}_\zeta) && \rho_a:=\nabla\zeta\cdot(\nabla\psi\cdot\nabla\mathbf{f}_\vartheta) && \rho_b:=\nabla\zeta\cdot(\nabla\psi\cdot\nabla\mathbf{f}_\zeta)\,.
\end{aligned}$$

Apart from μ_d, μ_l, λ_d these are Christoffel symbols. The scalar Laplacian is $\nabla^2=\nabla\cdot(\nabla\psi^i)\partial_i=(\nabla\psi^i\cdot\nabla\psi^j)\partial_i\partial_j+(\nabla^2\psi^i)\partial_i$, i.e.

$$\begin{aligned}
\nabla^2=(\nabla\psi)^2\partial_\psi^2+2(\nabla\psi\cdot\nabla\vartheta)\partial_\psi\partial_\vartheta+(\nabla\vartheta)^2\partial_\vartheta^2+2(\nabla\vartheta\cdot\nabla\zeta)\partial_\vartheta\partial_\zeta\\
+(\nabla\zeta)^2\partial_\zeta^2+2(\nabla\zeta\cdot\nabla\psi)\partial_\zeta\partial_\psi+(\nabla^2\psi)\partial_\psi+(\nabla^2\vartheta)\partial_\vartheta+(\nabla^2\zeta)\partial_\zeta\,.
\end{aligned}$$

The following further simplifications can be established using standard vector identities, the divergence theorem and Stokes' theorem (see Gilbert & Ponty 2000),

$$\overline{\mu}_a=\overline{\mu}_d=\overline{\mu}_g=\overline{\mu}_l=\overline{\lambda}_b=\overline{\rho}_b=0\,. \tag{2.11}$$

2.2 Asymptotic Expansion of the Magnetic Induction Equation

We employ the coordinate system described above in the asymptotic analysis of the magnetic induction equation for a single-roll flow in spherical geometry. In this section we follow Gilbert & Ponty (2000) and scale time t on the turn-over timescale $a/\mathcal{V}$, where a is the spherical radius and $\mathcal{V}$ is a typical flow speed. The times scaled on the turn-over and diffusion times are related by $t=\tau R_\mathrm{m}$. The non-dimensionalised magnetic induction equation in this case is

$$\partial_t\mathbf{B}=\nabla\times(\mathbf{v}\times\mathbf{B})+\varepsilon^4\nabla^2\mathbf{B}\,, \tag{2.12}$$

where $\varepsilon=R_\mathrm{m}^{-1/4}$ and $R_\mathrm{m}:=a\mathcal{V}/\eta$ is the magnetic Reynold's number. We are interested in the asymptotic behaviour of solutions for large R_m, i.e. as $\varepsilon\to0$.

The contravariant components of (2.12) are

$$D_tB_\psi=\varepsilon^4\nabla\psi\cdot\nabla^2\mathbf{B} \tag{2.13}$$

$$D_tB_\vartheta-\Omega'(\psi)B_\psi=\varepsilon^4\nabla\vartheta\cdot\nabla^2\mathbf{B} \tag{2.14}$$

$$D_tB_\zeta-\overline{W}'(\psi)B_\psi=\varepsilon^4\nabla\zeta\cdot\nabla^2\mathbf{B}\,. \tag{2.15}$$

The primes indicate derivatives with respect ψ. As noted above, regeneration of the magnetic field component B_ψ is solely due to diffusion, but regeneration of B_ϑ and B_ζ is partly due to distortion of B_ψ by meridional and azimuthal differential rotation, respectively.

Solutions of equation (2.12) or, equivalently equations (2.13)–(2.15), do not necessarily satisfy the solenoidal condition (1.2) on the magnetic field. The condition is satisfied identically by time separable solutions if the diffusion term is in the form $-\varepsilon^4\nabla\times\nabla\times\mathbf{B}$, but this form complicates the asymptotic analysis. Since $\nabla\cdot(\mathbf{f}_i/J)=0$, the coordinate form of (1.2) is

$$\Omega\partial_\psi(B_\psi/\Omega)+\partial_\vartheta B_\vartheta+\partial_\zeta B_\zeta=0\,. \tag{2.16}$$

This equation is independent of (2.13)–(2.15).

We assume that the magnetic field solutions obey the scaling of Ruzmaikin et al. (1988) for small ε,

$$\varepsilon^2B_\psi\sim B_\vartheta\sim B_\zeta\,,\quad p=\mathcal{O}(\varepsilon^2)\,,\quad m,k=\mathcal{O}(1)\,. \tag{2.17}$$

and that they can be separated into modes of the form $B_\psi,B_\vartheta,B_\zeta\propto e^{im\zeta+(p+i\omega)t}$. Thus $p+i\omega=\lambda/R_\mathrm{m}$. The constant m must be an integer for solutions single-valued in ζ. These modes localise upon a stream surface $\psi=\psi_o$ in a layer of thickness $\mathcal{O}(\varepsilon)$. Thus ϑ- and ζ-derivatives are $\mathcal{O}(1)$ but ψ-derivatives are $\mathcal{O}(\varepsilon^{-1})$. We therefore define a new variable Υ by

$$\psi=\psi_o+\varepsilon\Upsilon\,. \tag{2.18}$$

so that Υ-derivatives are $\mathcal{O}(1)$. The ψ-derivative and gradient operators become

$$\partial_\psi = \varepsilon^{-1}\partial_\Upsilon\,, \qquad \nabla = \varepsilon^{-1}\nabla\psi\,\partial_\Upsilon + \nabla\vartheta\,\partial_\vartheta + \nabla\zeta\,\partial_\zeta\,, \tag{2.19}$$

and the magnetic field components take the functional forms,

$$B_\psi = \varepsilon^2 b_\psi(\Upsilon,\vartheta)e^{im\zeta+i\omega t+pt}\,, \quad B_\vartheta = b_\vartheta(\Upsilon,\vartheta)e^{im\zeta+i\omega t+pt}\,, \quad B_\zeta = b_\zeta(\Upsilon,\vartheta)e^{im\zeta+i\omega t+pt}\,. \tag{2.20}$$

Equations (2.13)–(2.15) become, using (2.8)–(2.10),

$$\begin{aligned} D_t b_\psi = {}& \varepsilon 2\mu_a\partial_\Upsilon b_\vartheta + \varepsilon^2\{(\nabla\psi)^2\partial_\Upsilon^2 b_\psi + (2\mu_b\partial_\vartheta + 2im\mu_c + \mu_d)b_\vartheta + 2im\mu_g b_\zeta\} \\ & + \varepsilon^3\{2\mu_i + 2(\nabla\psi\cdot\nabla\vartheta)\partial_\vartheta + 2im\nabla\zeta\cdot\nabla\psi + \nabla^2\psi\}\partial_\Upsilon b_\psi \\ & + \varepsilon^4\{(\nabla\vartheta)^2\partial_\vartheta^2 + (2im\nabla\vartheta\cdot\nabla\zeta + \nabla^2\vartheta + 2\mu_j)\partial_\vartheta - m^2(\nabla\zeta)^2 + im\nabla^2\zeta + 2im\mu_k + \mu_l\}b_\psi\,, \end{aligned}$$

$$\begin{aligned} & D_t b_\vartheta - \varepsilon^2\Omega' b_\psi = \varepsilon^2(\nabla\psi)^2\partial_\Upsilon^2 b_\vartheta + \varepsilon^3\{2\lambda_a + 2(\nabla\psi\cdot\nabla\vartheta)\partial_\vartheta + 2im\nabla\zeta\cdot\nabla\psi + \nabla^2\psi\}\partial_\Upsilon b_\vartheta \\ & + \varepsilon^4\{[(\nabla\vartheta)^2\partial_\vartheta^2 + (2\lambda_b + 2im\nabla\vartheta\cdot\nabla\zeta + \nabla^2\vartheta)\partial_\vartheta - m^2(\nabla\zeta)^2 + im\nabla^2\zeta + 2im\lambda_c + \lambda_d]b_\vartheta + 2im\lambda_g b_\zeta\} + \mathcal{O}(\varepsilon^5)\,, \end{aligned}$$

$$\begin{aligned} D_t b_\zeta - \varepsilon^2\overline{W}' b_\psi = {}& \varepsilon^2(\nabla\psi)^2\partial_\Upsilon^2 b_\zeta \\ & + \varepsilon^3\{[2\rho_b + 2(\nabla\psi\cdot\nabla\vartheta)\partial_\vartheta + 2im\nabla\zeta\cdot\nabla\psi + \nabla^2\psi]\partial_\Upsilon b_\zeta + 2\rho_a\partial_\Upsilon b_\vartheta\} + \mathcal{O}(\varepsilon^4)\,, \end{aligned}$$

since

$$\begin{aligned} \varepsilon^4\nabla^2 = {}& \varepsilon^2(\nabla\psi)^2\partial_\Upsilon^2 + \varepsilon^3\{2(\nabla\psi\cdot\nabla\vartheta)\partial_\vartheta + 2im\nabla\zeta\cdot\nabla\psi + \nabla^2\psi\}\partial_\Upsilon \\ & + \varepsilon^4\{(\nabla\vartheta)^2\partial_\vartheta^2 + (2im\nabla\vartheta\cdot\nabla\zeta + \nabla^2\vartheta)\partial_\vartheta - m^2(\nabla\zeta)^2 + im\nabla^2\zeta\}\,. \end{aligned}$$

The solenoidal condition (2.16) becomes

$$\varepsilon\partial_\Upsilon b_\psi - \frac{\Omega'}{\Omega}\varepsilon^2 b_\psi + \partial_\vartheta b_\vartheta + imb_\zeta = 0\,. \tag{2.21}$$

We now expand ω and p in powers of ε with the ordering (2.17),

$$\omega = \omega_0 + \varepsilon\omega_1 + \varepsilon^2\omega_2 + \varepsilon^3\omega_3 + \varepsilon^4\omega_5 + \dots\,, \quad p = \varepsilon^2 p_2 + \varepsilon^3 p_3 + \varepsilon^4 p_4 + \dots\,, \tag{2.22}$$

and expand $\overline{W}(\psi)$ and $\Omega(\psi)$ in Taylor series about the streamline $\psi = \psi_o$,

$$\Omega(\psi_o + \varepsilon\Upsilon) = \Omega_o + \Omega_o'\varepsilon\Upsilon + \tfrac{1}{2}\Omega_o''\varepsilon^2\Upsilon^2 + \dots \tag{2.23}$$

$$\overline{W}(\psi_o + \varepsilon\Upsilon) = \overline{W}_o + \overline{W}_o'\varepsilon\Upsilon + \tfrac{1}{2}\overline{W}_o''\varepsilon^2\Upsilon^2 + \dots\,, \tag{2.24}$$

in which $\Omega_o = \Omega(\psi_o)$, $\Omega_o' = \Omega'(\psi_o)$, etc. Assuming the functional dependencies of (2.20) and substituting the expansions (2.22)–(2.24) into the advection operator (2.7) gives

$$D_t = d_0 + \varepsilon d_1 + \varepsilon^2 d_2 + \varepsilon^3 d_3 + \varepsilon^4 d_4 + \dots\,, \tag{2.25}$$

where

$$d_n = p_n + i\omega_n + \frac{\Upsilon^n}{n!}\left(\Omega_o^{(n)}\partial_\vartheta + im\overline{W}_o^{(n)}\right), \quad p_0 = p_1 = 0\,. \tag{2.26}$$

We also expand $(\nabla\psi)^2$ in the diffusion term in a Taylor series,

$$(\nabla\psi)^2 = \gamma_0 + \varepsilon\Upsilon\gamma_1 + \varepsilon^2\Upsilon^2\gamma_2 + \varepsilon^3\Upsilon^3\gamma_3 + \varepsilon^4\Upsilon^4\gamma_4 + \dots\,. \tag{2.27}$$

Finally we expand the magnetic field components,

$$b_\psi = b_{\psi 0} + \varepsilon b_{\psi 1} + \dots\,, \quad b_\vartheta = b_{\vartheta 0} + \varepsilon b_{\vartheta 1} + \dots\,, \quad b_\zeta = b_{\zeta 0} + \varepsilon b_{\zeta 1} + \dots\,. \tag{2.28}$$

We are now ready to derive the asymptotic equations at the various orders.

2.3 The ε^0, ε^1 and ε^2 Equations

In this section we describe the asymptotics to order ε^2. For a fuller account see Gilbert & Ponty (2000). We substitute expansions (2.22)–(2.25), (2.27) and (2.28) into the component equations (2.13)–(2.15), divide (2.13) by ε^2, and collect terms of like order.

The ε^0-equations are

$$d_0 b_{\psi 0} = 0\,, \qquad d_0 b_{\vartheta 0} = 0\,, \qquad d_0 b_{\zeta 0} = 0\,, \tag{2.29}$$

which have the solution,

$$b_{\psi 0} = F_{\psi 0}(\Upsilon) e^{ik\vartheta}\,, \quad b_{\vartheta 0} = F_{\vartheta 0}(\Upsilon) e^{ik\vartheta}\,, \quad b_{\zeta 0} = F_{\zeta 0}(\Upsilon) e^{ik\vartheta}\,, \tag{2.30}$$

where the functions $F_{\psi 0}$, $F_{\vartheta 0}$, $F_{\zeta 0}$ are determined at order ε^2 and must vanish as $|\Upsilon| \to \infty$. The constant k is an integer since $\mathbf{B}$ is single-valued. Solvability of (2.29) fixes the angular frequency ω to leading order for given m and k,

$$\omega_0 = -\Pi_o\,, \tag{2.31}$$

where we have introduced the frequency function $\Pi(\psi) := k\Omega + m\overline{W}$. The operator d_0 becomes $\Omega_o(\partial_\vartheta - ik)$, and hence annihilates any term with the ϑ-dependence $e^{ik\vartheta}$. The solenoidal ε^0-condition from (2.16) is

$$\partial_\vartheta b_{\vartheta 0} + imb_{\zeta 0} = 0\,. \tag{2.32}$$

Thus

$$kF_{\vartheta 0} + mF_{\zeta 0} = 0\,. \tag{2.33}$$

The ε^1-equations are

$$d_0 b_{\psi 1} + d_1 b_{\psi 0} = 2\mu_{a,o}\partial_\Upsilon b_{\vartheta 0}\,, \quad d_0 b_{\vartheta 1} + d_1 b_{\vartheta 0} = 0\,, \quad d_0 b_{\zeta 1} + d_1 b_{\zeta 0} = 0\,. \tag{2.34}$$

Their solvability requires

$$\omega_1 = 0\,, \qquad \Pi_o' = k\Omega_o' + m\overline{W}_o' = 0\,. \tag{2.35}$$

The last condition fixes the resonant streamline $\psi = \psi_o$, upon which the magnetic field is localised for given m and k. At this streamline the function $\Pi(\psi)$ possesses a critical point, and a maximum if $\Pi_o'' < 0$, which is the case for the simple roll flows we examine. The larger gradients in B_ϑ and B_ζ on this surface encourage diffusion of these fields and hence replenishment of B_ψ. The operator d_1 becomes $d_1 = \Upsilon\Omega_o'(\partial_\vartheta - ik)$ and hence also annihilates any term with ϑ-dependence $e^{ik\vartheta}$.

The last two equations in (2.34) can be solved similarly to (2.29). The first equation reduces to,

$$d_0 b_{\psi 1} = 2\mu_{a,o}\partial_\Upsilon b_{\vartheta 0} = 2\mu_{a,o} F_{\vartheta 0}'(\Upsilon) e^{ik\vartheta}\,,$$

which is solvable, since $\overline{\mu}_a = 0$ and the right side then possesses no term with the ϑ-dependence $e^{ik\vartheta}$. Thus the magnetic field at order ε^1 is

$$b_{\psi 1} = F_{\psi 1}(\Upsilon) e^{ik\vartheta} + G_{\psi 1}(\Upsilon, \vartheta) e^{ik\vartheta}\,, \quad b_{\vartheta 1} = F_{\vartheta 1}(\Upsilon) e^{ik\vartheta}\,, \quad b_{\zeta 1} = F_{\zeta 1}(\Upsilon) e^{ik\vartheta}\,, \tag{2.36}$$

where the functions $F_{\psi 1}$, $F_{\vartheta 1}$, $F_{\zeta 1}$ are determined at order ε^3 and the particular integral for equation (2.34)(a) is

$$G_{\psi 1} = \frac{2F_{\vartheta 0}'}{\Omega_o}\widehat{\mu}_{a,o}\,, \qquad \overline{G_{\psi 1}} = 0\,. \tag{2.37}$$

Here we have introduced the operator $\widehat{\ }$ defined by

$$\partial_\vartheta \widehat{f} = f - \overline{f}\,, \qquad \overline{\widehat{f}} = 0\,,$$

which implies

$$\widehat{f} = \int_0^\vartheta (f - \overline{f})\, d\vartheta - \overline{\int_0^\vartheta (f - \overline{f})\, d\vartheta}\,.$$

The properties

$$\overline{\widehat{f}g} = -\overline{f\widehat{g}}\,, \qquad \overline{f\widehat{f}} = 0 \tag{2.38}$$

are easily established.

The order ε^1 solenoidal condition is

$$\partial_\Upsilon b_{\psi 0} + \partial_\vartheta b_{\vartheta 1} + imb_{\zeta 1} = 0\,, \tag{2.39}$$

which becomes, on substituting (2.30) and (2.36),

$$\partial_\Upsilon F_{\psi 0} + ikF_{\vartheta 1} + imF_{\zeta 1} = 0\,, \tag{2.40}$$

The ε^2-equations are

$$\begin{aligned} d_0 b_{\psi 2} + d_1 b_{\psi 1} + (d_2 - \gamma_0\partial_\Upsilon^2) b_{\psi 0} &= 2\mu_{a,o}\partial_\Upsilon b_{\vartheta 1} + 2\mu'_{a,o}\Upsilon\partial_\Upsilon b_{\vartheta 0} \\ &\quad + (2\mu_{b,o}\partial_\vartheta + 2im\mu_{c,o} + \mu_{d,o}) b_{\vartheta 0} + 2im\mu_{g,o} b_{\zeta 0} \qquad (2.41)\\ d_0 b_{\vartheta 2} + d_1 b_{\vartheta 1} + (d_2 - \gamma_0\partial_\Upsilon^2) b_{\vartheta 0} &= \Omega'_o b_{\psi 0} \qquad (2.42)\\ d_0 b_{\zeta 2} + d_1 b_{\zeta 1} + (d_2 - \gamma_0\partial_\Upsilon^2) b_{\zeta 0} &= \overline{W}'_o b_{\psi 0}\,. \qquad (2.43) \end{aligned}$$

Gilbert & Ponty (2000) included subdominant terms from the Laplacian at this order arguing that these are comparable when employing the scalings of Gilbert (1988). However, they neglect to include the coordinate Laplacians, $\nabla^2\psi$, $\nabla^2\vartheta$, $\nabla^2\zeta$ which are of the same order. In the present analysis all these terms appear at the correct (higher) orders.

Equations (2.41)–(2.43) are solvable for the field components $b_{\psi 2}$, $b_{\vartheta 2}$ and $b_{\zeta 2}$, if the ϑ-dependence of the other terms is not $e^{ik\vartheta}$. This is true for the terms, $d_1 b_{\psi 1}$, $d_1 b_{\vartheta 1}$ and $d_1 b_{\zeta 1}$, since the operator d_1 annihilates $e^{ik\vartheta}$. It is also satisfied by the terms, $2\mu_{a,o}\partial_\Upsilon b_{\vartheta 1}$, $2\mu_{d,o} b_{\vartheta 0}$ and $2im\mu_{g,o} b_{\zeta 0}$, since the coefficients $\mu_{a,o}$, $\mu_{d,o}$, $\mu_{g,o}$ average to zero by (2.11). The sum of the remaining terms must average to zero after multiplication by $e^{-ik\vartheta}$. Consequently we may write the solvability condition for (2.41)–(2.43) as

$$\mathbf{L}\begin{pmatrix} F_{\psi 0} \\ F_{\vartheta 0} \\ F_{\zeta 0} \end{pmatrix} = \mathbf{0}\,, \qquad \mathbf{L} := \begin{pmatrix} \Xi & 2i\overline{\alpha}_o & 0 \\ \Omega'_o & \Xi & 0 \\ \overline{W}'_o & 0 & \Xi \end{pmatrix}\,, \tag{2.44}$$

where

$$\Xi := \overline{\gamma}_0\partial_\Upsilon^2 - \tfrac{1}{2}i\Pi''_o\Upsilon^2 - p_2 - i\omega_2\,, \qquad \alpha := k\mu_b + m\mu_c\,, \qquad \Pi''_o = k\Omega''_o + m\overline{W}''_o\,, \tag{2.45}$$

with $\overline{\gamma}_0 =< |\nabla\psi|^2_o >$. These equations determine the functions $F_{\psi 0}$, $F_{\vartheta 0}$, $F_{\zeta 0}$ and hence the magnetic field to leading order. The solutions are of the form

$$\begin{pmatrix} F_{\psi 0} \\ F_{\vartheta 0} \\ F_{\zeta 0} \end{pmatrix} = y_n(\Upsilon)\mathbf{a}\,, \qquad y_n(\Upsilon) = \mathrm{D}_n\left(\Upsilon/\kappa\right), \qquad \kappa := (\overline{\gamma}_0/2i\Pi''_o)^{1/4}. \tag{2.46}$$

Here $\mathbf{a}$ is a constant vector to be determined and $\mathrm{D}_n(z)$ is the parabolic cylinder function of degree n,

$$\mathrm{D}_n(z) = 2^{-n/2}e^{-z^2/4}\,\mathrm{H}_n(z/\sqrt{2})\,, \qquad n \geq 0\,,$$

where $\mathrm{H}_n(z)$ is the Hermite polynomial of degree n. It is a solution of the equation

$$\frac{d^2 D_n(z)}{dz^2} + (n + \tfrac{1}{2} - \tfrac{1}{4}z^2) D_n(z) = 0\,.$$

In order for this solution to satisfy the boundary conditions, i.e. $F_{\psi 0}, F_{\vartheta 0}, F_{\zeta 0} \to 0$ as $|\Upsilon| \to \infty$, we choose κ^{-2} with positive real part,

$$\kappa^{-2} = \sqrt{|\Pi''_o|/\overline{\gamma}_0}\,\left(1 + i\,\mathrm{sgn}\,\Pi''_o\right),$$

noting that $\overline{\gamma}_0 > 0$. The two eigenfunctions which arise from the ambiguous sign of κ differ only if n is odd and then only in sign. Thus

$$\kappa^{-1} = \sqrt[4]{2|\Pi''_o|/\overline{\gamma}_0}\;e^{i\pi(\mathrm{sgn}\,\Pi''_o)/8} = \sqrt[4]{|\Pi''_o|/\overline{\gamma}_0}\left(\sqrt{\tfrac{\sqrt{2}+1}{2}} + i\sqrt{\tfrac{\sqrt{2}-1}{2}}\;\mathrm{sgn}\,\Pi''_o\right).$$

The y_n are eigenfunctions of Ξ with eigenvalue ξ_n,

$$\Xi y_n = \xi_n y_n\,, \qquad \xi_n := -(n + \tfrac{1}{2})\sqrt{|\Pi''_o|\overline{\gamma}_0}\,\left(1 + i\,\mathrm{sgn}\,\Pi''_o\right) - (p_2 + i\omega_2)\,.$$

Substitution of the ansatz (2.46) into (2.44) gives

$$\mathbf{L}_n\mathbf{a} = \mathbf{0}\,, \qquad \mathbf{L}_n := \begin{pmatrix} \xi_n & 2i\overline{\alpha}_o & 0 \\ \Omega_o' & \xi_n & 0 \\ \overline{W}_o' & 0 & \xi_n \end{pmatrix}, \tag{2.47}$$

which has non-trivial solutions if $\det \mathbf{L}_n = 0$. This yields $\xi_n = 0$ or $\xi_n^2 = 2i\overline{\alpha}_o\Omega_o'$, i.e. $\xi_n = \pm(1 + i\,\mathrm{sgn}\,\overline{\alpha}_o\Omega_o')\sqrt{|\overline{\alpha}_o\Omega_o'|}$, and determines p_2 and ω_2. We shall ignore the solution for $\xi_n = 0$, since its growth rate has a negative real part and only its ζ component is non-zero. The other two solutions give for the nth mode

$$p_2 = \mp\sqrt{|\overline{\alpha}_o\Omega_o'|} - (n+\tfrac{1}{2})\sqrt{|\Pi_o''|\overline{\gamma}_0} \tag{2.48}$$

$$\omega_2 = \mp\sqrt{|\overline{\alpha}_o\Omega_o'|}\ \mathrm{sgn}(\overline{\alpha}_o\Omega_o') - (n+\tfrac{1}{2})\sqrt{|\Pi_o''|\overline{\gamma}_0}\ \mathrm{sgn}\,\Pi_o'' \tag{2.49}$$

$$\mathbf{a} = [-\xi_n, \Omega_o', \overline{W}_o']^T\,. \tag{2.50}$$

The real and imaginary parts of the growth rate in (2.48) and (2.49) agree with Gilbert & Ponty (2000) to order ϵ^2. The vector $\mathbf{a}$ is determined up to a constant factor. From (2.46) and (2.50) the order ε^0 solenoidal condition (2.33) is a consequence of the resonance condition (2.35)(b).

Equations (2.41)–(2.43) have solutions of the form,

$$b_{\psi 2} = F_{\psi 2}(\Upsilon)e^{ik\vartheta} + G_{\psi 2}(\Upsilon,\vartheta)e^{ik\vartheta}\,, \qquad \overline{G}_{\psi 2} = 0 \tag{2.51}$$

$$b_{\vartheta 2} = F_{\vartheta 2}(\Upsilon)e^{ik\vartheta} + G_{\vartheta 2}(\Upsilon,\vartheta)e^{ik\vartheta}\,, \qquad \overline{G}_{\vartheta 2} = 0 \tag{2.52}$$

$$b_{\zeta 2} = F_{\zeta 2}(\Upsilon)e^{ik\vartheta} + G_{\zeta 2}(\Upsilon,\vartheta)e^{ik\vartheta}\,, \qquad \overline{G}_{\zeta 2} = 0\,. \tag{2.53}$$

The particular integrals $G_{\psi 2}$, $G_{\vartheta 2}$ and $G_{\zeta 2}$ can be determined at this order by subtracting from (2.41)–(2.43) their projections on $e^{ik\vartheta}$ and integrating with respect to ϑ. The results are

$$\Omega_o G_{\psi 2} = -\frac{2\Omega_o'}{\Omega_o}\widehat{\mu}_{a,o}\Upsilon F_{\vartheta 0}' + \widehat{\gamma}_0 F_{\psi 0}'' + 2\widehat{\mu}_{a,o}F_{\vartheta 1}' + 2\widehat{\mu}_{a,o}'\Upsilon F_{\vartheta 0}' + (2i\widehat{\alpha}_o + \widehat{\mu}_{d,o})F_{\vartheta 0} + 2im\widehat{\mu}_{g,o}F_{\zeta 0}\,. \tag{2.54}$$

$$\Omega_o G_{\vartheta 2} = \widehat{\gamma}_0 F_{\vartheta 0}''\,. \tag{2.55}$$

$$\Omega_o G_{\zeta 2} = \widehat{\gamma}_0 F_{\zeta 0}''\,. \tag{2.56}$$

The order ε^2 solenoidal condition is

$$\partial_\Upsilon b_{\psi 1} - \frac{\Omega'}{\Omega}b_{\psi 0} + \partial_\vartheta b_{\vartheta 2} + imb_{\zeta 2} = 0\,, \tag{2.57}$$

which becomes, on substituting (2.30), (2.36) and (2.51)–(2.53),

$$\partial_\Upsilon(F_{\psi 1} + G_{\psi 1}) - \frac{\Omega'}{\Omega}F_{\psi 0} + \partial_\vartheta G_{\vartheta 2} + ik(F_{\vartheta 2} + G_{\vartheta 2}) + im(F_{\zeta 2} + G_{\zeta 2}) = 0\,.$$

Averaging this equation with respect to ϑ yields

$$\partial_\Upsilon F_{\psi 1} - \frac{\Omega'}{\Omega}F_{\psi 0} + ikF_{\vartheta 2} + imF_{\zeta 2} = 0\,, \tag{2.58}$$

leaving

$$\partial_\Upsilon G_{\psi 1} + \partial_\vartheta G_{\vartheta 2} + ikG_{\vartheta 2} + imG_{\zeta 2} = 0\,. \tag{2.59}$$

In section 6 following the numerical results we outline the method of solution at higher orders. In particular, we show there that $p_3 = \omega_3 = 0$, and give the full expressions for p_4 and ω_4.

2.4 The Asymptotic Magnetic Field Solution

The quantities b_ϑ, b_ζ, ϑ, μ_c, μ_j, μ_l, ρ_a, λ_b, λ_d, λ_g are explicitly independent of the weight factor σ. The explicit dependencies of other quantities on σ are given by

$$\Upsilon = \sigma\Upsilon^* \qquad b_\psi = \sigma b_\psi^* \qquad \Omega = \sigma\Omega^* \qquad \mu_a = \sigma^2\mu_a^* \qquad \mu_b = \sigma\mu_b^*$$

$$\mu_d = \sigma\mu_d^* \qquad \mu_g = \sigma\mu_g^* \qquad \mu_i = \sigma\mu_i^* \qquad \mu_k = \sigma^{-1}\mu_k^* \qquad \lambda_a = \sigma\lambda_a^*$$
$$\lambda_c = \sigma^{-1}\lambda_c^* \qquad Z = \sigma^{-1}Z^*\,,$$

where an asterisk indicates a quantity independent of σ. In this section we make the parameter σ explicit, use the asterisked quantities and suppress the asterisks.

Combining (2.5), (2.6) and (2.20) the magnetic field becomes

$$\mathbf{B} = \{\varepsilon^2 b_\psi \Omega^{-1}\nabla\vartheta\times\nabla\phi + b_\vartheta\Omega^{-1}\mathbf{V}_{\rm m} + (\varepsilon^2 b_\psi\sigma^{-1}\partial_\psi Z + b_\vartheta\sigma^{-1}\partial_\vartheta Z + b_\zeta)r\sin\theta\,\mathbf{1}_\phi\}e^{im\zeta+i\omega t+pt}\,.$$

To dominant order spatially,

$$\mathbf{B} = \{\varepsilon^2 F_{\psi 0}\Omega^{-1}\nabla\vartheta\times\nabla\phi + F_{\vartheta 0}\Omega^{-1}\mathbf{V}_{\rm m} + (\varepsilon^2 F_{\psi 0}\sigma^{-1}\partial_\psi Z + F_{\vartheta 0}\sigma^{-1}\partial_\vartheta Z + F_{\zeta 0})r\sin\theta\,\mathbf{1}_\phi\}e^{ik\vartheta+im\zeta+i\omega t+pt} + \mathcal{O}(\varepsilon)$$

or

$$\mathbf{B} = \{\Omega_o'\Omega^{-1}\mathbf{V}_{\rm m} + \sigma^{-1}(\Omega_o'\Omega^{-1}\widetilde{W} + \overline{W}_o')r\sin\theta\mathbf{1}_\phi\}D_n(\Upsilon/\kappa)e^{ik\vartheta+im\zeta+i\omega t+pt} + \mathcal{O}(\varepsilon)\,,$$

where

$$D_n(\Upsilon/\kappa) = 2^{-n/2}\exp\left(-\tfrac{1}{4}R_{\rm m}^{1/2}(\Psi-\Psi_o)^2\sqrt{|\Pi_o''/\overline{\gamma}_0|}\;(1+i\,\mathrm{sgn}\,\Pi_o'')\right)H_n(\Upsilon/\sqrt{2}\kappa)$$

with

$$\Upsilon/\kappa = R_{\rm m}^{1/4}(\Psi-\Psi_o)\sqrt[4]{|\Pi_o''|/\overline{\gamma}_0}\left(\sqrt{\tfrac{\sqrt{2}+1}{2}} + i\sqrt{\tfrac{\sqrt{2}-1}{2}}\;\mathrm{sgn}\,\Pi_o''\right).$$

The first four Hermite polynomials are $H_0(x)=1$, $H_1(x)=2x$, $H_2(x)=4x^2-2$, $H_3(x)=8x^3-12x$. As expected for large $R_{\rm m}$ the moduli of the eigenfunctions exhibit a Gaussian-like structure about the resonant curve, with spatial oscillations of rapidly diminishing amplitude as distance Υ from the curve increases. Higher n modes display more complex spatially varying behaviour within the envelope of the stream surface localization.

The magnetic field can be graphically represented by plotting the spherical polar components of $\mathrm{Re}\,C\mathbf{B}_0$ and $\mathrm{Im}\,C\mathbf{B}_0$ in the meridional plane, where

$$\mathbf{B}_0 = [\Omega^{-1}\mathbf{V}_{\rm m} + (\sigma^{-1}\Omega^{-1}\widetilde{W} - k/m)r\sin\theta\,\mathbf{1}_\phi]\,D_n(\Upsilon/\kappa)e^{i(k\vartheta - m\sigma^{-1}Z)}\,, \tag{2.60}$$

i.e. the ε^0-field obtained from $\mathbf{B}$ by removing the factor $e^{im\phi+i\omega t+pt}$, and choosing the complex normalisation constant C to minimise $\int_V |C\mathbf{B}_0-\mathbf{B}|^2\,dV$, where $\mathbf{B}$ is the magnetic field obtained by solving the dynamo eigen-problem,

$$C = \frac{\int_V \mathbf{B}_0^*\cdot\mathbf{B}\,dV}{\int_V|\mathbf{B}_0|^2\,dV}\,. \tag{2.61}$$

The real parts of the growth rates are

$$p = \pm\varepsilon^2\sqrt{|\sigma k\overline{\mu}_b + m\overline{\mu}_c||\Omega_o'|} - (n+\tfrac{1}{2})\varepsilon^2\sqrt{|\sigma k\Omega_o'' + m\overline{W}_o''|\overline{\gamma}_0} + \mathcal{O}(\varepsilon^4) \tag{2.62}$$

and the angular frequencies are

$$\omega = -\sigma k\Omega_o - m\overline{W}_o \pm \varepsilon^2\sqrt{|\sigma k\overline{\mu}_b + m\overline{\mu}_c||\Omega_o'|}\;\mathrm{sgn}\,[(\sigma k\overline{\mu}_b + m\overline{\mu}_c)\Omega_o'] \\ - (n+\tfrac{1}{2})\varepsilon^2\sqrt{|\sigma k\Omega_o'' + m\overline{W}_o''|\overline{\gamma}_0}\;\mathrm{sgn}\left(\sigma k\Omega_o'' + m\overline{W}_o''\right) + \mathcal{O}(\varepsilon^4)\,, \tag{2.63}$$

where the quantities appearing are evaluated upon the resonant stream surface $\psi=\psi_o$. The $n=0$ mode is the fastest growing magnetic field mode to dominant order for any m and k. The additional term, $-\varepsilon^4\left(k^2\overline{\beta}_k + m^2\overline{\beta}_m + 2mk\overline{\beta}_{mk}\right)$, must be added to the real part of the growth rate (2.62) to obtain Gilbert & Ponty's (2000) formula. The β's, which are independent of σ, are given by

$$\beta_k := |\nabla\vartheta|^2 - \overline{\gamma}_0^{-1}(\nabla\psi\cdot\nabla\vartheta)^2 \tag{2.64}$$
$$\beta_m := |\nabla\zeta|^2 - \overline{\gamma}_0^{-1}(\nabla\psi\cdot\nabla\zeta)^2 \tag{2.65}$$
$$\beta_{mk} := \nabla\vartheta\cdot\nabla\zeta - \overline{\gamma}_0^{-1}(\nabla\psi\cdot\nabla\vartheta)(\nabla\psi\cdot\nabla\zeta)\,, \tag{2.66}$$

These are not the complete contribution at order ε^4 but, as Gilbert (1989) argues, they should be the most important terms at that order for the fastest growing modes.

Finally, the streamline on which the field is localised is determined from the conditions,

$$k\sigma\Omega_o' + m\overline{W}_o' = 0\,, \qquad \sigma^2\Pi_o'' = k\sigma\Omega_o'' + m\overline{W}_o'' \neq 0\,. \tag{2.67}$$

In general, we find that $\Pi_o'' < 0$, which indicates that the resonant streamline corresponds to the maximal helical gradient of the magnetic mode. Equation (2.67)(a) is also the condition for the closure of the magnetic field lines on the surface $\psi = \psi_o$ to leading order. Since $d\mathbf{r} = \mathbf{f}_\psi d\psi + \mathbf{f}_\vartheta d\vartheta + \mathbf{f}_\zeta d\zeta$, the equation for the magnetic field lines, $\mathbf{B} \times d\mathbf{r} = \mathbf{0}$, reduces to

$$\begin{aligned} B_\psi d\vartheta - B_\vartheta d\psi &= 0 \\ B_\psi d\zeta - B_\zeta d\psi + (\partial_\vartheta Z)(B_\psi d\vartheta - B_\vartheta d\psi) &= 0 \\ B_\vartheta d\zeta - B_\zeta d\vartheta - (\partial_\psi Z)(B_\psi d\vartheta - B_\vartheta d\psi) &= 0\,, \end{aligned}$$

or simply

$$\frac{d\psi}{B_\psi} = \frac{d\vartheta}{B_\vartheta} = \frac{d\zeta}{B_\zeta}\,.$$

For the magnetic field (2.53)–(2.55) the field lines to leading order are

$$\Psi = \Psi_o\,, \qquad \vartheta - \vartheta_o = \frac{\overline{W}_o'}{\sigma\Omega_o'}(\zeta - \zeta_o)\,,$$

where $(\Psi_o, \vartheta_o, \zeta_o)$ is a given point on the field line. The magnetic field line is closed if there are integers k, m such that $\vartheta - \vartheta_o = -2\pi k$ and $\zeta - \zeta_o = 2\pi m$, which give the resonance condition (2.56)(a). So, unsurprisingly, a resonant surface also corresponds to the spatial localisation for which a magnetic mode reinforces itself. The resonance condition also ensures the ε^0-magnetic field is solenoidal, as noted following (2.50).

We could in principal find the resonant streamline $\Psi = \Psi_o$ for given values of (m, k, σ). However, we make the choices of the resonant streamline $\Psi = \Psi_o$ and the particular (m, k)-mode arbitrary by adjusting the parameter σ, and hence the flow, to satisfy the resonance condition (2.56)(a), i.e.

$$\sigma = -m\overline{W}_o'/k\Omega_o' = \sigma(m, k, \Psi_o)\,. \tag{2.68}$$

We thus use σ as a tuning parameter to tune the flow to the chosen streamline and magnetic modes.

3 Numerical Evaluation of the Asymptotic Expressions

In general the asymptotic approximations (2.51), (2.52), (2.53) to the growth rates and the eigenfunctions must be evaluated numerically. In this section we describe the method of computation.

The formula for the growth rate requires the evaluation of Ω, Ω', Ω'', $\overline{W}$, $\overline{W}'$, $\overline{W}''$, $\overline{\mu}_b$, $\overline{\mu}_c$, $\overline{\beta}_k$, $\overline{\beta}_m$, $\overline{\beta}_{mk}$ and $\overline{\gamma_0}$ on the resonant streamline $\psi = \psi_o$. Each of these quantities may be evaluated by line integrals along the streamline. Moreover a number of their constituent parts (such as $\nabla\vartheta$ and $\nabla\zeta$) may also be determined by line integrals. The integrals are usually too difficult to evaluate analytically and were evaluated numerically using the compound trapezoidal rule. The eigenfunctions require the evaluation of these quantities, except the β's, on a (ϑ, ψ)-grid, which must subsequently be interpolated onto the (s, z) coordinate system. A simple linear interpolation was sufficient.

We obtain Ω by integrating (2.1) and $\overline{W}$ by averaging. Their ψ derivatives may be procured as line integrals using the following technique. The average of a function $F(\psi, \vartheta)$ over the curve C_ψ given by constant ψ can be expressed, using (2.1), as

$$\overline{F}(\psi) = \frac{\Omega}{2\pi}\oint_{C_\psi} \frac{F\,\mathbf{v}_\mathrm{m}}{q^2}\cdot d\mathbf{r} = \frac{\Omega}{2\pi}\oint_{\partial S_\psi} \frac{F\,\mathbf{v}_\mathrm{m}}{q^2}\cdot d\mathbf{r} + \frac{\Omega}{2\pi}\oint_{C_0} \frac{F\,\mathbf{v}_\mathrm{m}}{q^2}\cdot d\mathbf{r} \tag{3.1}$$

$$= \frac{\Omega}{2\pi}\oint_{S_\psi} \nabla\times\left(\frac{F}{q^2}\mathbf{v}_\mathrm{m}\right)\cdot\mathbf{1}_\phi\, r\, dr\, d\theta + \Omega K\,, \tag{3.2}$$

where S_ψ is the annular region in the meridional plane bounded by C_ψ and a smaller fixed ψ-curve C_0, which encloses the stagnation point. The quantity K is independent of ψ. Now by (2.4), $r dr\, d\theta = (\Omega\, r \sin\theta)^{-1} d\psi\, d\vartheta$, and thus

$$\frac{\overline{F}}{\Omega} = \frac{1}{2\pi}\oint_{S_\psi} \nabla\times\left(\frac{F}{q^2}\mathbf{v}_\mathrm{m}\right)\cdot\frac{\mathbf{1}_\phi}{\Omega r\sin\theta}\, d\vartheta\, d\psi + K\,. \tag{3.3}$$

Differentiation gives

$$\frac{d}{d\psi}\left(\frac{\overline{F}}{\Omega}\right) = \frac{1}{2\pi}\oint_{C_\psi} \nabla\times\left(\frac{F}{q^2}\mathbf{v}_\mathrm{m}\right)\cdot\frac{\mathbf{1}_\phi}{\Omega r\sin\theta}\,d\vartheta = \frac{\overline{F_1}}{\Omega}\,, \tag{3.4}$$

where $F_1 := \nabla\times(F\mathbf{v}_\mathrm{m}/q^2)\cdot\mathbf{1}_\phi/r\sin\theta$. Iteration yields

$$d^n(\overline{F}/\Omega)/d\psi^n = \overline{F_n}/\Omega \tag{3.5}$$

where F_n is defined inductively for integer $n>1$ by

$$F_n := \nabla\times(F_{n-1}\mathbf{v}_\mathrm{m}/q^2)\cdot\mathbf{1}_\phi/r\sin\theta = -\nabla\cdot\left(\frac{F_{n-1}\nabla\psi}{(\nabla\psi)^2}\right). \tag{3.6}$$

Setting $F=1$ gives integral expressions for Ω', Ω'', etc. For azimuthal flows of the form $W(\vartheta,\psi)$, $F=W$ gives expressions for $\overline{W}$, $\overline{W}'$, $\overline{W}''$, etc. Let $Q := (\nabla\psi)^2$. Then

$$\begin{aligned} F_1 &= -\nabla\cdot(FQ\nabla\psi) = -(\nabla Q\cdot\nabla\psi + Q\nabla^2\psi)F - Q\nabla\psi\cdot\nabla F \\ F_2 &= -\nabla\cdot(F_1Q\nabla\psi) = -(\nabla Q\cdot\nabla\psi + Q\nabla^2\psi)F_1 - Q\nabla\psi\cdot\nabla F_1\,. \end{aligned}$$

If $R := \nabla Q\cdot\nabla\psi + Q\nabla^2\psi$, then

$$F_2 = (R^2 + Q\nabla\psi\cdot\nabla R)F + (2RQ + Q\nabla Q\cdot\nabla\psi)\nabla\psi\cdot\nabla F + \tfrac{1}{2}Q^2\nabla Q\cdot\nabla F + Q^2\nabla\psi\cdot\nabla\nabla F\cdot\nabla\psi\,.$$

As can be seen the integrands rapidly become very complicated with n. The motivation for persisting with these complicated expressions is that the numerical integration of smooth periodic functions over a period using the compound trapezoidal rule is spectrally accurate. Results were checked with a simpler but less accurate method of fitting a spline curve to the ψ-curve.

It soon becomes apparent that a number of the integrands are singular in spherical polar coordinates. If $\mathbf{V}_m = V_r\,\mathbf{1}_r + V_\theta\,\mathbf{1}_\theta$, we can write $d\vartheta = \Omega r d\theta/V_\theta = \Omega dr/V_r$. The spherical polar components of $\mathbf{V}_m$ vanish at two points on a $\mathbf{V}_m$-streamline, which can cause singular integrals, specifically those which evaluate $\nabla\vartheta$. To avoid this problem we transform to the toroidal coordinate system (R,Θ) shown in figure 1. The point $P_0(r_0,\theta_0)$ is a stagnation point of the meridional flow.

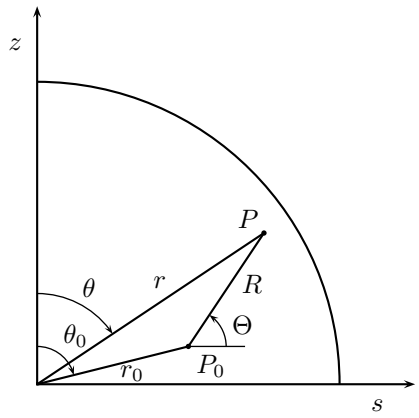

Figure 1: Toroidal coordinates (R,Θ).

Basic trigonometry gives a number of relationships between (r,θ) and (R,Θ), the most important of which are

$$r = \sqrt{r_0^2 + R^2 + 2r_0R\sin(\theta_0+\Theta)} \tag{3.7}$$

$$\theta = \theta_0 + \tan^{-1}\left|\frac{R\cos(\theta_0+\Theta)}{r_0 + R\sin(\theta_0+\Theta)}\right|, \tag{3.8}$$

The (R,Θ,ϕ) system is orthogonal but *left-handed*. For the flows we examine, we take (r_0,θ_0) to be the stagnation point at the centre of the concentric ψ curves. The radius r_0 can be evaluated using the Newton-Raphson method. We distinguish between different ψ curves by their largest s-intercept r_s. Each ψ curve

K	100	200	400	800
$\overline{\mu}_b$	4.63875	4.63936	4.63951	4.63955
$\overline{\mu}_c$	−0.20886	−0.20782	−0.20756	−0.20750
β_k	8.961	8.964	8.965	8.965
β_m ($\mathbf{v}_1$)	4.58627	4.58627	4.58627	4.58627
β_m ($\mathbf{v}_2$)	4.6719	4.6718	4.6718	4.6718
β_{mk}	0.2256	0.2278	0.2284	0.2285

Table 1: The quantities required by the asymptotic theory which converge more slowly with K. Here $r_s = 0.93$.

is thus described by an equation $\psi(r,\theta) = \psi(r_s, \pi/2)$. To determine the quadrature nodes we divide $[0, 2\pi]$, corresponding to one period of Θ, into n equal sub-intervals using the nodes $\Theta_i = 2\pi i/n$, $i = 0, 1, \ldots, n$. To calculate the corresponding values of R_i we use the Newton-Raphson method to solve

$$\psi(r(R_i, \Theta_i), \theta(R_i, \Theta_i)) - \psi(r_s, \pi/2) = 0$$

for R_i given Θ_i.

The integrands μ_b, μ_c, β_k, β_m, β_{mk} and γ_0 are expressed in terms of: Ω, $\overline{W}$; the R and Θ derivatives of ψ, ϑ, V_Θ, V_R; and the ψ and ϑ derivatives of Z; where $\mathbf{V}_m = V_R\,\mathbf{1}_R + V_\Theta\,\mathbf{1}_\Theta$. The derivatives of ψ, and V_R, V_Θ can be found analytically. The quantities $\partial_R\vartheta$, $\partial_\Theta\vartheta$ and $\partial_\psi Z$ must be determined. The angle ϑ is given by

$$\vartheta = \int_0^\vartheta d\vartheta^* = -\Omega \int_0^\Theta R^* \frac{(r_0 \sin\theta_0 + R^* \cos\Theta^*)}{\partial_{R^*}\psi^*} d\Theta^* \,, \tag{3.9}$$

where an asterisk denotes evaluation upon the $\psi = \psi^*$ curve. The two sets of variables (R, Θ) and (R^*, Θ^*) should not be confused: the asterisked pair are dependent on each other while the other pair are independent. With this in mind we differentiate the integral in (3.9). Using Leibniz's theorem we obtain

$$\partial_R\left(\frac{\vartheta}{\Omega}\right) = -\int_0^\Theta \partial_{R^*}\left(\frac{R^*(r_0 \sin\theta_0 + R^* \cos\Theta^*)}{\partial_{R^*}\psi^*}\right)\frac{\partial_R\psi}{\partial_{R^*}\psi^*} d\Theta^* \,, \tag{3.10}$$

and

$$\partial_\Theta\left(\frac{\vartheta}{\Omega}\right) = -\int_0^\Theta \partial_{R^*}\left(\frac{R^*(r_0 \sin\theta_0 + R^* \cos\Theta^*)}{\partial_{R^*}\psi^*}\right)\frac{\partial_\Theta\psi}{\partial_{R^*}\psi^*} d\Theta^* - \frac{R(r_0 \sin\theta_0 + R\cos\Theta)}{\partial_R\psi} \,. \tag{3.11}$$

Lastly, $\partial_\psi Z$ and $\partial_\vartheta Z$ are required for $\nabla\zeta$. Only the former issues a challenge. From the definition of $\widetilde{W}$,

$$\partial_\psi(\Omega Z) = \int_0^\vartheta \partial_\psi \widetilde{W}^* d\vartheta^* = \int_0^\vartheta \partial_\psi W^* d\vartheta^* - \overline{W}'\vartheta \,. \tag{3.12}$$

Thus from (2.2),

$$\partial_\psi Z = \frac{1}{\Omega}\int_0^\vartheta (\partial_\psi W^* - \frac{\Omega'}{\Omega} W^*) d\vartheta^* + \frac{\vartheta}{\Omega}\left(\frac{\Omega'}{\Omega}\overline{W} - \overline{W}'\right) \,. \tag{3.13}$$

This is expression is evaluated by converting the ϑ integral to an integral over Θ and using the formula

$$\partial_\psi W = J^{-1}(\partial_\Theta\vartheta\,\partial_R W - \partial_R\vartheta\,\partial_\Theta W) \,, \qquad J = \frac{\partial(\psi,\vartheta)}{\partial(R,\Theta)} \,. \tag{3.14}$$

Note that as the these integrals are not over closed curves, the trapezoidal rule does not give exponential accuracy for them. The μ's and β's also require further averaging so their convergence is not as fast, as shown in table 1.

The asymptotic estimates were computed in MATLAB. The convergence of quantities required by the asymptotic theory is shown in table 1 for different numbers K of numerical integration nodes along the chosen streamline, Ψ_0. Those quantities that issue from a single integration around the closed streamline converge very rapidly, typically for $K = 30$. These include Ω_0 and its ψ derivatives, $\overline{W}$ and its ψ derivatives, and $\overline{\gamma}_0$. Thus the quantities $\Omega_o = 5.3919$, $\Omega_o' = 7.2807$, $\Omega_o'' = -16.662$, $\overline{W}_o = 0.93043$, $\overline{W}_o' = 1.4927$, $\overline{W}_o''' = -2.7786$ are accurate to the figures shown here for $K = 100$. However, quantities which are evaluated by line integrals with variable limits converge more slowly, and settle down only for $K = 800$. The convergence of these quantities is displayed in table 1.

4 Numerical Solution of the Spherical Dynamo Eigenproblem

As indicated above, for steady flows the magnetic field is a linear combination of modes, which have the time separable form (1.4). (We ignore the possibility of generalised eigenfunctions.) The kinematic dynamo problem reduces to an eigenvalue problem for the growth rate λ and the spatial eigenfunction $\mathbf{B}(\mathbf{r})$. The magnetic induction equation is usually scaled in these problems on the diffusive time-scale, as in (1.1). In order to test the asymptotic theory outlined in sections 2 and 3 we must solve the eigen-problem numerically. The solenoidal conditions on the magnetic field and the velocity are satisfied identically by the poloidal-toroidal representation,

$$\mathbf{B} = \nabla \times T\mathbf{r} + \nabla \times \nabla \times S\mathbf{r}\,, \tag{4.1}$$

for the magnetic field and (1.6). The problem is then discretised using a spectral method in angle and fourth-order finite-differences in radius, and techniques of linear algebra are used to solve discretised eigenproblem.

4.1 Spectral Equations in Angle

The numerical method uses a hybrid form of the spectral equations of James (1974). These are a compact form of the poloidal-toroidal spectral equations derived by Bullard & Gellman (1954), apart from a factor of r in the poloidal-toroidal representations and the normalisation of the spherical harmonics. The poloidal and toroidal potentials of $\mathbf{B}$ are expanded in spherical harmonics,

$$Y_n^m(\theta,\phi) := (-)^m \sqrt{\frac{(2n+1)(n-m)!}{(n+m)!}} P_{n,m}(\cos\theta) e^{im\phi}\,, \tag{4.2}$$

where $P_{n,m}$ is the the Neumann associated Legendre function defined by

$$P_{n,m}(z) := (-)^n \frac{(1-z^2)^{m/2}}{2^n n!} \frac{d^{m+n}(1-z^2)^n}{dz^{m+n}}\,.$$

$$Y_n^{m*} = (-)^m Y_n^{-m} \tag{4.3}$$

Thus

$$S = \sum_{n,m} S_n^m(r,t) Y_n^m(\theta,\phi)\,, \qquad T = \sum_{n,m} T_n^m(r,t) Y_n^m(\theta,\phi)\,. \tag{4.4}$$

The summations are over $n = 1, 2, \ldots$, $m = -n\!:\!n$.

The compact poloidal-toroidal spectral equations are derived by first expanding the magnetic field and the velocity in vector spherical harmonics,

$$\mathbf{v} = \sum_{n,n_1,m} v_{n,n_1}^m \mathbf{Y}_{n,n_1}^m\,, \qquad \mathbf{B} = \sum_{n,n_1,m} B_{n,n_1}^m \mathbf{Y}_{n,n_1}^m\,, \tag{4.5}$$

where the vector spherical harmonics, which form a complete set, are defined by

$$\mathbf{Y}_{n,n_1}^m := (-)^{n-m}\sqrt{2n+1} \sum_{m_1,\mu} \begin{pmatrix} n & n_1 & 1 \\ m & -m_1 & -\mu \end{pmatrix} Y_{n_1}^{m_1} \mathbf{e}_\mu\,. \tag{4.6}$$

The complex unit vectors $\mathbf{e}_\mu$ are defined by $\mathbf{e}_0 := \mathbf{1}_z$ and $\mathbf{e}_{\pm1} := \mp(\mathbf{1}_x \pm i\mathbf{1}_y)/\sqrt{2}$. The summations in equation (4.5) are over $n = 0, 1, 2, \ldots$, $n_1 = n, n\pm1 \geq 0$, $m = -n\!:\!n$. The vector spherical harmonics are orthonormal with respect to the inner product,

$$(\mathbf{F},\mathbf{G}) := \frac{1}{4\pi} \oint \mathbf{F}\cdot\mathbf{G}^*\, d\Omega\,,$$

where $d\Omega = \sin\theta\, d\theta d\phi$. Substituting the expansions (4.5) of the magnetic field and the velocity into the magnetic induction equation (4.1) and taking the inner product with $\mathbf{Y}_{n,n_1}^m$ yields vector spherical harmonic spectral equations.

However, the vector spherical harmonic coefficients of the magnetic field are given in terms of the spherical harmonic coefficients of the magnetic potentials S and T by

$$B_{n,n-1}^m = (n+1)\sqrt{n/(2n+1)}\,\partial_n^{n-1} S_n^m \tag{4.7}$$

$$B^m_{n,n} = -i\sqrt{n(n+1)}T^m_n \tag{4.8}$$

$$B^m_{n,n+1} = n\sqrt{(n+1)/(2n+1)}\partial^{n+1}_n S^m_n\,, \tag{4.9}$$

where

$$\partial^{n'}_n := \begin{cases} \dfrac{\partial}{\partial r} + \dfrac{n+1}{r}, & \text{if } n' = n-1; \\ \dfrac{\partial}{\partial r} - \dfrac{n}{r}, & \text{if } n' = n+1. \end{cases}$$

Inversion of (4.7)–(4.9) gives

$$S^m_n = \frac{B^m_{n,n-1}}{(n+1)\sqrt{n(2n+1)}} - \frac{B^m_{n,n+1}}{n\sqrt{(n+1)(2n+1)}}\,, \qquad T^m_n = \frac{iB^m_{n,n}}{\sqrt{n(n+1)}}\,. \tag{4.10}$$

Spectral equations for S^m_n and T^m_n are derived by taking the combinations of the B^m_{n,n_1}-equations as indicated by (4.10) and considering the time derivative. Thus

$$(\partial_t - D_n)S^m_n = R_\mathrm{m}\sum_{\alpha,\beta} e_B(n,n)(\mathbf{Y}^{m_\alpha}_{n_\alpha,n_{1\alpha}} \times \mathbf{Y}^{m_\beta}_{n_\beta,n_{1\beta}}, \mathbf{Y}^m_{n,n}) v^{m_\alpha}_{n_\alpha,n_{1\alpha}} B^{m_\beta}_{n_\beta,n_{1\beta}} \tag{4.11}$$

$$(\partial_t - D_n)T^m_n = R_\mathrm{m}\sum_{\substack{\alpha,\beta,n_1 \\ (n_1=n\pm1)}} e_B(n,n_1)(\mathbf{Y}^{m_\alpha}_{n_\alpha,n_{1\alpha}} \times \mathbf{Y}^{m_\beta}_{n_\beta,n_{1\beta}}, \mathbf{Y}^m_{n,n_1})\partial^n_{n_1}(v^{m_\alpha}_{n_\alpha,n_{1\alpha}} B^{m_\beta}_{n_\beta,n_{1\beta}})\,, \tag{4.12}$$

where the operator $D_n := r^{-2}\{\partial_r(r^2\partial_r) - n(n+1)\}$ and the factor

$$e_B(n,n_1) := \begin{cases} -1/\sqrt{n(2n+1)}, & \text{if } n_1 = n-1; \\ i/\sqrt{n(n+1)}, & \text{if } n_1 = n; \\ -1/\sqrt{(n+1)(2n+1)}, & \text{if } n_1 = n+1. \end{cases}$$

The single coupling integral $(\mathbf{Y}^{m_\alpha}_{n_\alpha,n_{1\alpha}} \times \mathbf{Y}^{m_\beta}_{n_\beta,n_{1\beta}}, \mathbf{Y}^m_{n,n})$ can be evaluated explicitly in terms of $3j$- and $6j$-symbols (James 1976). The hybrid spectral equations follow from (4.11) and (4.12) by replacing the coefficients B^m_{n,n_1} are throughout by S^m_n and T^m_m using (4.7)–(4.9). The compact poloidal-toroidal spectral equations of James (1974) follow by also replacing the velocity coefficients v^m_{n,n_1} throughout with the coefficients s^m_n and t^m_n of the velocity potentials using equations analogous to (4.7)–(4.9).

Equations (4.11)–(4.12) are solved subject to

$$S^m_n = \mathcal{O}(r^n)\,, \quad T^m_n = \mathcal{O}(r^n) \qquad \text{as } r \to 0; \tag{4.13}$$

$$\frac{\partial S^m_n}{\partial r} + \frac{n+1}{r}S^m_n = 0\,, \quad T^m_n = 0\,, \qquad \text{at } r = 1. \tag{4.14}$$

Conditions (4.13) and (4.15) are implied by the differentiability of $\mathbf{B}$ with respect to x, y, z at $r = 0$. Equations (4.14) arise from the self-exciting dynamo condition (1.5) for an insulating exterior. If $\mathbf{B}$ is analytic at $r = 0$, as assumed herein, additional useful conditions hold,

$$S^m_n(-r) = (-)^n S^m_n(r)\,, \quad T^m_n(-r) = (-)^n T^m_n(r)\,. \tag{4.15}$$

The magnetic field eigenfunctions decouple for each azimuthal wavenumber m, since the flows considered herein are axisymmetric. Moreover, by property (4.3), only modes with $m \geq 0$ need be considered, since the fields are real. The case $m = 0$, which gives only decaying modes by the axisymmetric antidynamo theorem (see Ivers & James 1985), was ignored.

In numerical work the expansions (4.4) and (4.4) were truncated at $n = N$, and $n_1 = N + 1$ in (4.5), giving $2(N - m + 1)$ spherical harmonic coefficient functions S^m_n and T^m_n for $n = m, \ldots, N$ with m fixed.

4.2 Radial Discretisation

The radial dependence is discretised using fourth-order finite-differences over a uniform grid $r_j := j/J$, $j = 0 : J$ on $0 \leq r \leq 1$. Centred-difference formulas are applied to the truncated poloidal and toroidal spectral equations at the interior points r_j, $j = 1 : J - 2$, using conditions (4.15) at $j = 1$ and the one-sided formulas,

$$f^{(1)}_0 = \frac{-f_{-3} + 6f_{-2} - 18f_{-1} + 10f_0 + 3f_1}{12h} - \frac{1}{20}f^{(5)}(\eta)h^4$$

	Re λ			Im λ		
$J\backslash N$	20	30	40	20	30	40
100	236.4	255.0	254.7	52786.7	52733.2	52731.1
200	258.5	277.7	277.7	52721.2	52688.3	52688.0
400	261.5	279.1	279.2	52716.5	52685.6	52685.4
800	261.7	279.2	279.3	52716.3	52685.4	52785.2

Table 2: Convergence of the dominant mode's eigenvalue λ with J and N for $\mathbf{v}_1$ at $R_\mathrm{m} = 100,000$.

$$f_0^{(2)} = \frac{f_{-4} - 6f_{-3} + 14f_{-2} - 4f_{-1} - 15f_0 + 10f_1}{12h^2} - \frac{13}{180} f^{(6)}(\eta) h^4$$

for the toroidal equation at r_{J-1},

$$f_0^{(1)} = \frac{f_{-2} - 9f_{-1} - 9f_0 + 17f_1 - 6hf_1^{(1)}}{18h} + \frac{1}{60} f^{(5)}(\eta) h^4$$
$$f_0^{(2)} = \frac{3f_{-3} - 32f_{-2} + 252f_{-1} - 480f_0 + 257f_1 - 60hf_1^{(1)}}{144h^2} - \frac{1}{360} f^{(6)}(\eta) h^4$$

for the poloidal equation at r_{J-1} and

$$f_0^{(2)} = \frac{-9f_{-4} + 64f_{-3} - 216f_{-2} + 576f_{-1} - 415f_0 + 300hf_0^{(1)}}{72h^2} + \frac{1}{15} f^{(6)}(\eta) h^4$$

for the poloidal equation at r_J. There are thus $(2J+1)(N-m+1)$ unknowns, $S_n^m(r_j)$ for $j = 1:J$ and $T_n^m(r_j)$ for $j = 1:J-1$

4.3 Computation of the Eigenvalues and Eigenfunctions

For a given magnetic Reynolds number R_m the discretisation leads to an eigenvalue problem

$$\mathbf{A}\mathbf{x} = \lambda \mathbf{x}\,, \tag{4.16}$$

where $\mathbf{A}$ is an $(2J+1)(N-m+1) \times (2J+1)(N-m+1)$ matrix, which depends linearly on R_m.

The matrix $\mathbf{A}$ is banded with the bandwidth minimized by ordering the unknowns to block together all harmonic coefficients at each grid-point. Thus $\mathbf{x} = [\mathbf{x}_1, \ldots, \mathbf{x}_j, \ldots, \mathbf{x}_N]$, where the vector $\mathbf{x}_j$ of unknowns at r_j is

$$\mathbf{x}_j := [S_m^m(r_j), T_m^m(r_j), S_{m+1}^m(r_j), T_{m+1}^m(r_j), S_{m+2}^m(r_j), T_{m+2}^m(r_j), ..., S_N^m(r_j), T_N^m(r_j)]$$

for $j = 1:J-1$ and

$$\mathbf{x}_N := [S_m^m(r_J), S_{m+1}^m(r_J), S_{m+2}^m(r_J), ..., S_N^m(r_J)]\,.$$

The equations are ordered identically. Moreover, the matrix band itself is sparse, with many zero elements due to the selection rules (James 1973) for the coupling integral in (4.11) and (4.12).

We determined the eigenvalues and eigenfunctions by inverse iteration and the implicitly restarted Arnoldi method using ARPACK (Sorensen 1992). The Arnoldi method was particularly helpful in identifying the mode of fastest growth at large R_m as the ratio of the real part of the growth rate to the imaginary part is $\mathcal{O}(R_\mathrm{m}^{-1/2})$. Consequently inverse iteration had difficulty in converging to the eigenvalue of largest real part without a good estimate of the true eigenvalue.

The solution of (4.16) was straightforward except that very large dimensions were required in some cases to achieve convergence (on increasing J and N) for very large R_m ($=5\times10^5$). The truncation levels J and N were restricted by the memory limit. The largest matrix computed was $64,040 \times 64,040$ for $J = 800$, $N = 40$, $m = 1$. Convergence of the eigenvalue λ of largest real part with respect to J and N is shown at $R_\mathrm{m} = 10^5$ for $\mathbf{v}_1$ in table 2 and for $\mathbf{v}_2$ in table 3. The higher modes with $n = 1, 2$ require even higher truncation levels, as they exhibit greater spatial variation. As R_m is increased greater truncation levels are required as the length-scale of the fastest growing mode decreases like $\mathcal{O}(R_\mathrm{m}^{-1/4})$. Difficulties were encountered for $R_\mathrm{m} > 5\times10^5$ as the truncation required (and consequently the size of the matrices generated) became prohibitive.

The eigenfunctions are normalised so that $\max_{r,\theta}\{(\mathrm{Re}\,\hat{\mathbf{B}})^2 + (\mathrm{Im}\,\hat{\mathbf{B}})^2\} = 1$ and $\mathrm{Re}\,\hat{B}_r = 0$ at the maximum, where $\mathbf{B} = \hat{\mathbf{B}}(r,\theta)\, e^{im\phi + \lambda\tau}$.

	Re λ			Im λ		
$J\backslash N$	20	30	40	20	30	40
200	687.7	688.2	688.3	16390.6	16391.6	16392.8
400	688.2	687.5	687.5	16390.6	16391.9	16392.1
800	688.2	687.5	687.5	16390.6	16392.0	16392.3

Table 3: Convergence of the dominant mode's eigenvalue λ with J and N for $\mathbf{v}_2$ at $R_\mathrm{m} = 100,000$.

R_m	Re λ_0	Im λ_0	Re λ_1	Im λ_1	Re λ_2	Im λ_2
416.1864	0	170.2922	–	–	–	–
500	3.1054	208.8	−88.05	198.2411	–	–
750	11.2432	325.55	–	–	–	–
1000	17.9967	444.19	−77.7	425.57	−237.2588	421.808
1500	28.3164	684.99	–	–	–	–
2000	35.3415	929.29	–	–	–	–
3000	43.1781	1426.89	–	–	−207.5813	1353.06
5000	54.6313	2445.51	−180.165	2306.466	–	–
10000	78.5208	5032.19	−133.484	4788.276	−387.1595	4678.515
20000	115.6785	10270.02	–	–	–	–
50000	193.5259	26118.99	−324.540	25560.96	−811.1473	25003.12
100000	279.162	52685.35	−467.662	51898.48	−1182.71	51107.84
150000	344.9439	79324.97	–	–	–	–
200000	400.2472	106002.52	−668.846	104897.5	−1726.128	103768.5
300000	492.6508	159423.87	−825.961	158069	−2024.529	156876.3
400000	571.3119	212899.37	–	–	−1968.609	209731.6
500000	641.1343	266407.22	−1080.54	264712.9	−1863.246	262300.9

Table 4: The growth rates of the leading modes as computed by the numerical eigenproblem for $\mathbf{v}_1$, $m = k = 1$ at different R_m. The subscript of λ indicates the corresponding n mode number.

5 Results

We present results for each of the flows $\mathbf{v}_1$ and $\mathbf{v}_2$, corresponding to a representative configuration of the parameters for the same resonant curve. For both $\mathbf{v}_1$ and $\mathbf{v}_2$ the resonant curve is $\Psi_o = \Psi(r_s, \pi/2) \approx -0.20287\ldots$ with $r_s = 0.93$. The resonance is ensured for given m and k by setting the tuning parameter σ according to (2.68). The resonance conditions for $\mathbf{v}_1$ and $\mathbf{v}_2$ may be expressed as $\sigma = \sigma_1(m, k, \Psi)$ and $\sigma = \sigma_2(m, k, \Psi)$. We find that $\sigma_1(1, 1, \Psi_0) \approx 0.1373$, $\sigma_1(2, 1, \Psi_0) \approx 0.2747$, and $\sigma_2(1, 1, \Psi_0) \approx 0.2050$ to 4 significant figures. Moreover, for the flows we examine there is no degeneracy in σ, i.e. for a given σ there is only one possible set of (m, k, Ψ), so there can only be one resonant curve for a given flow.

The different times t, τ of the asymptotic and numerical results are related by $t/\tau = R_\mathrm{m}$. Thus to compare the asymptotic and numerical results, the numerical growth rates are divided by R_m, i.e. $p = \mathrm{Re}\,\lambda/R_\mathrm{m}$, $\omega = \mathrm{Im}\,\lambda/R_\mathrm{m}$. Moreover, asymptotic and numerical modes must be correctly matched. There is no difficulty with the azimuthal wavenumber m, since it coincides in the asymptotic and numerical results for $\mathbf{v}_1$, and also for $\mathbf{v}_2$, when ζ is decomposed and the factor $e^{im\phi}$ is extracted from the eigenfunction. We assumed that, once the resonant curve and the wavenumbers m, k are chosen, which sets the tuning parameter $\sigma(m, k, \Psi)$, the collection of modes determined by the numerical eigenproblem correspond to the various asymptotic n modes. The strongest growing exact (numerical) mode was identified with $n = 0$.

5.1 Growth Rates

The growth rates of the $n = 0, 1, 2$ magnetic modes for $k = 1$ and $m = 1, 2$ in the spherical helical dynamos, which we considered, are presented below. Tables 4 and 5 show the growth rates of the $n = 0, 1, 2$ modes, as computed by the numerical eigenproblem for $\mathbf{v}_1$ and $\mathbf{v}_2$ at the truncation levels $N = 40$ and $J = 800$. The scaling $\mathrm{Im}\,\lambda/\,\mathrm{Re}\,\lambda \sim R_\mathrm{m}^{1/2}$ predicted by the asymptotic theory for large R_m [see equations (2.15)] is clearly evident. Moreover the leading modes possess growth rates whose imaginary parts asymptote to a common value $(-\Pi_o R_\mathrm{m})$. This closely clustered property of the eigenvalues in spherical helical dynamos explains the difficulty of algebraic eigen-solvers in separating the eigenvalues at large R_m. In this regime a partial eigen-solver, such as the implicitly restarted Arnoldi method, is invaluable.

Figures 2 to 8 present the (real) growth rates p and angular frequencies ω calculated using the asymptotic theory with the higher order terms (the solid lines) of Gilbert & Ponty (2000) included, the asymptotic theory

R_m	$\mathrm{Re}\,\lambda_0$	$\mathrm{Im}\,\lambda_0$	$\mathrm{Re}\,\lambda_1$	$\mathrm{Im}\,\lambda_1$	$\mathrm{Re}\,\lambda_2$	$\mathrm{Im}\,\lambda_2$
500	17.8	18.2	−60.3	17.8	–	–
1,000	38.0	74.7	−48.0	66.1	−642.4	113.6
2,000	68.9	206.3	−25.0	187.4	−384.8	196.7
3,000	93.6	347.2	−5.2	320.8	−375.0	322.2
5,000	133.2	641.3	27.4	602.2	−348.1	592.7
10,000	203.8	1408.9	87.8	1344.3	−282.1	1303.8
20,000	293.9	3006.6	178.5	2878.7	−211.5	2747.8
30,000	363.0	4645.6	224.4	4423.7	−237.0	4339.7
50,000	477.1	7969.4	250.7	7697.2	−86.1	7546.4
100,000	687.5	16392.3	348.9	16000.0	−19.2	15566.2
200,000	982.4	33432.1	486.2	32867.1	−57.2	32299.4

Table 5: The growth rates of the leading modes as computed by the numerical eigenproblem for $\mathbf{v}_2$, $m = k = 1$ at different R_m. The subscript of λ indicates the corresponding n mode number.

correct to order ε^2 (the dashed line) and the numerical method (the data points). The truncation levels for the asymptotic values and the numerical values are $K = 400$, $J = 800$, $N = 40$. Figures 2–4 show the growth rates p_n and angular frequencies ω_n for the $m = 1$, $k = 1$, $n = 0, 1, 2$ magnetic modes of the $\mathbf{v}_1$ flow with $\sigma = \sigma_1(1, 1, \Psi_0)$. Of the three modes shown, only the $n = 0$ mode is a dynamo, above the critical magnetic Reynolds number at $R_\mathrm{m} \approx 416$ (see table 4) with a maximum positive growth rate at $R_\mathrm{m} \approx 1500$. For $R_\mathrm{m} \gtrsim 1500$, the asymptotic theory and figure 2 imply that $p_0 \to 0$ monotonically, as $R_\mathrm{m} \to \infty$, and hence that the dynamo is slow. Figures 3,4 and the asymptotic theory imply that the $n = 1, 2$ modes decay for all $R_\mathrm{m} \gtrsim 100$. Figure 5 shows p_0, ω_0 for the $m = 2$, $k = 1$, $n = 0$ mode of the $\mathbf{v}_1$ flow with $\sigma = \sigma_1(2, 1, \Psi_0)$. Observe that the flows are actually different for the $k = 1$,$n = 0$ magnetic modes with the azimuthal wavenumbers $m = 1, 2$, since the modes share the same resonance curve. This requires different σ and hence different amplitude ratios of meridional to azimuthal flow.

Figures 6–8 show p_n, ω_n for the $m = 1$, $k = 1$, $n = 0, 1, 2$ magnetic modes of the $\mathbf{v}_2$ flow with $\sigma = \sigma_2(1, 1, \Psi_0)$. The $n = 0$ mode is a dynamo above the critical magnetic Reynolds number at $R_\mathrm{m} \sim 100$ with a maximum growth rate at $R_\mathrm{m} \sim 800$. For the v_2 flow the $n = 1$ mode also acts as a dynamo above $R_\mathrm{m} \sim 2000$ with a maximum growth rate at $R_\mathrm{m} \sim 2 \times 10^4$. The $n = 2$ mode decays for all $R_\mathrm{m} \gtrsim 2000$ with $p_2 \to 0$ as $R_\mathrm{m} \to \infty$.

There is excellent agreement between the asymptotic growth rates of order ε^2 and the numerical growth rates when $R_\mathrm{m} \gtrsim 10^5$ for $\mathbf{v}_1$ and when $R_\mathrm{m} \gtrsim 4 \times 10^4$ for $\mathbf{v}_2$, with even better agreement in the angular frequencies. If the additional terms of Gilbert & Ponty (2000) are retained in the asymptotic growth rates the agreement extends down to $R_\mathrm{m} \gtrsim 10^4$, substantiating their neglect of the other terms at this order, at least for the modes of small n. This agreement strongly supports the asymptotic theory. It also indicates that the identification of the numerical modes with the asymptotic modes is correct.

5.2 Magnetic Field Structure

Figures 9–17 show magnetic modes for various parameter values. Figure 9 plots the real and imaginary parts of the magnetic field components, $\hat{B}_r$, $\hat{B}_\theta$, $\hat{B}_\phi$, of the $m = 1$, $k = 1$, $n = 0$ mode for the $\mathbf{v}_1$ flow with $\sigma = \sigma_1(1, 1, \Psi_0)$ and $R_\mathrm{m} = 10^5$. The asymptotic field to leading order and the numerical magnetic field are shown. Solid (dashed) contours represent positive (negative) magnetic field. Superimposed on the plots is the resonant curve to highlight the localisation of the magnetic field. It is apparent from the figures that the asymptotic and numerical magnetic fields agree in their dominant features: the position, orientation and shape of the local maxima and minima, but with a slight offset outwards away from the resonant streamline. This is clearer in figures 10 and 11, which show $|\hat{B}_r|$, $|\hat{B}_\theta|$, $|\hat{B}_\phi|$, and $|\hat{\mathbf{B}}|$ respectively, for the same mode. The localisation of the field to the resonant stream line is readily observed in figures 9–11, with marked flux expulsion inside the resonant streamline and even outdside. The $k = 1$ nature of the field is readily apparent from its variation around the streamline.

Figures 12–14 show the $m = 1$, $k = 1$, $n = 0$ mode for the $\mathbf{v}_1$ flow with $\sigma = \sigma_1(1, 1, \Psi_0)$, but with $R_\mathrm{m} = 5 \times 10^5$. The structure in $\mathrm{Im}\,\hat{B}_r$, $\mathrm{Im}\,\hat{B}_\theta$, $|\hat{B}_r|$, $|\hat{B}_\theta|$ and $|\hat{\mathbf{B}}|$ near the z-axis, which is present at $R_\mathrm{m} = 10^5$, has disappeared at $R_\mathrm{m} = 5 \times 10^5$ and the magnetic field is more localised and intense. The offset of the maxima and minima from the resonant streamline is substantially reduced compared to Figures 9–11.

Finally, Figures 13–17 show the $m = 1$, $k = 1$, $n = 1$ mode for the $\mathbf{v}_1$ flow with $\sigma = \sigma_1(1, 1, \Psi_0)$ and $R_\mathrm{m} = 10^5$. This mode decays slowly with time as shown in figure 3. Its spatial structure is more complicated

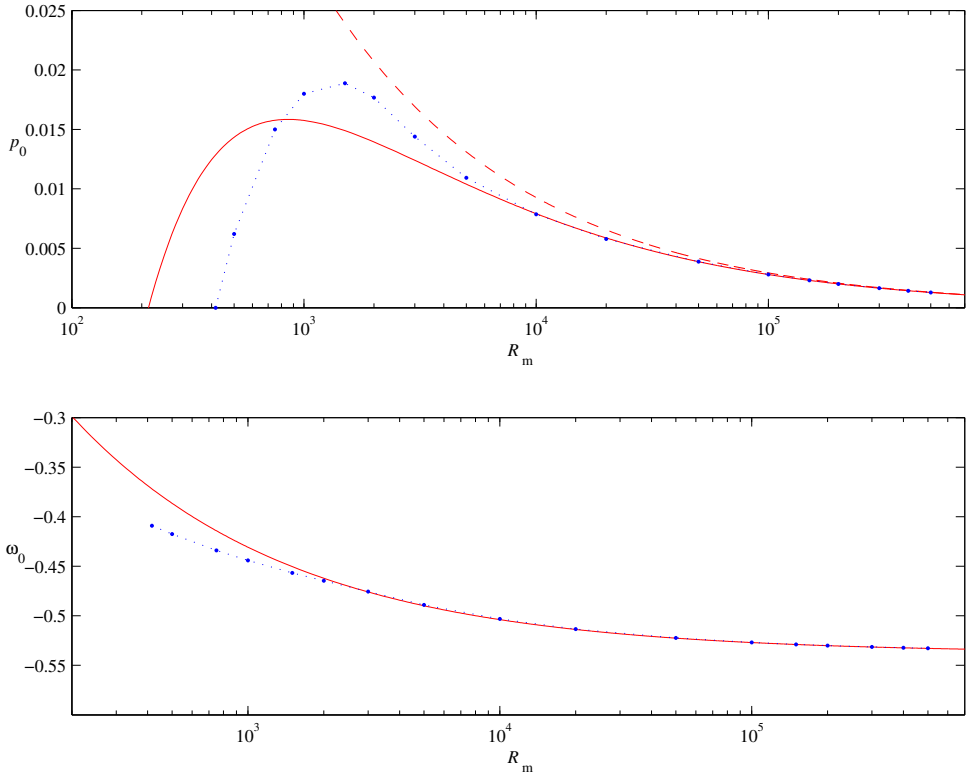

Figure 2: The growth rate p_0 and angular frequency ω_0 for the $m = 1$, $k = 1$, $n = 0$ mode of $\mathbf{v}_1$ calculated using the asymptotic formulae with the extra terms of Gilbert & Ponty (2000) (solid lines), the asymptotic formulae correct to order ε^2 (dashed line) and the numerical method (points on the dotted lines).

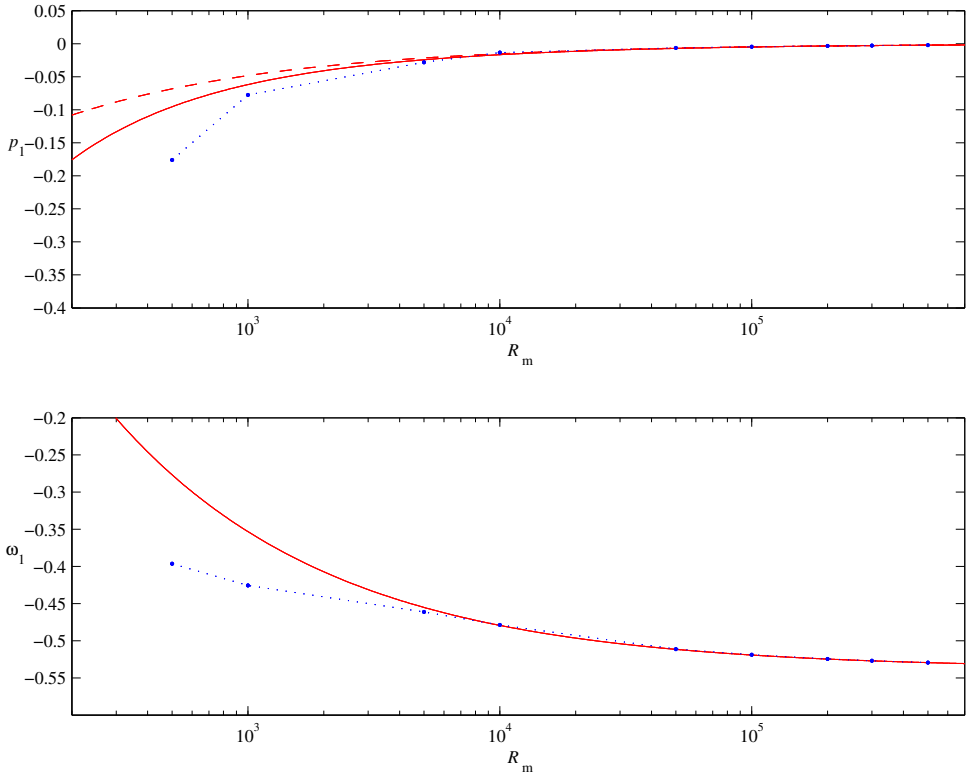

Figure 3: The growth rate p_1 and angular frequency ω_1 for the $m = 1$, $k = 1$, $n = 1$ mode of $\mathbf{v}_1$.

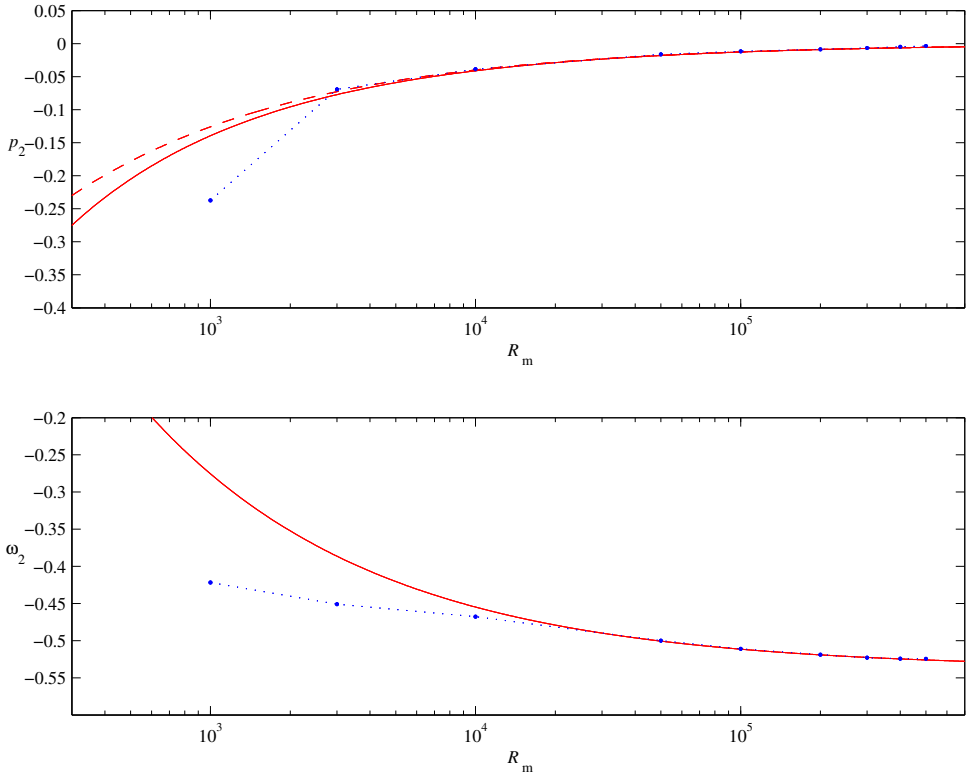

Figure 4: The growth rate p_2 and angular frequency ω_2 for the $m = 1$, $k = 1$, $n = 2$ mode of $\mathbf{v}_1$.

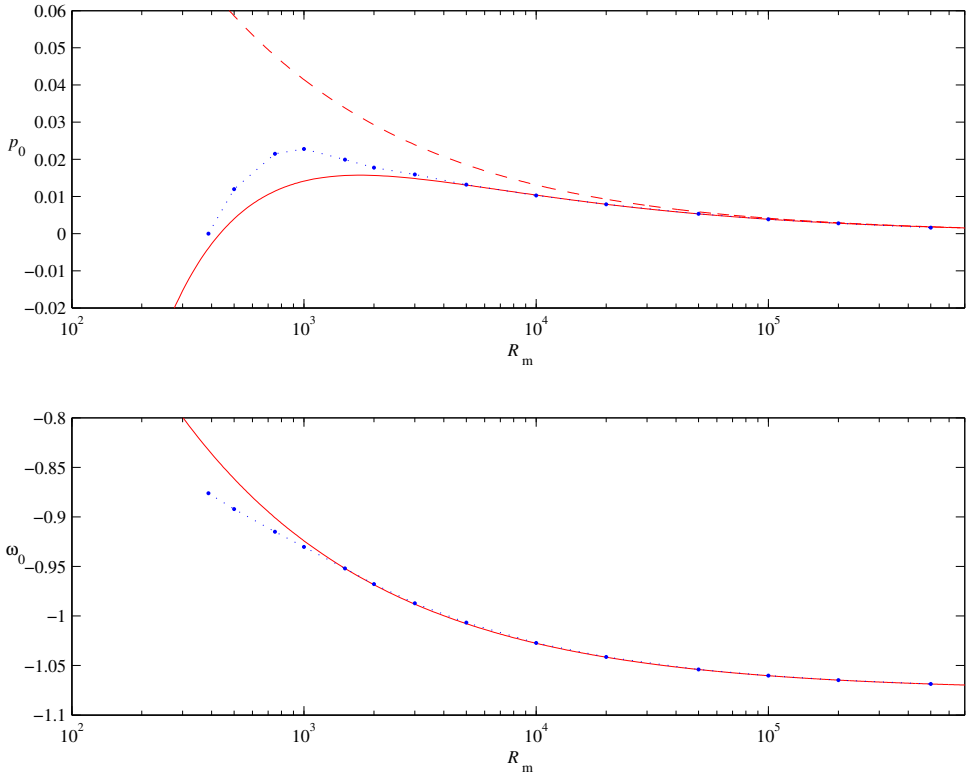

Figure 5: The growth rate p_0 and angular frequency ω_0 for the $m = 2$, $k = 1$, $n = 0$ mode of $\mathbf{v}_1$.

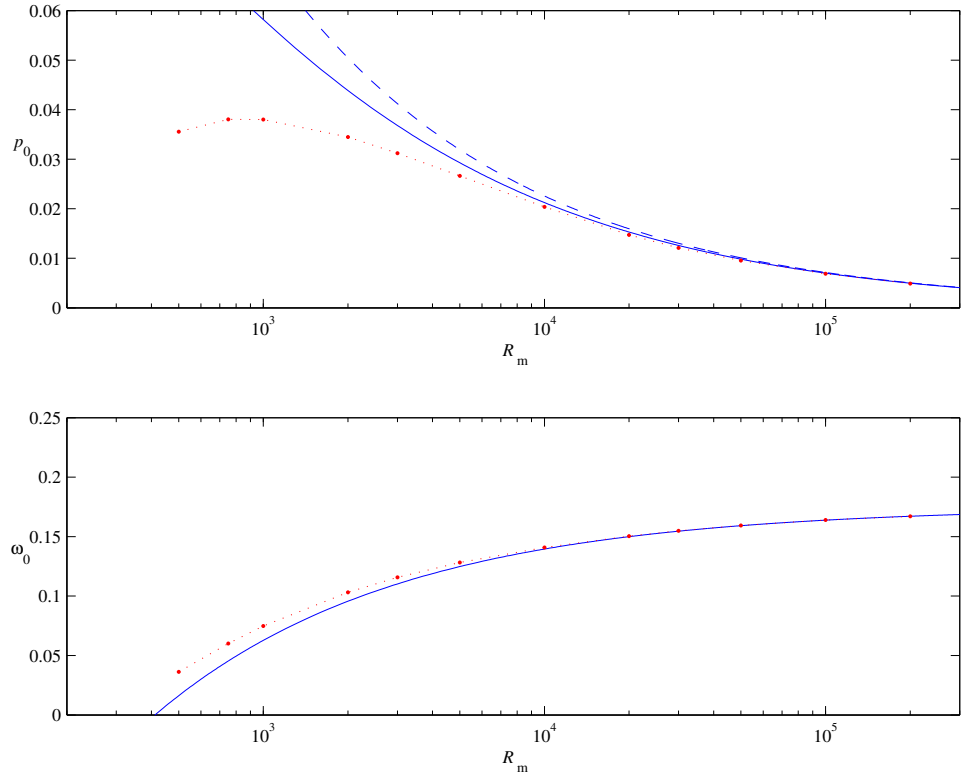

Figure 6: The growth rate p_0 and angular frequency ω_0 for the $m = 1$, $k = 1$, $n = 0$ mode of $\mathbf{v}_2$.

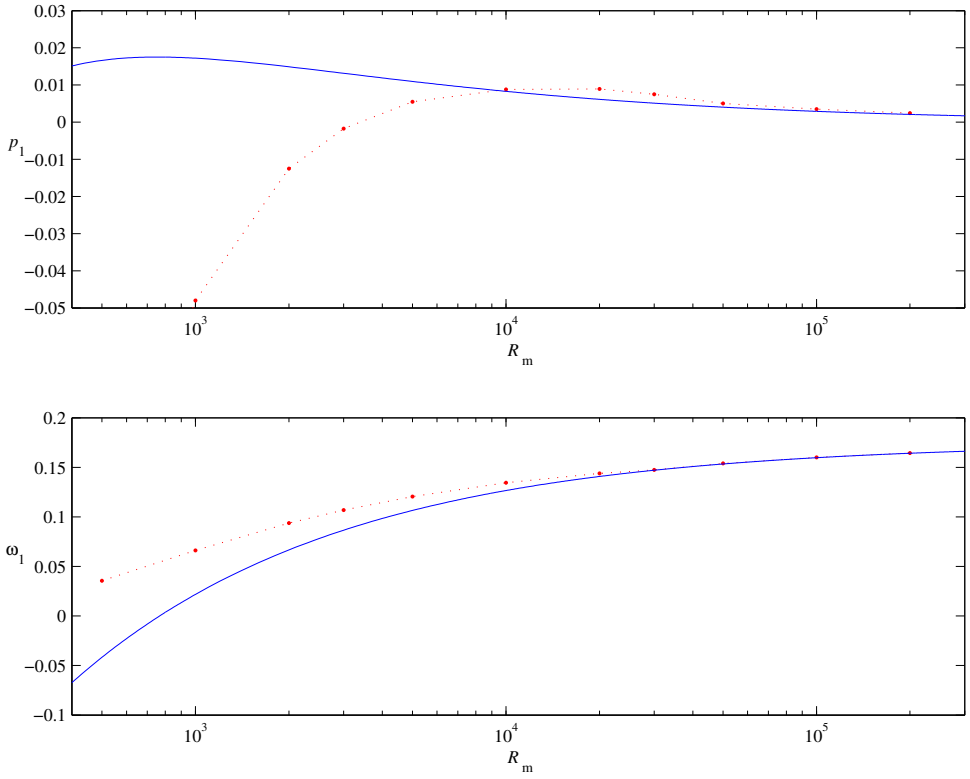

Figure 7: The growth rate p_0 and angular frequency ω_0 for the $m = 1$, $k = 1$, $n = 1$ mode of $\mathbf{v}_2$.

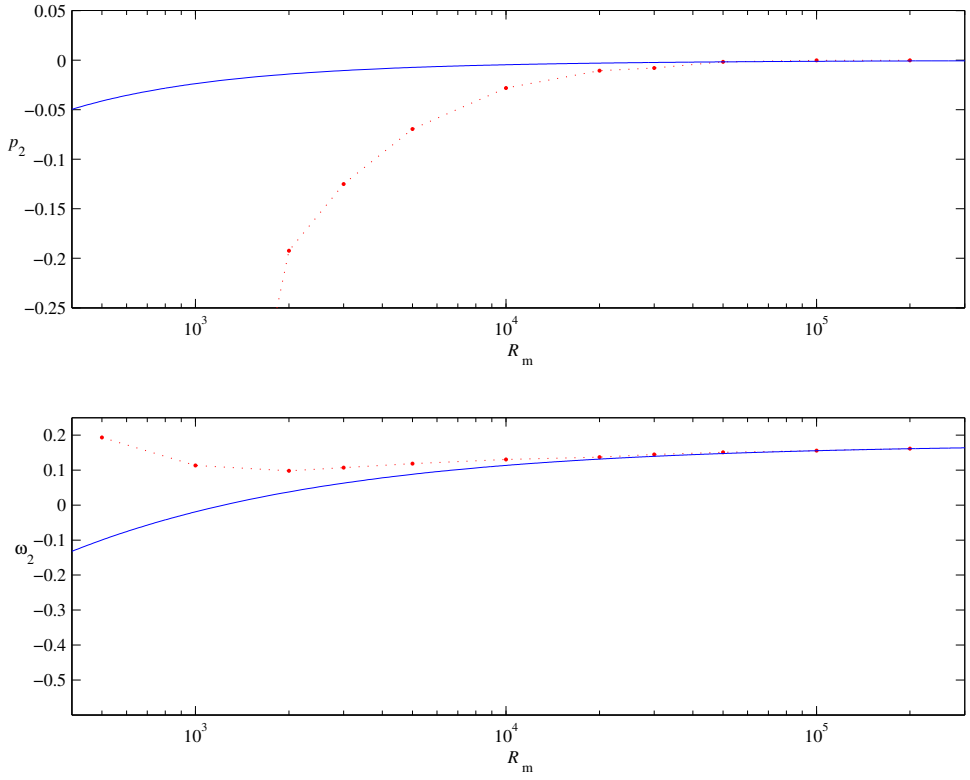

Figure 8: The growth rate p_0 and angular frequency ω_0 for the $m = 1$, $k = 1$, $n = 2$ mode of $\mathbf{v}_2$.

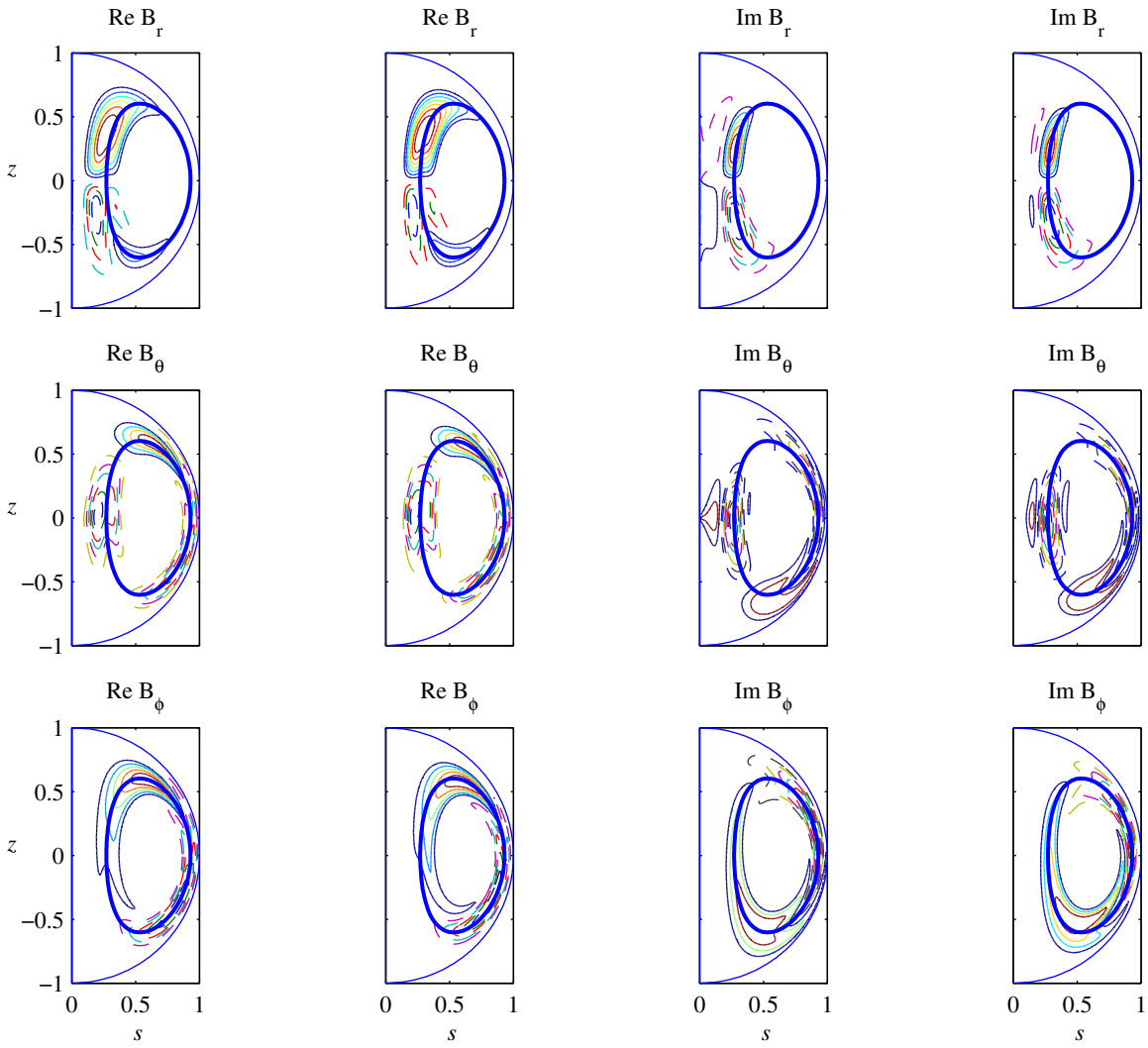

Figure 9: Plots of the real and imaginary parts of $\hat{B}_r$, $\hat{B}_\theta$, $\hat{B}_\phi$ for the $m = 1$, $k = 1$, $n = 0$ mode of $\mathbf{v}_1$ at $R_\mathrm{m} = 10^5$, determined asymptotically (left) to leading order and numerically (right), and the resonant stream line (thick lines).

due to the variation with ψ under the gaussian envelope of $D_1(\Upsilon/\kappa)$. In particular, the field components vanish on the resonant streamline. The field is not fully localised at this magnetic Reynolds number, with some structure in $|\hat{B}_r|$ still present near the z-axis. The maxima and minima of the leading order asymptotic field components are broader and displaced further away from the resonant streamline. The asymptotic field also shows structure in $\mathrm{Re}\,\hat{B}_r$, $\mathrm{Im}\,\hat{B}_r$, $\mathrm{Re}\,\hat{B}_\theta$, $|\hat{B}_r|$, $|\hat{B}_\theta|$ and $|\hat{\mathbf{B}}|$ near the z-axis absent from the numerical field.

6 The Asymptotic Theory to $\mathcal{O}(\varepsilon^4)$

6.1 The $\mathcal{O}(\varepsilon^1)$ Magnetic Field

The asymptotic analysis of section 2 is extended to determine the growth rate up to order ε^4. At order ε^3 it is found that there is no contribution to the growth rate, which partially explains the good agreement between the asymptotic and numerical growth rates, and the magnetic field in (2.28) is fully determined to order ε^1. The tuning parameter σ is suppressed in this section.

The ε^3-equations are

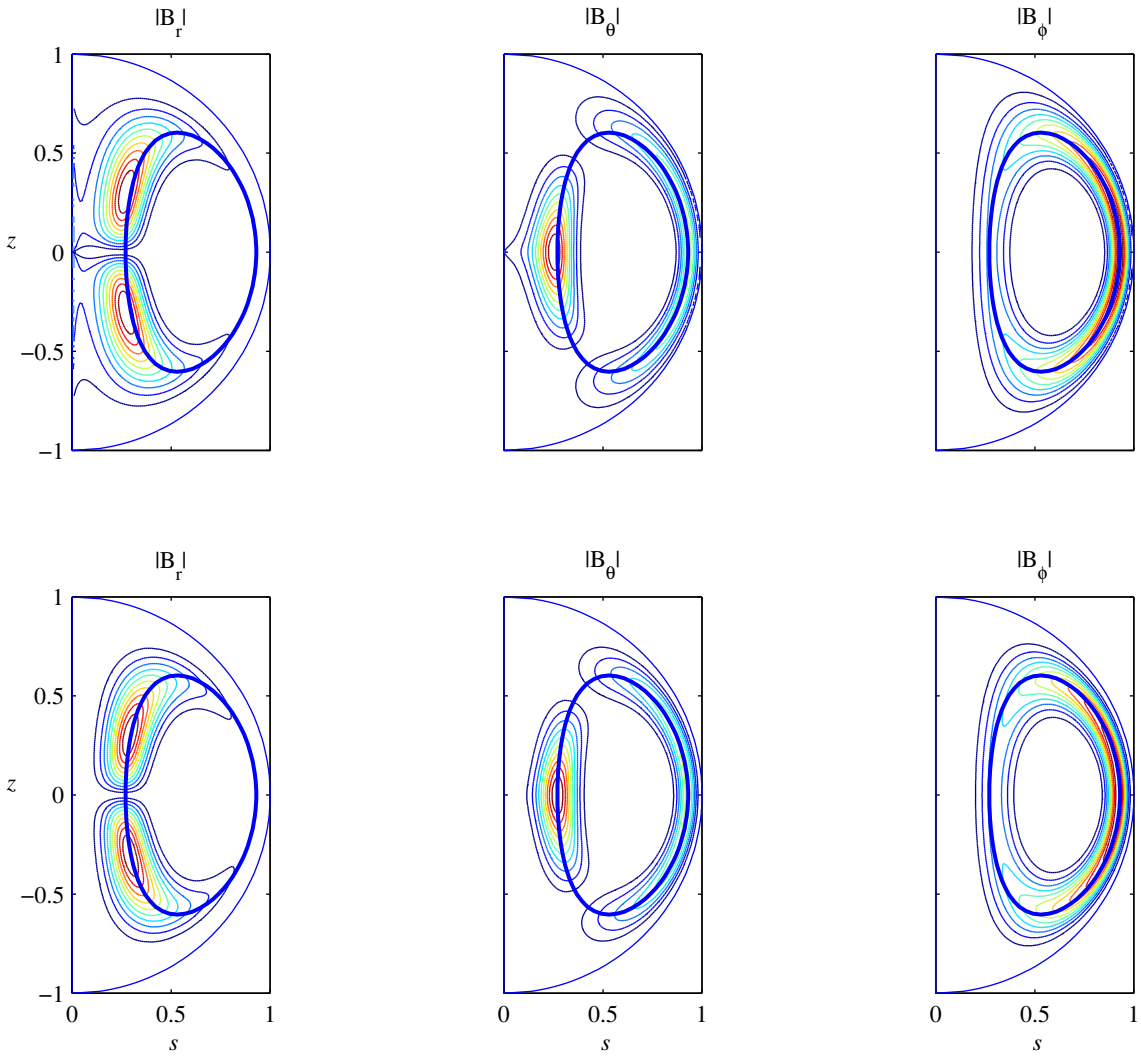

Figure 10: Plots of $|\hat{B}_r|$, $|\hat{B}_\theta|$, $|\hat{B}_\phi|$ for the $m = 1$, $k = 1$, $n = 0$ mode of $\mathbf{v}_1$ at $R_\mathrm{m} = 10^5$, determined asymptotically (left) to leading order and numerically (right), and the resonant stream line (thick lines).

$$d_0 b_{\psi 3} + d_1 b_{\psi 2} + (d_2 - \gamma_0 \partial_\Upsilon^2) b_{\psi 1} + (d_3 - \gamma_1 \Upsilon \partial_\Upsilon^2) b_{\psi 0} = 2(\chi_{0,1} + \mu_{i,o}) \partial_\Upsilon b_{\psi 0} + 2\mu_{a,o} \partial_\Upsilon b_{\vartheta 2} + 2\mu'_{a,o} \Upsilon \partial_\Upsilon b_{\vartheta 1} + \mu''_{a,o} \Upsilon^2 \partial_\Upsilon b_{\vartheta 0} + (2\mu_{b,o} \partial_\vartheta + 2im\mu_{c,o} + \mu_{d,o}) b_{\vartheta 1} + (2\mu'_{b,o} \partial_\vartheta + 2im\mu'_{c,o} + \mu'_{d,o}) \Upsilon b_{\vartheta 0} + 2im\mu_{g,o} b_{\zeta 1} + 2im\mu'_{g,o} \Upsilon b_{\zeta 0} \quad (6.1)$$

$$d_0 b_{\vartheta 3} + d_1 b_{\vartheta 2} + (d_2 - \gamma_0 \partial_\Upsilon^2) b_{\vartheta 1} + (d_3 - \gamma_1 \Upsilon \partial_\Upsilon^2) b_{\vartheta 0} = 2(\chi_{1,o} + \lambda_{a,o}) \partial_\Upsilon b_{\vartheta 0} + \Omega'_o b_{\psi 1} + \Upsilon \Omega''_o b_{\psi 0} \quad (6.2)$$

$$d_0 b_{\zeta 3} + d_1 b_{\zeta 2} + (d_2 - \gamma_0 \partial_\Upsilon^2) b_{\zeta 1} + (d_3 - \gamma_1 \Upsilon \partial_\Upsilon^2) b_{\zeta 0} = 2(\chi_{1,o} + \rho_{b,o}) \partial_\Upsilon b_{\zeta 0} + 2\rho_{a,o} \partial_\Upsilon b_{\vartheta 0} + \overline{W}'_o b_{\psi 1} + \Upsilon \overline{W}''_o b_{\psi 0} \,, \quad (6.3)$$

introducing

$$\chi_1 := \tfrac{1}{2} \nabla^2 \psi + i(k \nabla\psi \cdot \nabla\vartheta + m \nabla\psi \cdot \nabla\zeta) \,.$$

The operator $d_2 - \gamma_0 \partial_\Upsilon^2 = -\Xi + \frac{1}{2} \Upsilon^2 \Omega''_o (\partial_\vartheta - ik) - (\gamma_0 - \overline{\gamma}_0) \partial_\Upsilon^2$. The solutions of equations (6.1)–(6.3) can be written in the form,

$$b_{\psi 3} = F_{\psi 3}(\Upsilon) e^{ik\vartheta} + G_{\psi 3}(\Upsilon, \vartheta) e^{ik\vartheta} \,, \qquad \overline{G}_{\psi 3} = 0 \quad (6.4)$$

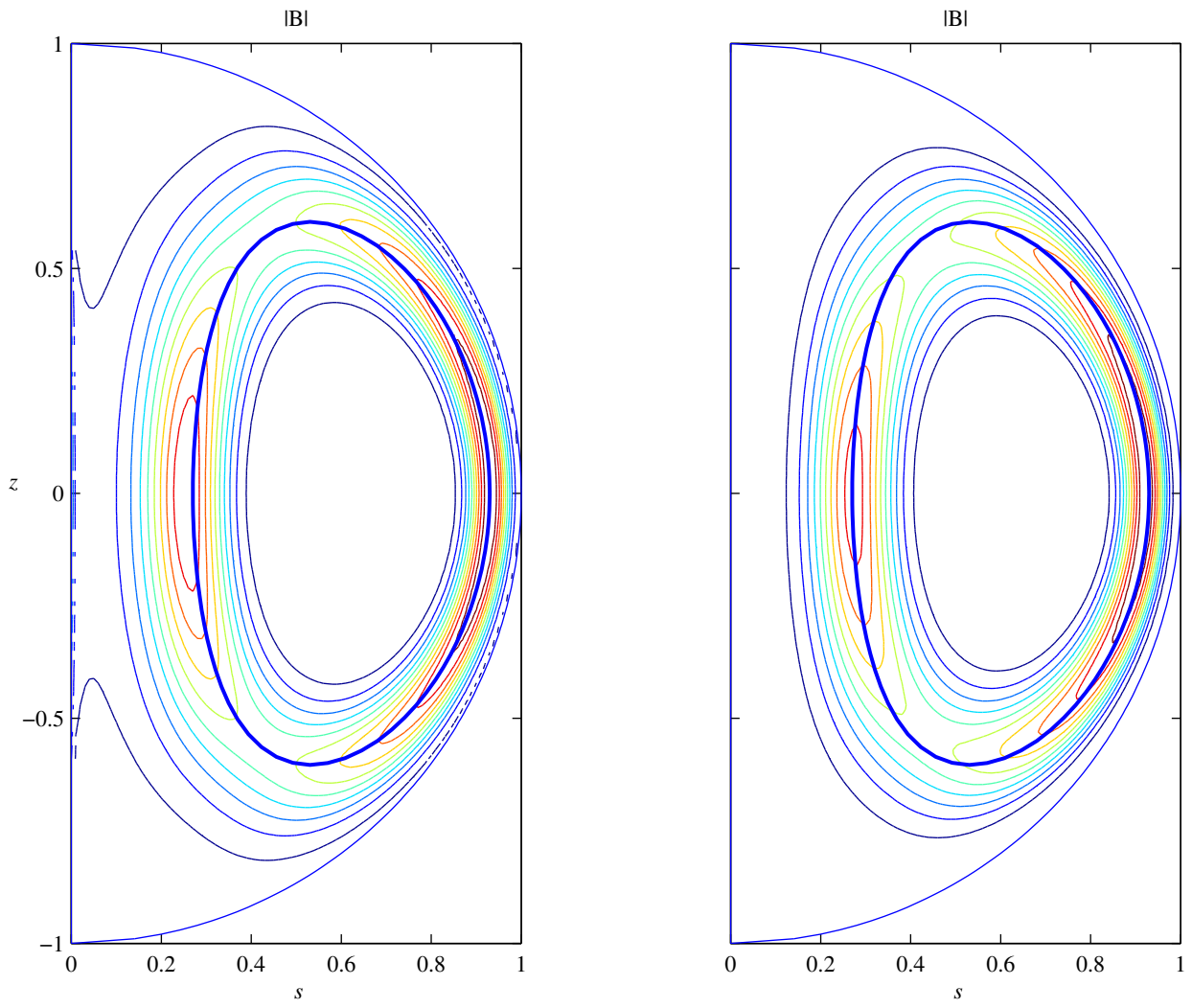

Figure 11: Plots of $|\hat{\mathbf{B}}|$ for the $m = 1$, $k = 1$, $n = 0$ mode of $\mathbf{v}_1$ at $R_{\rm m} = 10^5$, determined asymptotically (left) to leading order and numerically (right), and the resonant stream line (thick lines).

$$b_{\vartheta 3} = F_{\vartheta 3}(\Upsilon)e^{ik\vartheta} + G_{\vartheta 3}(\Upsilon,\vartheta)e^{ik\vartheta}\,, \qquad \overline{G}_{\vartheta 3} = 0 \tag{6.5}$$

$$b_{\zeta 3} = F_{\zeta 3}(\Upsilon)e^{ik\vartheta} + G_{\zeta 3}(\Upsilon,\vartheta)e^{ik\vartheta}\,, \qquad \overline{G}_{\zeta 3} = 0\,. \tag{6.6}$$

Projecting equations (6.1)–(6.3) onto $e^{ik\vartheta}$ and using (2.11) gives

$$\begin{aligned}
\Xi F_{\psi 1} + 2i\overline{\alpha}_o F_{\vartheta 1} &= (p_3 + i\omega_3 + \tfrac{1}{6}i\Pi_o'''\Upsilon^3 - \overline{\gamma}_1\Upsilon\partial_\Upsilon^2)F_{\psi 0} - 2(\overline{\chi}_{1,o} + \overline{\mu}_{i,o})F_{\psi 0}' - 2i\overline{\alpha}_o'\Upsilon F_{\vartheta 0}\\
\Xi F_{\vartheta 1} + \Omega_o' F_{\psi 1} &= (p_3 + i\omega_3 + \tfrac{1}{6}i\Pi_o'''\Upsilon^3 - \overline{\gamma}_1\Upsilon\partial_\Upsilon^2)F_{\vartheta 0} - 2(\overline{\chi}_{1,o} + \overline{\lambda}_{a,o})F_{\vartheta 0}' - \Upsilon\Omega_o'' F_{\psi 0}\\
\Xi F_{\zeta 1} + \overline{W}_o' F_{\psi 1} &= (p_3 + i\omega_3 + \tfrac{1}{6}i\Pi_o'''\Upsilon^3 - \overline{\gamma}_1\Upsilon\partial_\Upsilon^2)F_{\zeta 0} - 2\overline{\chi}_{1,o}F_{\zeta 0}' - 2\overline{\rho}_{a,o}F_{\vartheta 0}' - \Upsilon\overline{W}_o'' F_{\psi 0}\,,
\end{aligned}$$

since $\overline{G_{\psi 1}'} = 0$, $\overline{G_{\psi 1}''} = 0$, $\overline{\mu}_{a,o} = \overline{\mu}_{a,o}' = \overline{\mu}_{a,o}'' = 0$, $\overline{\mu}_{d,o} = \overline{\mu}_{d,o}' = 0$, $\overline{\mu}_{g,o} = \overline{\mu}_{g,o}' = 0$, $\overline{\rho}_{b,o} = 0$. The primes on the G functions denote differentiation with respect to Υ. Note from (2.37) and (2.55),

$$\overline{\gamma_0 G_{\psi 1}''} + 2\overline{\mu_{a,o}G_{\vartheta 2}'} = \frac{2F_{\vartheta 0}'''}{\Omega_o}(\overline{\gamma_0\widehat{\mu}_{a,o} + \widehat{\gamma}_0\mu_{a,o}}) = 0\,.$$

In vector form the projected equations are

$$\mathbf{L}\mathbf{F}_1 = \{(p_3 + i\omega_3)y_n + \tfrac{1}{6}i\Pi_o'''\Upsilon^3 y_n - \overline{\gamma}_1\Upsilon y_n'' - 2\overline{\chi}_{1,o}y_n'\}\mathbf{a} - \Upsilon y_n\mathbf{a}_1 - 2y_n'\mathbf{a}_2\,, \tag{6.7}$$

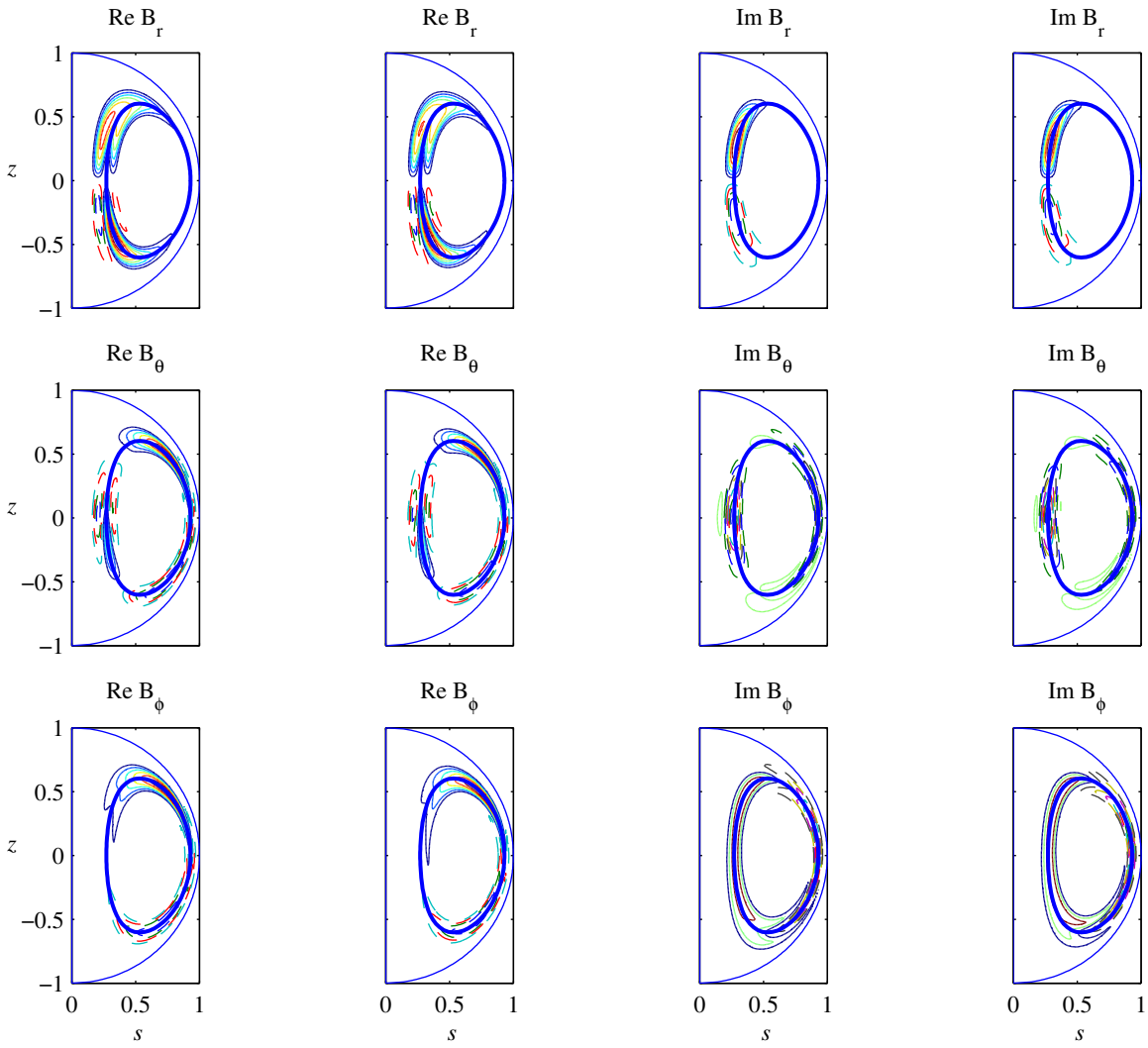

Figure 12: Plots of the real and imaginary parts of $\hat{B}_r$, $\hat{B}_\theta$, $\hat{B}_\phi$ for the $m = 1$, $k = 1$, $n = 0$ mode of $\mathbf{v}_1$ at $R_\mathrm{m} = 5\times10^5$, determined asymptotically (left) to leading order and numerically (right), and the resonant stream line (thick lines).

where $\mathbf{L}$ is defined in (2.44), $\mathbf{F}_1 := (F_{\psi1}, F_{\vartheta1}, F_{\zeta1})^T$ and

$$\mathbf{a}_1 := [2i\overline{\alpha}'_o\Omega'_o, -\Omega''_o\xi_n, -\overline{W}''_o\xi_n]^T\,, \quad \mathbf{a}_2 := [-\overline{\mu}_{i,o}\xi_n, \overline{\lambda}_{a,o}\Omega'_o, \overline{\rho}_{a,o}\Omega'_o]^T\,. \tag{6.8}$$

The primes on y_n indicate derivatives with respect to Υ.

We next express the derivatives and terms multiplied by Υ on the right side of (6.7) in terms of parabolic cylinder functions of different orders by using the recurrence relations,

$$y'_n = \tfrac{1}{2}\kappa^{-1}(ny_{n-1} - y_{n+1})\,, \qquad \Upsilon y_n = \kappa(ny_{n-1} + y_{n+1})\,, \tag{6.9}$$

which are derived from the parabolic cylinder function recurrence relations, $(d/dz + z/2)D_n(z) = nD_{n-1}(z)$, $(d/dz - z/2)D_n(z) = -D_{n+1}(z)$. Iteration yields equations (B.1)–(B.5) in Appendix B. Thus (6.7) becomes

$$\mathbf{L}\mathbf{F}_1 = \sum_{j=-3}^{3}{}' \mathbf{g}_{n,j}\, y_{n+j}\,, \tag{6.10}$$

where the prime on the summation sign indicates summation over every second index. The vectors $\mathbf{g}_{n,j}$ are given by

$$\mathbf{g}_{n,0} = (p_3 + i\omega_3)\mathbf{a}$$

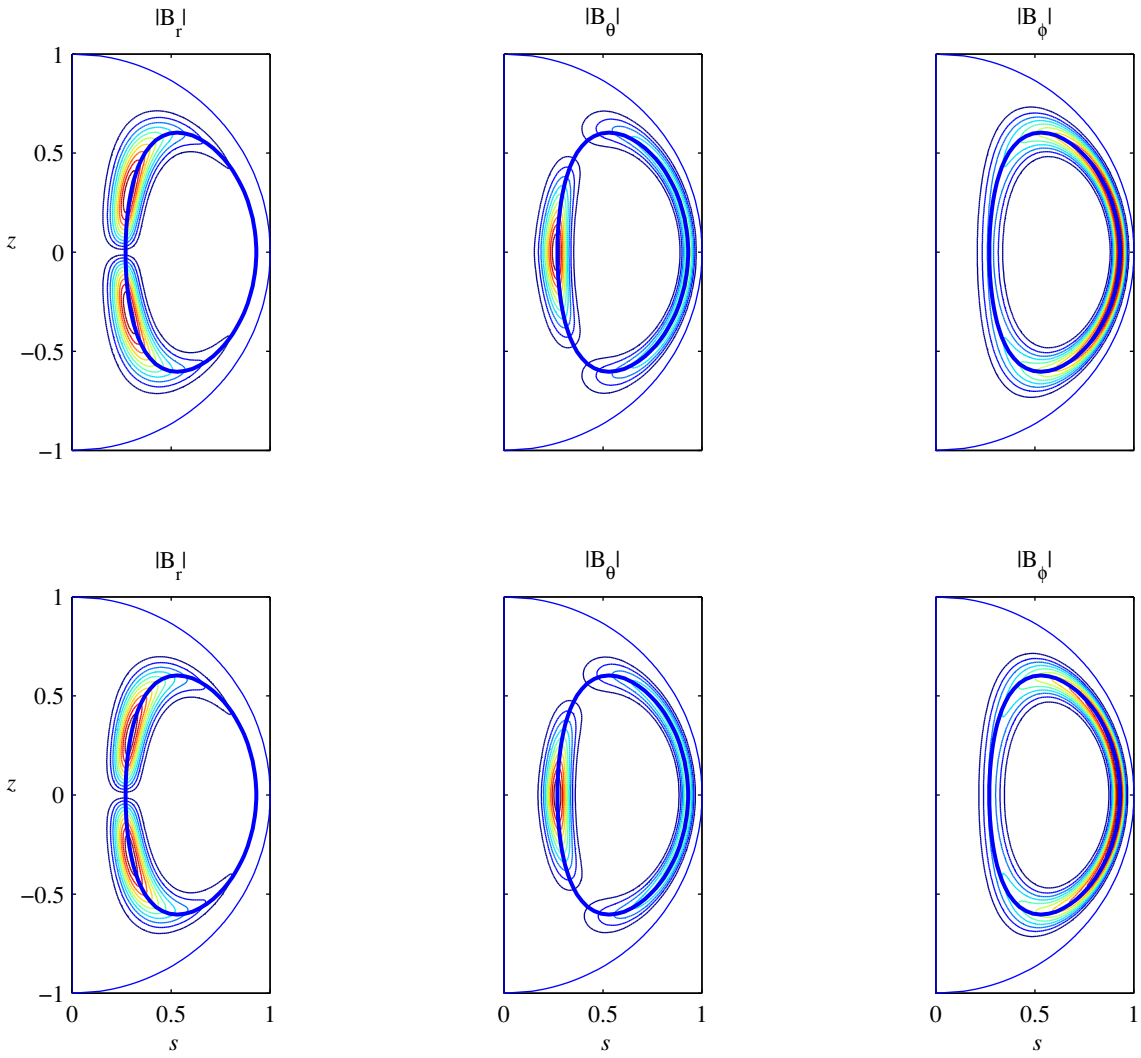

Figure 13: Plots of $|\hat{B}_r|$, $|\hat{B}_\theta|$, $|\hat{B}_\phi|$ for the $m=1$, $k=1$, $n=0$ mode of $\mathbf{v}_1$ at $R_\mathrm{m}=5\times10^5$, determined asymptotically (left) to leading order and numerically (right), and the resonant stream line (thick lines).

$$
\begin{aligned}
\mathbf{g}_{n,-3} &= \tfrac{1}{4}n(n-1)(n-2)(\tfrac{1}{3}\overline{\gamma}_0\Pi_o'''/\Pi_o''-\overline{\gamma}_1)\,\kappa^{-1}\mathbf{a}\\
\mathbf{g}_{n,-1} &= \tfrac{1}{4}[n^2\overline{\gamma}_0\Pi_o'''/\Pi_o''+n(n-2)\overline{\gamma}_1-4n\overline{\chi}_{1,o}]\kappa^{-1}\mathbf{a}-n\kappa\mathbf{a}_1-n\kappa^{-1}\mathbf{a}_2\\
\mathbf{g}_{n,1} &= \tfrac{1}{4}[(n+1)\overline{\gamma}_0\Pi_o'''/\Pi_o''+(n+3)\overline{\gamma}_1+4\overline{\chi}_{1,o}]\kappa^{-1}\mathbf{a}-\kappa\mathbf{a}_1+\kappa^{-1}\mathbf{a}_2\\
\mathbf{g}_{n,3} &= \tfrac{1}{4}(\tfrac{1}{3}\overline{\gamma}_0\Pi_o'''/\Pi_o''-\overline{\gamma}_1)\,\kappa^{-1}\mathbf{a}\,,
\end{aligned}
$$

since $i\kappa^4=\overline{\gamma}_0/2\Pi_o''$. We assume a solution to (6.7) of the form

$$
\mathbf{F}_1=\sum_{j=-3}^{3}{}'\,\mathbf{b}_{n,j}\,y_{n+j}\,. \tag{6.11}
$$

By (6.10) the coefficient vectors in (6.11) are determined from

$$
\mathbf{L}_{n+j}\mathbf{b}_{n,j}=\mathbf{g}_{n,j}\,,\qquad j=0,\pm1,\pm3\,, \tag{6.12}
$$

where $\mathbf{L}_{n+j}$ is defined in (2.47)(b). When $j\neq0$ the determination of $\mathbf{b}_{n,j}$ is straightforward, since $\mathbf{L}_{n+j}$ is invertible,

$$
\mathbf{L}(\xi)^{-1}=\frac{1}{\xi^2-\xi_n^2}\begin{pmatrix}\xi & -2i\overline{\alpha}_o & 0\\ -\Omega_o' & \xi & 0\\ -\overline{W}_o' & 2i\overline{\alpha}_o\overline{W}_o'/\xi & (\xi^2-\xi_n^2)/\xi\end{pmatrix}. \tag{6.13}
$$

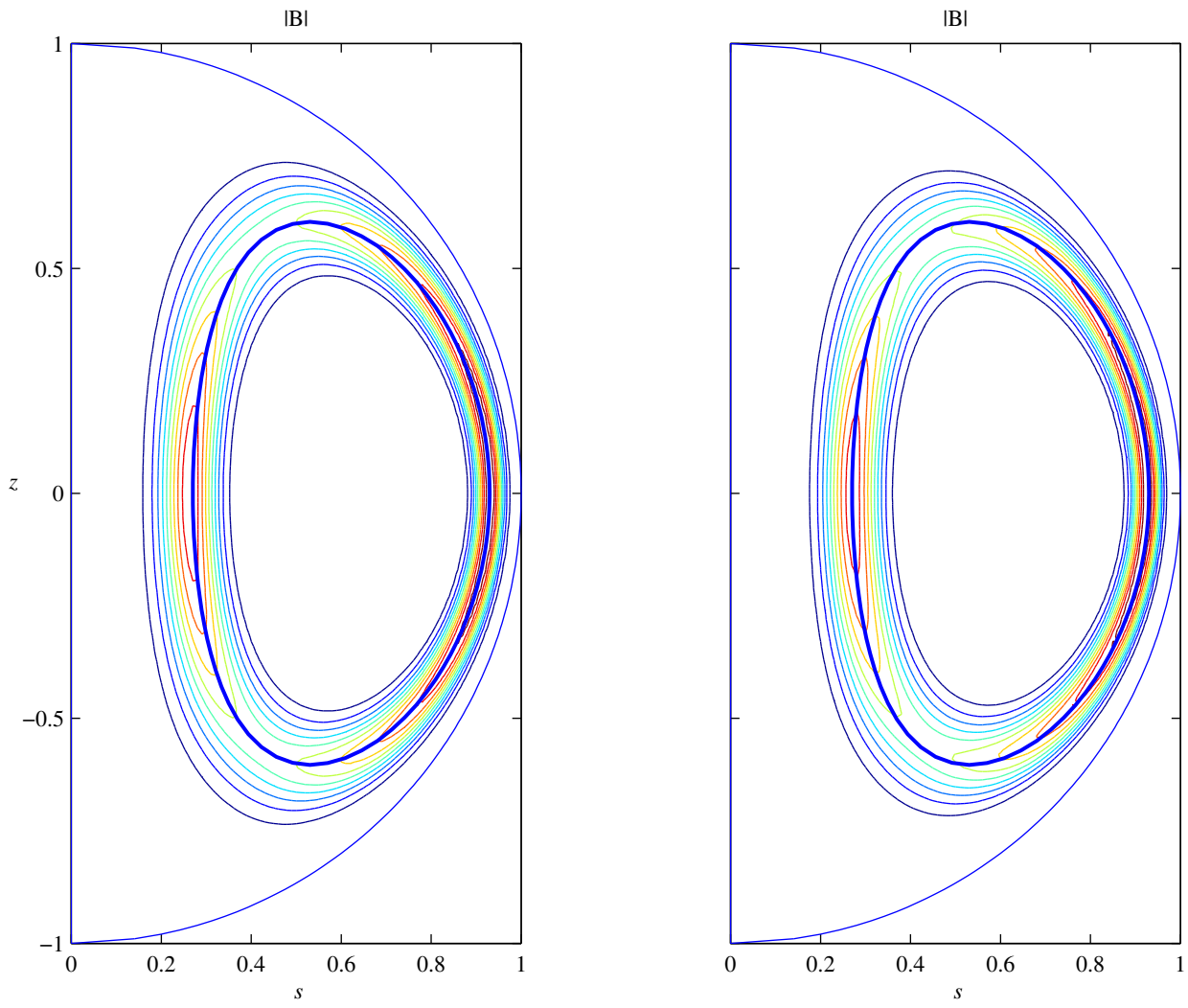

Figure 14: Plots of $|\hat{\mathbf{B}}|$ for the $m=1$, $k=1$, $n=0$ mode of $\mathbf{v}_1$ at $R_{\rm m}=5\times10^5$, determined asymptotically (left) to leading order and numerically (right), and the resonant stream line (thick lines).

In particular,

$$\mathbf{L}(\xi)^{-1}\mathbf{a}=\frac{\mathbf{a}}{\xi-\xi_n}\,,\qquad \xi_{n+j}-\xi_n=-j\overline{\gamma}_0\kappa^{-2}\,. \tag{6.14}$$

Thus

$$\mathbf{L}_{n\pm1}^{-1}\mathbf{a}=\mp\frac{\kappa^2}{\overline{\gamma}_0}\mathbf{a}\,,\qquad \mathbf{L}_{n\pm3}^{-1}\mathbf{a}=\mp\frac{\kappa^2}{3\overline{\gamma}_0}\mathbf{a}\,,$$

$$\mathbf{L}_{n\pm1}^{-1}\mathbf{a}_1=\frac{1}{\xi_{n\pm1}^2-\xi_n^2}\begin{pmatrix}2i\overline{\alpha}_o'\Omega_o'\xi_{n\pm1}+2i\overline{\alpha}_o\Omega_o''\xi_n\\ -2i\overline{\alpha}_o'(\Omega_o')^2-\Omega_o''\xi_n\xi_{n\pm1}\\ -2i\overline{\alpha}_o'\Omega_o'\overline{W}_o'-2i\overline{\alpha}_o\overline{W}_o'\Omega_o''\xi_n/\xi_{n\pm1}-(\xi_{n\pm1}^2-\xi_n^2)\overline{W}_o''\xi_n/\xi_{n\pm1}\end{pmatrix}\,, \tag{6.15}$$

and

$$\mathbf{L}_{n\pm1}^{-1}\mathbf{a}_2=\frac{1}{\xi_{n\pm1}^2-\xi_n^2}\begin{pmatrix}-\overline{\mu}_{i,o}\xi_n\xi_{n\pm1}-2i\overline{\alpha}_o\overline{\lambda}_{a,o}\Omega_o'\\ \Omega_o'\overline{\mu}_{i,o}\xi_n+\overline{\lambda}_{a,o}\Omega_o'\xi_{n\pm1}\\ \overline{W}_o'\overline{\mu}_{i,o}\xi_n+2i\overline{\alpha}_o\overline{W}_o'\Omega_o'\overline{\lambda}_{a,o}/\xi_{n\pm1}+(\xi_{n\pm1}^2-\xi_n^2)\overline{\rho}_{a,o}\Omega_o'/\xi_{n\pm1}\end{pmatrix}\,. \tag{6.16}$$

Hence the solution vectors in (6.11) determined from (6.12) for $j\neq0$ are

$$\mathbf{b}_{n,-3}=\tfrac{1}{12}n(n-1)(n-2)(\tfrac{1}{3}\overline{\gamma}_0\Pi_o'''/\Pi_o''-\overline{\gamma}_1)\frac{\kappa}{\overline{\gamma}_0}\,\mathbf{a} \tag{6.17}$$

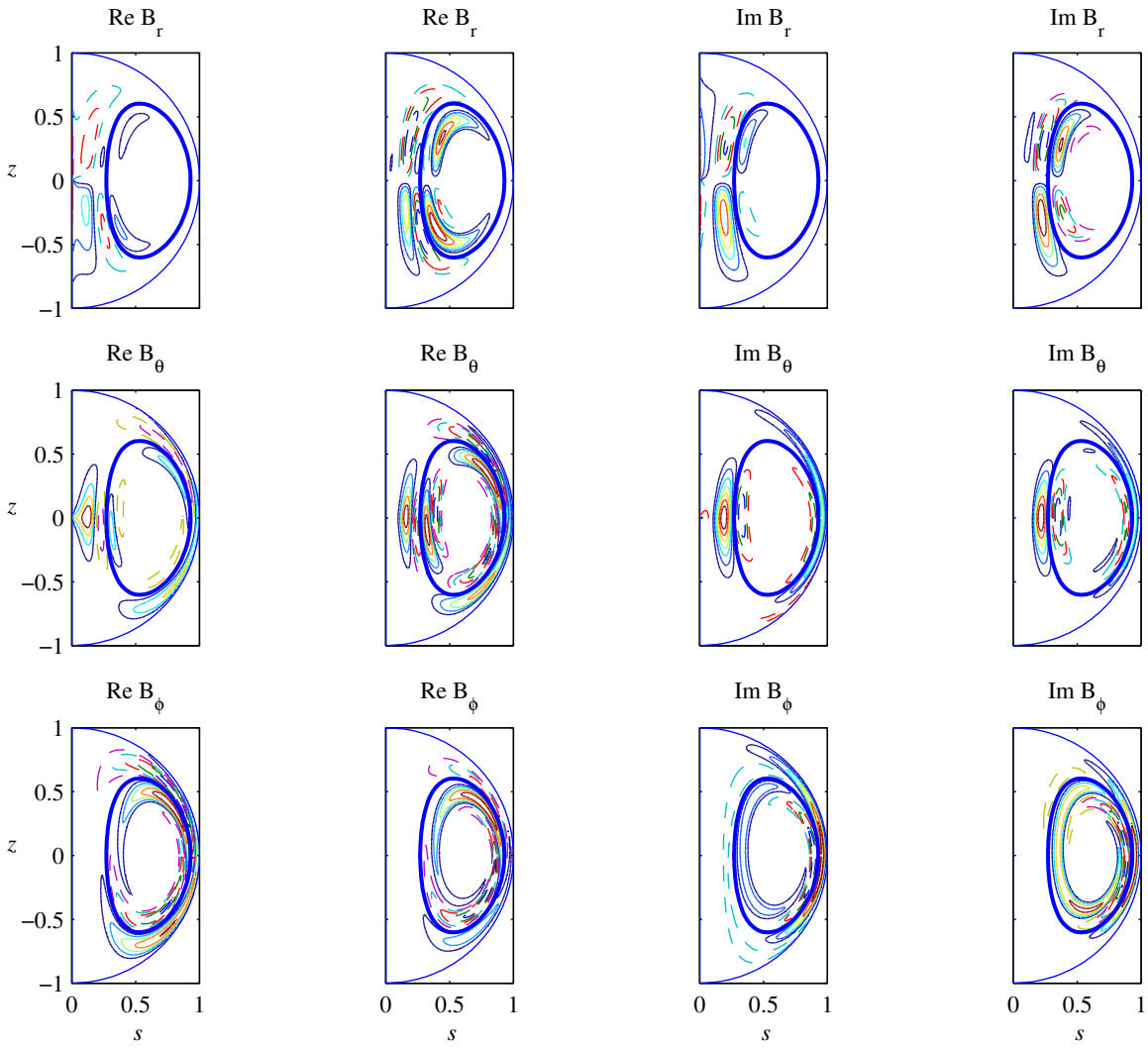

Figure 15: Plots of the real and imaginary parts of $\hat{B}_r$, $\hat{B}_\theta$, $\hat{B}_\phi$ for the $m = 1$, $k = 1$, $n = 1$ mode of $\mathbf{v}_1$ at $R_\mathrm{m} = 10^5$, determined asymptotically (left) to leading order and numerically (right), and the resonant stream line (thick lines).

$$\mathbf{b}_{n,-1} = \tfrac{1}{4}[n^2\overline{\gamma}_0\Pi_o'''/\Pi_o'' + n(n-2)\overline{\gamma}_1 - 4n\overline{\chi}_{1,o}]\frac{\kappa}{\overline{\gamma}_0}\mathbf{a} - n\mathbf{L}_{n-1}^{-1}(\kappa\mathbf{a}_1 + \kappa^{-1}\mathbf{a}_2) \tag{6.18}$$

$$\mathbf{b}_{n,1} = -\tfrac{1}{4}[(n+1)\overline{\gamma}_0\Pi_o'''/\Pi_o'' + (n+3)\overline{\gamma}_1 + 4\overline{\chi}_{1,o}]\frac{\kappa}{\overline{\gamma}_0}\mathbf{a} - \mathbf{L}_{n+1}^{-1}(\kappa\mathbf{a}_1 - \kappa^{-1}\mathbf{a}_2) \tag{6.19}$$

$$\mathbf{b}_{n,3} = -\tfrac{1}{12}(\tfrac{1}{3}\overline{\gamma}_0\Pi_o'''/\Pi_o'' - \overline{\gamma}_1)\frac{\kappa}{\overline{\gamma}_0}\mathbf{a}\,. \tag{6.20}$$

In the $j = 0$ case the matrix $\mathbf{L}_n$ is singular. It satisfies $\mathbf{c}^T\mathbf{L}_n = \mathbf{0}$, where

$$\mathbf{c} := [-\Omega_o'\,, \xi_n\,, 0]^T/2\Omega_o'\xi_n \tag{6.21}$$

and $\mathbf{c}^T\mathbf{a} = 1$. Thus the $j = 0$ equation in (6.11) furnishes us with the solvability condition $\mathbf{c}^T\mathbf{g}_{n,0} = 0$, i.e. $p_3 + i\omega_3 = 0$, which ensures that $\mathbf{g}_{n,0} = \mathbf{0}$ and that $\mathbf{b}_{n,0}$ is a constant multiple of $\mathbf{a}$. Thus the term $\mathbf{b}_{n,0}\,y_n$ can be absorbed into the order ε^0 solution. Without loss of generality we can set $\mathbf{b}_{n,0} = \mathbf{0}$. To complete the derivation of the magnetic field to order ε^1, it remains to show that the ε^1 solenoidal condition is satisfied. Equation (2.40) reduces to

$$ikF_{\vartheta 1} + imF_{\zeta 1} = \xi_n y_n'\,, \tag{6.22}$$

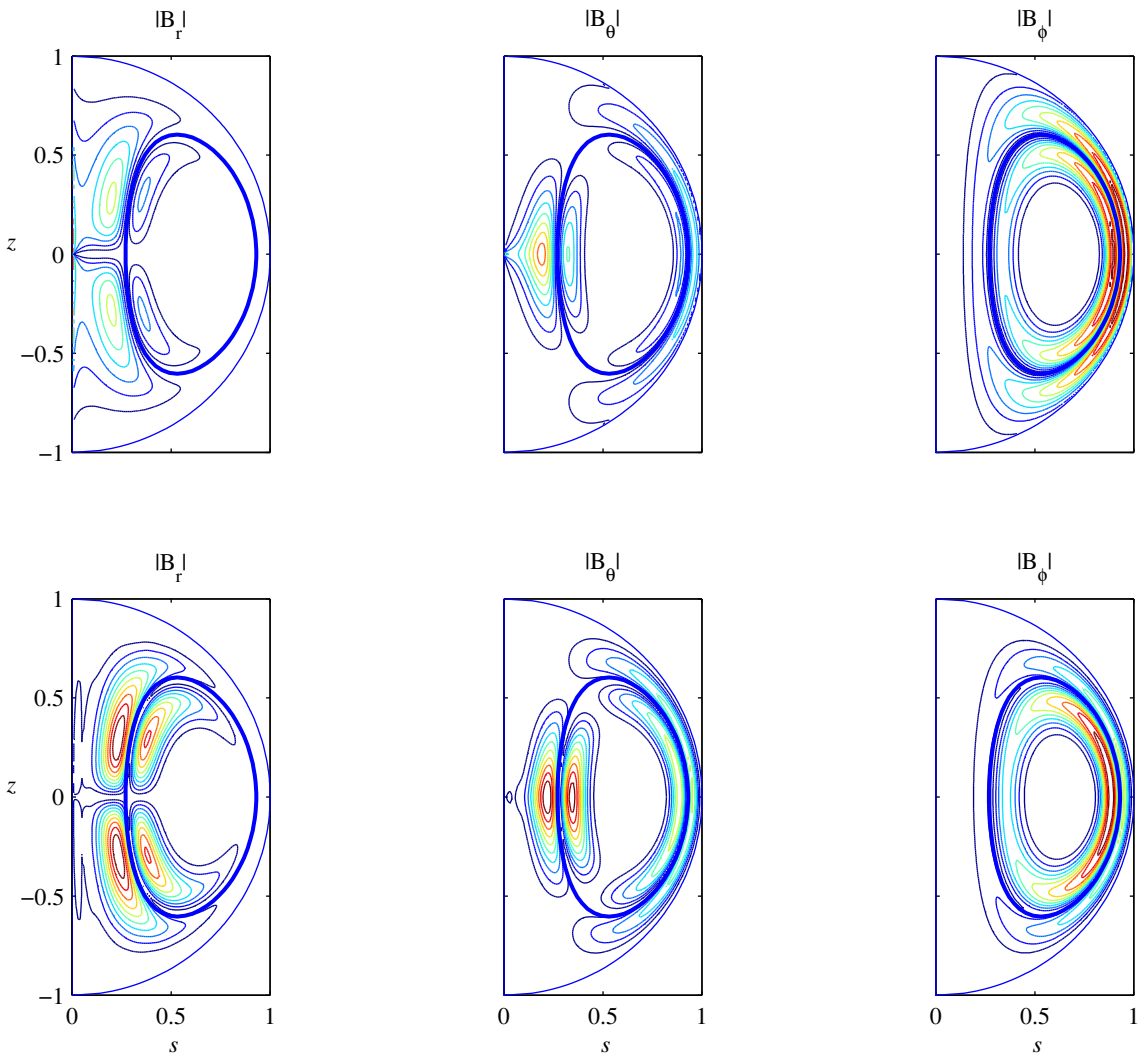

Figure 16: Plots of $|\hat{B}_r|$, $|\hat{B}_\theta|$, $|\hat{B}_\phi|$ for the $m = 1$, $k = 1$, $n = 1$ mode of $\mathbf{v}_1$ at $R_\mathrm{m} = 10^5$, determined asymptotically (left) to leading order and numerically (right), and the resonant stream line (thick lines).

using (2.46) and (2.50). Substituting (6.10) and equating coefficients of y_n, using (6.9)(a), yields

$$i\mathbf{k}\cdot[\mathbf{b}_{n,-3},\mathbf{b}_{n,-1},\mathbf{b}_{n,1},\mathbf{b}_{n,3}] = [0,\tfrac{1}{2}n\kappa^{-1}\xi_n,-\tfrac{1}{2}\kappa^{-1}\xi_n,0]\,,$$

where $\mathbf{k} = k\mathbf{1}_\vartheta + m\mathbf{1}_\zeta$. Substituting (6.17)–(6.20) and noting $(k\mathbf{1}_\vartheta + m\mathbf{1}_\zeta)\cdot\mathbf{a} = 0$ by the resonance condition (2.35)(b), the first and last equations are satisfied, and the remaining two equations reduce to

$$i\mathbf{k}\cdot\mathbf{L}_{n\mp1}^{-1}(\kappa\mathbf{a}_1 \pm \kappa^{-1}\mathbf{a}_2) = \mp\tfrac{1}{2}\kappa^{-1}\xi_n\,.$$

But a simple calculation gives $\mathbf{k}\cdot\mathbf{L}(\xi)^{-1} = \xi^{-1}(k\mathbf{1}_\vartheta + m\mathbf{1}_\zeta)$. Thus

$$\mathbf{k}\cdot\mathbf{L}(\xi)^{-1}\mathbf{a}_1 = -\xi^{-1}\xi_n\Pi_o''\,,\qquad \mathbf{k}\cdot\mathbf{L}(\xi)^{-1}\mathbf{a}_2 = \xi^{-1}(k\overline{\lambda}_{a,o} + m\overline{\rho}_{a,o})\Omega_o'\,.$$

Hence, noting $\xi_{n\pm1} = \xi_n \mp \overline{\gamma}_0\kappa^{-2}$,

$$\tfrac{1}{2}\xi_n^2 \mp (\tfrac{1}{2}\overline{\gamma}_0\kappa^{-2} - i\kappa^2\xi_n\Pi_o'') + i(k\overline{\lambda}_{a,o} + m\overline{\rho}_{a,o})\Omega_o' = 0\,.$$

By (2.46)(c) these two conditions reduce to the single condition,

$$\xi_n^2 = -2i(k\overline{\lambda}_{a,o} + m\overline{\rho}_{a,o})\Omega_o'\,,$$

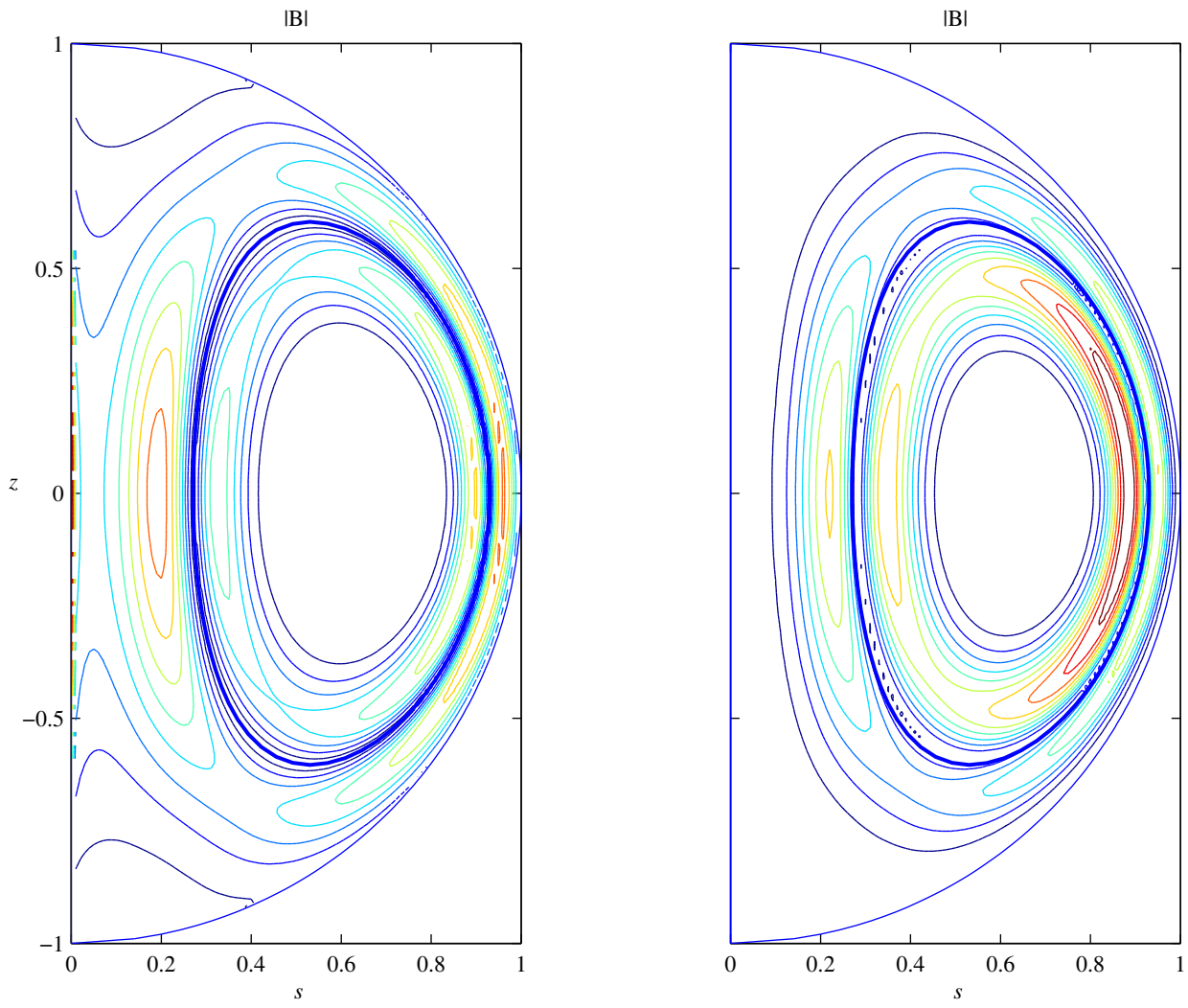

Figure 17: Plots of $|\hat{\mathbf{B}}|$ for the $m = 1$, $k = 1$, $n = 1$ mode of $\mathbf{v}_1$ at $R_\mathrm{m} = 10^5$, determined asymptotically (left) to leading order and numerically (right), and the resonant stream line (thick lines).

Thus, since $\xi_n^2 = 2i\overline{\alpha}_o\Omega_o'$, condition(6.22) is equivalent to

$$\overline{\alpha}_o = -(k\overline{\lambda}_{a,o} + m\overline{\rho}_{a,o})\,.$$

From

$$k\lambda_a + m\rho_a = \nabla(k\vartheta + m\zeta)\cdot(\nabla\psi\cdot\nabla\mathbf{f}_\vartheta)\,,$$
$$\alpha := k\mu_b + m\mu_c = \nabla\psi\cdot[\nabla(k\vartheta + m\zeta)\cdot\nabla\mathbf{f}_\vartheta]\,,$$
$$\mathbf{f}_\vartheta\cdot\nabla\psi = \partial_\vartheta\psi = 0$$

and

$$\mathbf{f}_\vartheta\cdot\nabla(k\vartheta + m\zeta) = k\,,$$

it follows that

$$\alpha + (k\lambda_a + m\rho_a) = -\mathbf{f}_\vartheta\cdot\nabla[\nabla\psi\cdot\nabla(k\vartheta + m\zeta)] = -\partial_\vartheta[\nabla\psi\cdot\nabla(k\vartheta + m\zeta)]\,.$$

Hence

$$\overline{\alpha} = -(k\overline{\lambda}_a + m\overline{\rho}_a)$$

and the solenoidal condition (**??**) is satisfied.

Only the particular solution $G_{\vartheta 3}$ to (6.4)–(6.6) is required below,

$$\Omega_o G_{\vartheta 3} + \Omega_o' \Upsilon G_{\vartheta 2} = \widehat{\gamma}_0 F_{\vartheta 1}'' + \widehat{\gamma}_1 \Upsilon F_{\vartheta 0}'' + 2(\widehat{\chi}_{1,o} + \widehat{\lambda}_{a,o}) F_{\vartheta 0}' + \Omega_o' \widehat{G}_{\psi 1} \,.$$

Substituting for $G_{\psi 1}$ from (2.37) and $G_{\vartheta 2}$ from (2.55),

$$\Omega_o G_{\vartheta 3} = -\frac{\Omega_o'}{\Omega_o}\widehat{\gamma}_0 \Upsilon F_{\vartheta 0}'' + \widehat{\gamma}_0 F_{\vartheta 1}'' + \widehat{\gamma}_1 \Upsilon F_{\vartheta 0}'' + 2(\widehat{\chi}_{1,o} + \widehat{\lambda}_{a,o}) F_{\vartheta 0}' + 2\frac{\Omega_o'}{\Omega_o}\widehat{\mu}_{a,o} F_{\vartheta 0}' \tag{6.23}$$

6.2 The $\mathcal{O}(\varepsilon^4)$ Growth Rate and Angular Frequency

Finally we consider the ε^4-equations. At this order we are only interested in finding the solvability condition which determines p_4 and ω_4. Only the ψ and ϑ equations are required,

$$\begin{aligned} d_0 b_{\psi 4} + d_1 b_{\psi 3} + (d_2 - \gamma_0 \partial_\Upsilon^2) b_{\psi 2} + (d_3 - \gamma_1 \Upsilon \partial_\Upsilon^2) b_{\psi 1} + (d_4 - \tfrac{1}{2}\gamma_2 \Upsilon^2 \partial_\Upsilon^2) b_{\psi 0} = \\ 2(\chi_1 + \mu_i)_o \partial_\Upsilon b_{\psi 1} + 2(\chi_1 + \mu_i)_o' \Upsilon \partial_\Upsilon b_{\psi 0} \\ + (\chi_2 + 2ik\mu_j + 2im\mu_k + \mu_l)_o b_{\psi 0} + 2\mu_{a,o} \partial_\Upsilon b_{\vartheta 3} + 2\mu_{a,o}' \Upsilon \partial_\Upsilon b_{\vartheta 2} + \mu_{a,o}'' \Upsilon^2 \partial_\Upsilon b_{\vartheta 1} + \tfrac{1}{3}\mu_{a,o}''' \Upsilon^3 \partial_\Upsilon b_{\vartheta 0} \\ + (2\mu_b \partial_\vartheta + 2im\mu_c + \mu_d)_o b_{\vartheta 2} + (2\mu_b \partial_\vartheta + 2im\mu_c + \mu_d)_o' \Upsilon b_{\vartheta 1} + \tfrac{1}{2}(2\mu_b \partial_\vartheta + 2im\mu_c + \mu_d)_o'' \Upsilon^2 b_{\vartheta 0} \\ + 2im\mu_{g,o} b_{\zeta 2} + 2im\mu_{g,o}' \Upsilon b_{\zeta 1} + im\mu_{g,o}'' \Upsilon^2 b_{\zeta 0} \end{aligned} \tag{6.24}$$

and

$$\begin{aligned} d_0 b_{\vartheta 4} + d_1 b_{\vartheta 3} + (d_2 - \gamma_0 \partial_\Upsilon^2) b_{\vartheta 2} + (d_3 - \gamma_1 \Upsilon \partial_\Upsilon^2) b_{\vartheta 1} + (d_4 - \tfrac{1}{2}\gamma_2 \Upsilon^2 \partial_\Upsilon^2) b_{\vartheta 0} = \\ 2(\chi_1 + \lambda_a)_o \partial_\Upsilon b_{\vartheta 1} + 2(\chi_1 + \lambda_a)_o' \Upsilon \partial_\Upsilon b_{\vartheta 0} + (\chi_2 + 2ik\lambda_b + 2im\lambda_c + \lambda_d)_o b_{\vartheta 0} \\ + 2im\lambda_{g,o} b_{\zeta 0} + \Omega_o' b_{\psi 2} + \Upsilon \Omega_o'' b_{\psi 1} + \tfrac{1}{2}\Omega_o''' \Upsilon^2 b_{\psi 0} \,, \end{aligned} \tag{6.25}$$

where

$$\chi_2 := -k^2 |\nabla\vartheta|^2 - m^2 |\nabla\zeta|^2 - 2mk \nabla\vartheta \cdot \nabla\zeta + i(k\nabla^2\vartheta + m\nabla^2\zeta) \,.$$

We project onto $e^{ik\vartheta}$, noting (2.11) and $\overline{\mu}_{a,o} = \overline{\mu}_{a,o}' = \overline{\mu}_{a,o}'' = \overline{\mu}_{a,o}''' = 0$, $\overline{\mu}_{d,o} = \overline{\mu}_{d,o}' = \overline{\mu}_{d,o}'' = 0$, $\overline{\mu}_{g,o} = \overline{\mu}_{g,o}' = \overline{\mu}_{g,o}'' = 0$. From equation (6.24) we obtain

$$\begin{aligned} &- \Xi F_{\psi 2} - 2i\overline{\alpha}_o F_{\vartheta 2} = \overline{\gamma_0 G_{\psi 2}''} - \tfrac{1}{6} i\Upsilon^3 \Pi_o''' F_{\psi 1} + \overline{\gamma}_1 \Upsilon F_{\psi 1}'' + \overline{\gamma_1 G_{\psi 1}''}\Upsilon - (p_4 + i\omega_4 + \tfrac{1}{24} i\Upsilon^4 \Pi_o'''') F_{\psi 0} + \tfrac{1}{2}\overline{\gamma}_2 \Upsilon^2 F_{\psi 0}'' \\ &+ 2(\overline{\chi}_{1,o} + \overline{\mu}_{i,o}) F_{\psi 1}' + 2\overline{(\chi_{1,o} + \mu_{i,o}) G_{\psi 1}'} + 2\overline{(\nabla\psi \cdot \nabla\vartheta)_o \partial_\vartheta G_{\psi 1}'} + 2(\overline{\chi}_{1,o}' + \overline{\mu}_{i,o}')\Upsilon F_{\psi 0}' + (\overline{\chi}_{2,o} + 2ik\overline{\mu}_{j,o} + 2im\overline{\mu}_{k,o} + \overline{\mu}_{l,o}) F_{\psi 0} \\ &+ 2\overline{\mu_{a,o} G_{\vartheta 3}'} + 2\overline{\mu_{a,o}' G_{\vartheta 2}'}\Upsilon + \overline{(2i\alpha_o + \mu_{d,o}) G_{\vartheta 2}} + 2\overline{\mu_{b,o} \partial_\vartheta G_{\vartheta 2}} + 2i\overline{\alpha}_o' \Upsilon F_{\vartheta 1} + i\overline{\alpha}_o'' \Upsilon^2 F_{\vartheta 0} + 2im\overline{\mu_{g,o} G_{\zeta 2}} \end{aligned} \tag{6.26}$$

and from (6.25),

$$\begin{aligned} &- \Xi F_{\vartheta 2} - \Omega_o' F_{\psi 2} = \overline{\gamma_0 G_{\vartheta 2}''} - \tfrac{1}{6} i\Upsilon^3 \Pi_o''' F_{\vartheta 1} + \overline{\gamma_1}\Upsilon F_{\vartheta 1}'' - (p_4 + i\omega_4 + \tfrac{1}{24} i\Upsilon^4 \Pi_o'''') F_{\vartheta 0} + \tfrac{1}{2}\overline{\gamma}_2 \Upsilon^2 F_{\vartheta 0}'' \\ &+ 2(\overline{\chi}_{1,o} + \overline{\lambda}_{a,o}) F_{\vartheta 1}' + 2(\overline{\chi}_{1,o}' + \overline{\lambda}_{a,o}')\Upsilon F_{\vartheta 0}' + (\overline{\chi}_{2,o} + 2ik\overline{\lambda}_{b,o} + 2im\overline{\lambda}_{c,o} + \overline{\lambda}_{d,o}) F_{\vartheta 0} \\ &+ 2im\overline{\lambda}_{g,o} F_{\zeta 0} + \Upsilon \Omega_o'' F_{\psi 1} + \tfrac{1}{2}\Omega_o''' \Upsilon^2 F_{\psi 0} \,, \end{aligned} \tag{6.27}$$

Substituting for $G_{\psi 1}$, $G_{\psi 2}$, $G_{\vartheta 2}$, $G_{\zeta 2}$, $G_{\vartheta 3}$ from (2.37), (2.54)–(2.56), (6.23), respectively, into (6.26) gives

$$\begin{aligned} &- \Xi F_{\psi 2} - 2i\overline{\alpha}_o F_{\vartheta 2} = \{ -\frac{2\Omega_o'}{\Omega_o}\overline{\gamma_0 \widehat{\mu}_{a,o}} (\Upsilon F_{\vartheta 0}')'' + \overline{\gamma_0 \widehat{\gamma}_0} F_{\psi 0}'''' + 2\overline{\gamma_0 \widehat{\mu}_{a,o}} F_{\vartheta 1}''' \\ &\qquad + 2\overline{\gamma_0 \widehat{\mu}_{a,o}'} (\Upsilon F_{\vartheta 0}')'' + \overline{\gamma_0 (2i\widehat{\alpha}_o + \widehat{\mu}_{d,o})} F_{\vartheta 0}'' + 2im\overline{\gamma_0 \widehat{\mu}_{g,o}} F_{\zeta 0}'' \} / \Omega_o \\ &- \tfrac{1}{6} i\Upsilon^3 \Pi_o''' F_{\psi 1} + \overline{\gamma_1}\Upsilon F_{\psi 1}'' + \overline{\gamma_1 \widehat{\mu}_{a,o}} \Upsilon \frac{2F_{\vartheta 0}'''}{\Omega_o} - (p_4 + i\omega_4 + \tfrac{1}{24} i\Upsilon^4 \Pi_o'''') F_{\psi 0} + \tfrac{1}{2}\overline{\gamma}_2 \Upsilon^2 F_{\psi 0}'' + 2(\overline{\chi}_{1,o} + \overline{\mu}_{i,o}) F_{\psi 1}' \\ &+ 4\overline{(\chi_{1,o} + \mu_{i,o})\widehat{\mu}_{a,o}} \frac{F_{\vartheta 0}''}{\Omega_o} + 4\overline{(\nabla\psi \cdot \nabla\vartheta)_o \mu_{a,o}} \frac{F_{\vartheta 0}''}{\Omega_o} + 2(\overline{\chi}_{1,o}' + \overline{\mu}_{i,o}')\Upsilon F_{\psi 0}' + (\overline{\chi}_{2,o} + 2ik\overline{\mu}_{j,o} + 2im\overline{\mu}_{k,o} + \overline{\mu}_{l,o}) F_{\psi 0} \\ &\{ -2\overline{\mu_{a,o}\widehat{\gamma}_0} \frac{\Omega_o'}{\Omega_o} (\Upsilon F_{\vartheta 0}'')' + 2\overline{\mu_{a,o}\widehat{\gamma}_0} F_{\vartheta 1}''' + 2\overline{\mu_{a,o}\widehat{\gamma}_1} (\Upsilon F_{\vartheta 0}'')' + 4\overline{\mu_{a,o}(\widehat{\chi}_{1,o} + \widehat{\lambda}_{a,o})} F_{\vartheta 0}'' + 4\overline{\mu_{a,o}\widehat{\widehat{\mu}}_{a,o}} \frac{\Omega_o'}{\Omega_o} F_{\vartheta 0}'' \} / \Omega_o \\ &+ 2\overline{\mu_{a,o}'\widehat{\gamma}_0} \frac{1}{\Omega_o} \Upsilon F_{\vartheta 0}''' + \overline{(2i\alpha_o + \mu_{d,o})\widehat{\gamma}_0} \frac{F_{\vartheta 0}''}{\Omega_o} + 2\overline{\mu_{b,o}\partial_\vartheta \widehat{\gamma}_0} \frac{F_{\vartheta 0}''}{\Omega_o} + 2i\overline{\alpha}_o' \Upsilon F_{\vartheta 1} + i\overline{\alpha}_o'' \Upsilon^2 F_{\vartheta 0} + 2im\overline{\mu_{g,o}\widehat{\gamma}_0} \frac{F_{\zeta 0}''}{\Omega_o} \,. \end{aligned}$$

Using the relations,

$$\begin{aligned}
\overline{\gamma_0\widehat{\mu}_{a,o}} + \overline{\mu_{a,o}\widehat{\gamma}_0} &= 0\\
\overline{\gamma_0\widehat{\gamma}_0} &= 0\\
\overline{\gamma_0\widehat{\mu}'_{a,o}} + \overline{\mu'_{a,o}\widehat{\gamma}_0} &= 0\\
\overline{\gamma_0(2i\widehat{\alpha}_o + \widehat{\mu}_{d,o})} + \overline{(2i\alpha_o + \mu_{d,o})\widehat{\gamma}_0} &= 0\\
\overline{\gamma_0\widehat{\mu}_{g,o}} + \overline{\mu_{g,o}\widehat{\gamma}_0} &= 0\\
\overline{\gamma_1\widehat{\mu}_{a,o}} + \overline{\mu_{a,o}\widehat{\gamma}_1} &= 0\\
\overline{\chi_{1,o}\widehat{\mu}_{a,o}} + \overline{\mu_{a,o}\widehat{\chi}_{1,o}} &= 0\,,
\end{aligned}$$

which follow from the property (2.38)(a) of the operator $\widehat{\ }$, this equation reduces to

$$\begin{aligned}
-\Xi F_{\psi 2} - 2i\overline{\alpha}_o F_{\vartheta 2} = &-\tfrac{1}{6}i\Pi'''_o\Upsilon^3 F_{\psi 1} + \overline{\gamma}_1\Upsilon F''_{\psi 1} - (p_4 + i\omega_4 + \tfrac{1}{24}i\Upsilon^4\Pi''''_o)F_{\psi 0} + \tfrac{1}{2}\overline{\gamma}_2\Upsilon^2 F''_{\psi 0}\\
&+ 2(\overline{\chi}_{1,o} + \overline{\mu}_{i,o})F'_{\psi 1} + 2(\overline{\chi}'_{1,o} + \overline{\mu}'_{i,o})\Upsilon F'_{\psi 0} + (\overline{\chi}_{2,o} + 2ik\overline{\mu}_{j,o} + 2im\overline{\mu}_{k,o} + \overline{\mu}_{l,o})F_{\psi 0}\\
&+ \overline{\chi}_{3,o}F''_{\vartheta 0} + 2i\overline{\alpha}'_o\Upsilon F_{\vartheta 1} + i\overline{\alpha}''_o\Upsilon^2 F_{\vartheta 0} \qquad (6.28)
\end{aligned}$$

where the real quantity χ_3 is defined by

$$\Omega_o\chi_3 := -\frac{2\Omega'}{\Omega}\gamma_0\widehat{\mu}_a + 4\gamma_0\widehat{\mu}'_a + 2\mu_a\widehat{\gamma}_1 + 4\mu_a\widehat{\lambda}_a + 4\mu_a\widehat{\widehat{\mu}}_a\frac{\Omega'}{\Omega} + 2\mu_b\partial_\vartheta\widehat{\gamma}_0 + 4\mu_i\widehat{\mu}_a + 4(\nabla\psi\cdot\nabla\vartheta)\mu_a\,.$$

The ϑ-equation (6.27) becomes

$$\begin{aligned}
-\Xi F_{\vartheta 2} - \Omega'_o F_{\psi 2} = &-\tfrac{1}{6}i\Pi'''_o\Upsilon^3 F_{\vartheta 1} + \overline{\gamma_1}\Upsilon F''_{\vartheta 1} - (p_4 + i\omega_4 + \tfrac{1}{24}i\Upsilon^4\Pi''''_o)F_{\vartheta 0} + \tfrac{1}{2}\overline{\gamma}_2\Upsilon^2 F''_{\vartheta 0}\\
&+ 2(\overline{\chi}_{1,o} + \overline{\lambda}_{a,o})F'_{\vartheta 1} + 2(\overline{\chi}'_{1,o} + \overline{\lambda}'_{a,o})\Upsilon F'_{\vartheta 0} + (\overline{\chi}_{2,o} + 2ik\overline{\lambda}_{b,o} + 2im\overline{\lambda}_{c,o} + \overline{\lambda}_{d,o})F_{\vartheta 0}\\
&+ 2im\overline{\lambda}_{g,o}F_{\zeta 0} + \Upsilon\Omega''_o F_{\psi 1} + \tfrac{1}{2}\Omega'''_o\Upsilon^2 F_{\psi 0}\,. \qquad (6.29)
\end{aligned}$$

Using the y_n recurrence relations (6.9), equations (6.28), (6.29) and an analogous equation for $F_{\zeta 2}$, can be written in the form

$$\mathbf{L}\mathbf{F}_2 = \sum_{j=-6}^{6}{}' \mathbf{d}_{n,j}\, y_{n+j}\,, \qquad (6.30)$$

where the solution $\mathbf{F}_2 := (F_{\psi 2}, F_{\vartheta 2}, F_{\zeta 2})^T$ must be of the form,

$$\mathbf{F}_2 = \sum_{j=-6}^{6}{}' \mathbf{h}_{n,j}\, y_{n+j}\,, \qquad (6.31)$$

with constant vectors $\mathbf{d}_{n,j}$ and $\mathbf{h}_{n,j}$. Thus

$$\mathbf{L}_{n+j}\mathbf{h}_{n,j} = \mathbf{d}_{n,j}\,.$$

Since $\mathbf{L}_n$ is singular, a necessary condition for the existence of solutions to (6.30) is that the coefficient of y_n in $\mathbf{c}^T\mathbf{L}\mathbf{F}_2$ vanish, i.e. $\mathbf{c}^T\mathbf{d}_{n,0} = 0$.

We now construct $2\Omega'_o\xi_n\mathbf{c}^T\mathbf{L}\mathbf{F}_2$ from (6.28) and (6.29),

$$\begin{aligned}
\mathbf{c}^T\mathbf{L}\mathbf{F}_2 = \mathbf{c}^T[&-\tfrac{1}{6}i\Pi'''_o\Upsilon^3\mathbf{F}_1 + \overline{\gamma}_1\Upsilon\mathbf{F}''_1 - (p_4 + i\omega_4 + \tfrac{1}{24}i\Upsilon^4\Pi''''_o)\mathbf{F}_0 + \tfrac{1}{2}\overline{\gamma}_2\Upsilon^2\mathbf{F}''_0 + 2\overline{\chi}_{1,o}\mathbf{F}'_1 + 2\overline{\chi}'_{1,o}\Upsilon\mathbf{F}'_0 + \overline{\chi}_{2,o}\mathbf{F}_0]\\
&- \tfrac{1}{2}\xi_n^{-1}\left[2\overline{\mu}'_{i,o}\Upsilon F'_{\psi 0} + (2ik\overline{\mu}_{j,o} + 2im\overline{\mu}_{k,o} + \overline{\mu}_{l,o})F_{\psi 0} + \chi_{3,o}F''_{\vartheta 0} + i\overline{\alpha}''_o\Upsilon^2 F_{\vartheta 0}\right]\\
&+ \tfrac{1}{2}{\Omega'_o}^{-1}\left[2\overline{\lambda}'_{a,o}\Upsilon F'_{\vartheta 0} + (2ik\overline{\lambda}_{b,o} + 2im\overline{\lambda}_{c,o} + \overline{\lambda}_{d,o})F_{\vartheta 0} + \tfrac{1}{2}\Omega'''_o\Upsilon^2 F_{\psi 0} + 2im\overline{\lambda}_{g,o}F_{\zeta 0}\right] + 2\mathbf{c}_1^T\mathbf{F}'_1 + \Upsilon\mathbf{c}_2^T\mathbf{F}_1\,,
\end{aligned}$$

introducing

$$\mathbf{c}_1^T := [-\Omega'_o\overline{\mu}_{i,o}, \xi_n\overline{\lambda}_{a,o}, 0]/2\Omega'_o\xi_n\,, \qquad \mathbf{c}_2^T := [\xi_n\Omega''_o, -\Omega'_o 2i\overline{\alpha}'_o, 0]/2\Omega'_o\xi_n\,.$$

We need the y_n terms of the right side. Using

$$\mathbf{c}^T[\mathbf{F}_0,\, \Upsilon\mathbf{F}_0',\, \Upsilon^2\mathbf{F}_0'',\, \Upsilon^4\mathbf{F}_0] = [y_n,\, \Upsilon y_n',\, \Upsilon^2 y_n'',\, \Upsilon^4 y_n]$$

the equation reduces to

$$\begin{aligned}\mathbf{c}^T\mathbf{L}\mathbf{F}_2 = {}& [-(p_4+i\omega_4)+\overline{\chi}_{2,o}+i(k\overline{\mu}_{j,o}+m\overline{\mu}_{k,o}+k\overline{\lambda}_{b,o}+m\overline{\lambda}_{c,o})+\tfrac{1}{2}(\overline{\mu}_{l,o}+\overline{\lambda}_{d,o})+im\overline{\lambda}_{g,o}\overline{W}_o'/\Omega_o'-\tfrac{1}{24}i\Pi_o''''\Upsilon^4]y_n\\ &+\tfrac{1}{2}\overline{\gamma}_2\Upsilon^2 y_n''+2(\overline{\chi}_{1,o}'+\tfrac{1}{2}\overline{\chi}_{4,o}')\Upsilon y_n'-\tfrac{1}{2}(\Omega_o'\chi_{3,o}/\xi_n)y_n''-\tfrac{1}{2}(\Omega_o'i\overline{\alpha}_o''/\xi_n+\tfrac{1}{2}\xi_n\Omega_o'''/\Omega_o')\Upsilon^2 y_n\\ &+\mathbf{c}^T[-\tfrac{1}{6}i\Pi_o'''\Upsilon^3\mathbf{F}_1+\overline{\gamma}_1\Upsilon\mathbf{F}_1''+2\overline{\chi}_{1,o}\mathbf{F}_1']+2\mathbf{c}_1^T\mathbf{F}_1'+\Upsilon\mathbf{c}_2^T\mathbf{F}_1\,, \quad (6.32)\end{aligned}$$

where

$$\chi_4 := \mu_i + \lambda_a\,.$$

The y_n terms in y_n'', $\Upsilon^2 y_n$, $\Upsilon y_n'$, $\Upsilon^2 y_n''$ and $\Upsilon^4 y_n$ can be extracted using the identities (B.1), (B.3), (B.6)–(B.8) in Appendix B, derived from (6.9). Extracting these terms gives

$$p_4 + i\omega_4 = C_1 + C_2 + C_3 + C_4 + C_5\,, \quad (6.33)$$

where

$$\begin{aligned}C_1 = {}& \overline{\chi}_{2,o} + [i(k\overline{\mu}_{j,o}+m\overline{\mu}_{k,o}+k\overline{\lambda}_{b,o}+m\overline{\lambda}_{c,o})+\tfrac{1}{2}(\overline{\mu}_{l,o}+\overline{\lambda}_{d,o})]+im\overline{\lambda}_{g,o}\overline{W}_o'/\Omega_o'-\tfrac{1}{8}(n^2+n+\tfrac{1}{2})\overline{\gamma}_0\Pi_o''''/\Pi_o''\\ &-\tfrac{1}{4}(n^2+n-\tfrac{1}{2})\overline{\gamma}_2+(\overline{\chi}_{1,o}'+\tfrac{1}{2}\overline{\chi}_{4,o}')+\tfrac{1}{4}(n+\tfrac{1}{2})(\Omega_o'\overline{\chi}_{3,o}/q)-\tfrac{1}{2}(n+\tfrac{1}{2})\overline{\chi}_{5,o}''q\,,\end{aligned}$$

with

$$\chi_5 := \alpha/\overline{\alpha}_o + \Omega'/\Omega_o'\,,$$

and C_2, C_3, C_4, C_5 are the coefficients of y_n from the terms $-\frac{1}{6}i\Pi_o'''\Upsilon^3\mathbf{c}^T\mathbf{F}_1$, $\overline{\gamma}_1\Upsilon\mathbf{c}^T\mathbf{F}_1''$, $2\overline{\chi}_{1,o}\mathbf{c}^T\mathbf{F}_1'$, $2\mathbf{c}_1^T\mathbf{F}_1' + \Upsilon\mathbf{c}_2^T\mathbf{F}_1$. The quantity $q := \kappa^2\xi_n$ is either real or purely imaginary, since $q^2 = \kappa^4\xi_n^2 = \overline{\gamma}_0\overline{\alpha}_o\Omega_o'/\Pi_o''$ is real. In the flows we consider $q^2 < 0$.

The coefficients C_2, C_3, C_4, C_5 are more difficult to extract. From the form (6.11) of the solution $\mathbf{F}_1$,

$$\mathbf{c}^T[\Upsilon^3\mathbf{F}_1,\, \Upsilon\mathbf{F}_1'',\, \mathbf{F}_1'] = \sum_{j=-3}^{3}{}' \mathbf{c}^T\mathbf{b}_{n,j}\,[\Upsilon^3 y_{n+j},\, \Upsilon y_{n+j}'',\, y_{n+j}']\,, \quad (6.34)$$

where

$$\begin{aligned}\mathbf{c}^T\mathbf{b}_{n,-3} &= \tfrac{1}{12}n(n-1)(n-2)(\tfrac{1}{3}\overline{\gamma}_0\Pi_o'''/\Pi_o''-\overline{\gamma}_1)\frac{\kappa}{\overline{\gamma}_0}\\ \mathbf{c}^T\mathbf{b}_{n,-1} &= \tfrac{1}{4}\left(n^2\overline{\gamma}_0\Pi_o'''/\Pi_o''+n(n-2)\overline{\gamma}_1-4n\overline{\chi}_{1,o}\right)\frac{\kappa}{\overline{\gamma}_0}-n\mathbf{c}^T\mathbf{L}_{n-1}^{-1}(\kappa\mathbf{a}_1+\kappa^{-1}\mathbf{a}_2)\\ \mathbf{c}^T\mathbf{b}_{n,1} &= -\tfrac{1}{4}\left((n+1)\overline{\gamma}_0\Pi_o'''/\Pi_o''+(n+3)\overline{\gamma}_1+4\overline{\chi}_{1,o}\right)\frac{\kappa}{\overline{\gamma}_0}-\mathbf{c}^T\mathbf{L}_{n+1}^{-1}(\kappa\mathbf{a}_1-\kappa^{-1}\mathbf{a}_2)\\ \mathbf{c}^T\mathbf{b}_{n,3} &= -\tfrac{1}{12}(\tfrac{1}{3}\overline{\gamma}_0\Pi_o'''/\Pi_o''-\overline{\gamma}_1)\frac{\kappa}{\overline{\gamma}_0}\,,\end{aligned}$$

using $\mathbf{c}^T\mathbf{a} = 1$. By (6.15) and (6.16),

$$\mathbf{c}^T\mathbf{L}_{n\pm1}^{-1}\mathbf{a}_1 = -\frac{\xi_n\overline{\chi}_{5,o}'}{2(\xi_{n\pm1}-\xi_n)}\,, \quad \mathbf{c}^T\mathbf{L}_{n\pm1}^{-1}\mathbf{a}_2 = \frac{\overline{\chi}_{4,o}}{2(\xi_{n\pm1}-\xi_n)}\,, \quad (6.35)$$

since $\mathbf{c}^T\mathbf{L}(\xi)^{-1} = \mathbf{c}^T/(\xi-\xi_n)$. Hence by (6.14)(b),

$$\mathbf{c}^T\mathbf{L}_{n\pm1}^{-1}\mathbf{a}_1 = \pm\tfrac{1}{2}\overline{\chi}_{5,o}'q/\overline{\gamma}_0\,, \qquad \mathbf{c}^T\mathbf{L}_{n\pm1}^{-1}\mathbf{a}_2 = \mp\tfrac{1}{2}\overline{\chi}_{4,o}\kappa^2/\overline{\gamma}_0\,. \quad (6.36)$$

Thus

$$\mathbf{c}^T\mathbf{b}_{n,-3} = \tfrac{1}{12}n(n-1)(n-2)\left(\tfrac{1}{3}\overline{\gamma}_0\Pi_o'''/\Pi_o''-\overline{\gamma}_1\right)\frac{\kappa}{\overline{\gamma}_0} \quad (6.37)$$

$$\mathbf{c}^T\mathbf{b}_{n,-1} = \tfrac{1}{4}\left(n^2\overline{\gamma}_0\Pi_o'''/\Pi_o''+n(n-2)\overline{\gamma}_1-4n(\overline{\chi}_{1,o}+\tfrac{1}{2}\overline{\chi}_{4,o})+2n\overline{\chi}_{5,o}'q\right)\frac{\kappa}{\overline{\gamma}_0} \quad (6.38)$$

$$\mathbf{c}^T\mathbf{b}_{n,1} = -\tfrac{1}{4}\left((n+1)\overline{\gamma}_0\Pi_o'''/\Pi_o'' + (n+3)\overline{\gamma}_1 + 4(\overline{\chi}_{1,o} + \tfrac{1}{2}\overline{\chi}_{4,o}) + 2\overline{\chi}'_{5,o}q\right)\frac{\kappa}{\overline{\gamma}_0} \tag{6.39}$$

$$\mathbf{c}^T\mathbf{b}_{n,3} = -\tfrac{1}{12}\left(\tfrac{1}{3}\overline{\gamma}_0\Pi_o'''/\Pi_o'' - \overline{\gamma}_1\right)\frac{\kappa}{\overline{\gamma}_0}\,. \tag{6.40}$$

The coefficients of y_n in each component of (6.34) are of the following form,

$$\frac{\overline{\gamma}_0}{\kappa}(A\mathbf{c}^T\mathbf{b}_{n,-3}+B\mathbf{c}^T\mathbf{b}_{n,-1}+C\mathbf{c}^T\mathbf{b}_{n,1}+D\mathbf{c}^T\mathbf{b}_{n,3}) = \tfrac{1}{12}\overline{\gamma}_0\Pi_o'''/\Pi_o''[\tfrac{1}{3}n(n-1)(n-2)A+3n^2B-3(n+1)C-\tfrac{1}{3}D]$$
$$-\tfrac{1}{4}\overline{\gamma}_1[\tfrac{1}{3}n(n-1)(n-2)A - n(n-2)B + (n+3)C - \tfrac{1}{3}D] - (\overline{\chi}_{1,o} + \tfrac{1}{2}\overline{\chi}_{4,o})(nB+C) + \tfrac{1}{2}\overline{\chi}'_{5,o}q(nB-C)$$

Now, from the recurrence relations (6.9), identities (B.9)–(B.12) in Appendix B, give $A = \kappa^3$, $B = 3\kappa^3 n$, $C = 3\kappa^3(n+1)^2$, $D = \kappa^3(n+1)(n+2)(n+3)$. Thus

$$C_2 := \{\tfrac{5}{24}(n^2+n+\tfrac{11}{30})\frac{\overline{\gamma}_0\Pi_o'''}{\Pi_o''} + \tfrac{3}{8}(n^2+n+\tfrac{7}{18})\overline{\gamma}_1 + \tfrac{1}{2}(n^2+n+\tfrac{1}{2})(\overline{\chi}_{1,o}+\tfrac{1}{2}\overline{\chi}_{4,o}) + \tfrac{1}{4}(n+\tfrac{1}{2})\overline{\chi}'_{5,o}q\}\frac{\Pi_o'''}{\Pi_o''}\,.$$

Similarly, (B.13)–(B.16) in Appendix B, give $A = \frac{1}{4}\kappa^{-1}$, $B = -\frac{1}{4}\kappa^{-1}(n+2)$, $C = -\frac{1}{4}\kappa^{-1}(n-1)(n+1)$, $D = \frac{1}{4}\kappa^{-1}(n+1)(n+2)(n+3)$, which imply

$$C_3 := \{-\tfrac{1}{8}(n^2+n+\tfrac{5}{6})\overline{\gamma}_0\frac{\Pi_o'''}{\Pi_o''} + \tfrac{3}{8}(n^2+n-\tfrac{1}{6})\overline{\gamma}_1 + \tfrac{1}{2}(n^2+n-\tfrac{1}{2})(\overline{\chi}_{1,o}+\tfrac{1}{2}\overline{\chi}_{4,o}) - \tfrac{1}{4}(n+\tfrac{1}{2})\overline{\chi}'_{5,o}q\}\overline{\gamma}_1/\overline{\gamma}_0\,.$$

For the last component in (6.34) the relation (6.9)(a) gives $A = 0$, $B = -\frac{1}{2}\kappa^{-1}$, $C = \frac{1}{2}(n+1)\kappa^{-1}$, $D = 0$, which imply

$$C_4 = \{-\tfrac{1}{4}(n^2+n+\tfrac{1}{2})\overline{\gamma}_0\frac{\Pi_o'''}{\Pi_o''} - \tfrac{1}{4}(n^2+n+\tfrac{3}{2})\overline{\gamma}_1 - \tfrac{1}{2}(\overline{\chi}_{0,o}+\tfrac{1}{2}\overline{\chi}_{4,o}) - \tfrac{1}{2}(n+\tfrac{1}{2})\overline{\chi}'_{5,o}q\}2\overline{\chi}_{1,o}/\overline{\gamma}_0\,.$$

To derive C_5 note that the coefficients of y_n in $y'_{n\pm1}$, $y'_{n\pm3}$ are $\frac{1}{2}\kappa^{-1}(n+1)$, $-\frac{1}{2}\kappa^{-1}$ 0, 0, respectively, by (6.9)(a). Similarly, the coefficients of y_n in $\Upsilon y_{n\pm1}$, $\Upsilon y_{n\pm3}$ are $\kappa(n+1)$, κ 0, 0, respectively, by (6.9)(b). Thus $C_5 := (-\kappa^{-1}\mathbf{c}_1^T + \kappa\mathbf{c}_2^T)\mathbf{b}_{n,-1} + (n+1)(\kappa^{-1}\mathbf{c}_1^T + \kappa\mathbf{c}_2^T)\mathbf{b}_{n,1}$.

Since

$$\mathbf{c}_1^T\mathbf{a} = \tfrac{1}{2}\overline{\chi}_{4,o}\,, \qquad \mathbf{c}_2^T\mathbf{a} = -\tfrac{1}{2}\xi_n\overline{\chi}'_{5,o}\,,$$

it follows that

$$(-\kappa^{-1}\mathbf{c}_1^T + \kappa\mathbf{c}_2^T)\kappa\mathbf{a} = -\tfrac{1}{2}\overline{\chi}_{4,o} - \tfrac{1}{2}\overline{\chi}'_{5,o}q$$
$$(\kappa^{-1}\mathbf{c}_1^T + \kappa\mathbf{c}_2^T)\kappa\mathbf{a} = \tfrac{1}{2}\overline{\chi}_{4,o} - \tfrac{1}{2}\overline{\chi}'_{5,o}q\,.$$

From (6.36),

$$\mathbf{c}_1^T\mathbf{L}_{n\mp1}^{-1}(\mathbf{a}_1 \pm \kappa^{-2}\mathbf{a}_2) = -\frac{1}{2\overline{\gamma}_0(\pm2q+\overline{\gamma}_0)}\{[\mp q\overline{\chi}_{4,o} - \overline{\gamma}_0\overline{\mu}_{i,o}](\mp q\overline{\alpha}'_o/\overline{\alpha}_o + \overline{\mu}_{i,o}) + [\mp q\overline{\chi}_{4,o} - \overline{\gamma}_0\overline{\lambda}_{a,o}](\mp q\Omega_o''/\Omega_o' + \overline{\lambda}_{a,o})\}\,,$$

using $\kappa^2\xi_{n\mp1} = q \pm \overline{\gamma}_0$, and

$$\mathbf{c}_2^T\mathbf{L}_{n\mp1}^{-1}(\mathbf{a}_1 \pm \kappa^{-2}\mathbf{a}_2) = \frac{\xi_n}{2\overline{\gamma}_0(\pm2q+\overline{\gamma}_0)}\{[\mp q\overline{\chi}'_{5,o} - \overline{\gamma}_0\Omega_o''/\Omega_o'](\mp q\overline{\alpha}'_o/\overline{\alpha}_o + \overline{\mu}_{i,o}) + [\mp\overline{\chi}'_{5,o}q - \overline{\gamma}_0\overline{\alpha}'_o/\overline{\alpha}_o](\mp q\Omega_o''/\Omega_o' + \overline{\lambda}_{a,o})\}\,.$$

Hence

$$(\mp\kappa^{-1}\mathbf{c}_1^T + \kappa\mathbf{c}_2^T)\mathbf{L}_{n\mp1}^{-1}(\kappa\mathbf{a}_1 \pm \kappa^{-1}\mathbf{a}_2) = \frac{1}{2\overline{\gamma}_0(2q\pm\overline{\gamma}_0)}\{[\mp q(\overline{\chi}_{4,o} + \overline{\gamma}_0\Omega_o''/\Omega_o') - \overline{\gamma}_0\overline{\mu}_{i,o} - \overline{\chi}'_{5,o}q^2](\mp q\overline{\alpha}'_o/\overline{\alpha}_o + \overline{\mu}_{i,o})$$
$$+ [\mp q(\overline{\chi}_{4,o} + \overline{\gamma}_0\overline{\alpha}'_o/\overline{\alpha}_o) - \overline{\gamma}_0\overline{\lambda}_{a,o} - \overline{\chi}'_{5,o}q^2](\mp q\Omega_o''/\Omega_o' + \overline{\lambda}_{a,o})\}\,.$$

Finally,

$$C_5 = -\tfrac{1}{8}[n^2\overline{\gamma}_0\Pi_o'''/\Pi_o'' + n(n-2)\overline{\gamma}_1 - 4n\overline{\chi}_{1,o}]\frac{1}{\overline{\gamma}_0}[\overline{\chi}_{4,o} + \overline{\chi}'_{5,o}q]$$

$$
\begin{aligned}
&- \frac{n}{2\overline{\gamma}_0(2q+\overline{\gamma}_0)}\{[-q(\overline{\chi}_{4,o}+\overline{\gamma}_0\Omega_o''/\Omega_o')-\overline{\gamma}_0\overline{\mu}_{i,o}-\overline{\chi}_{5,o}'q^2](-q\overline{\alpha}_o'/\overline{\alpha}_o+\overline{\mu}_{i,o}) \\
&\qquad + [-q(\overline{\chi}_{4,o}+\overline{\gamma}_0\overline{\alpha}_o'/\overline{\alpha}_o)-\overline{\gamma}_0\overline{\lambda}_{a,o}-\overline{\chi}_{5,o}'q^2](-q\Omega_o''/\Omega_o'+\overline{\lambda}_{a,o})\} \\
&- \tfrac{1}{8}[(n+1)^2\overline{\gamma}_0\Pi_o'''/\Pi_o''+(n+1)(n+3)\overline{\gamma}_1+4(n+1)\overline{\chi}_{1,o}]\frac{1}{\overline{\gamma}_0}[\overline{\chi}_{4,o}-\overline{\chi}_{5,o}'q] \\
&\quad - \frac{n+1}{2\overline{\gamma}_0(2q-\overline{\gamma}_0)}\{[q(\overline{\chi}_{4,o}+\overline{\gamma}_0\Omega_o''/\Omega_o')-\overline{\gamma}_0\overline{\mu}_{i,o}-\overline{\chi}_{5,o}'q^2](q\overline{\alpha}_o'/\overline{\alpha}_o+\overline{\mu}_{i,o}) \\
&\qquad\qquad + [q(\overline{\chi}_{4,o}+\overline{\gamma}_0\overline{\alpha}_o'/\overline{\alpha}_o)-\overline{\gamma}_0\overline{\lambda}_{a,o}-\overline{\chi}_{5,o}'q^2](q\Omega_o''/\Omega_o'+\overline{\lambda}_{a,o})\}
\end{aligned}
$$

From (6.33) the additional term of Gilbert & Ponty (2000) in $p_4+i\omega_4$ is $\mathrm{Re}\,\overline{\chi}_{2,o}+\overline{\gamma}_0^{-1}(\mathrm{Im}\,\overline{\chi}_{1,o})^2$.

7 Conclusions

The asymptotic theory of Gilbert & Ponty (2000) for axisymmetric roll dynamos in a sphere has been compared to the numerically computed results of the exact dynamo theory for two simple flows, with azimuthal components of the special form $v_\phi = r\sin\theta\, W(\psi)$ and of general form. Good agreement has been found between the asymptotic theory to $\mathcal{O}(R_\mathrm{m}^{-1/2})$ and the numerical results for the growth rate and angular frequency if the magnetic Reynolds number $R_\mathrm{m} \gtrsim 10^5$. The asymptotic formulas for the growth rate and the angular frequency have been extended to $\mathcal{O}(R_\mathrm{m}^{-1})$, with no contribution at $\mathcal{O}(R_\mathrm{m}^{-3/4})$. For the magnetic field the agreement between the asymptotic theory at leading order and the numerical results is reasonable if $R_\mathrm{m}=10^5$ and good if $R_\mathrm{m}=5\times10^5$. The asymptotic formula for the magnetic field has also been extended but only to second order.

Only the simplest class of axisymmetric roll dynamos have been considered: those which consist of a single roll flow with a single resonant streamline. The magnetic field in these dynamos is localised to the resonant stream surface and can interact only with itself. Further work is required on more complicated spherical roll flows, those with a single roll but more than one resonant streamline, or those with several rolls. Such flows offer the possibility of interaction between magnetic fields localised to separate regions of the flow. This may produce interacting modes of non-Ponomarenko type, e.g. Gailitis type modes, besides Ponomarenko type modes. A related question for future work, which arises from the localised nature of the Ponomarenko type modes at large R_m, is whether they depend on the magnetic boundary conditions at the surface of the conducting fluid.

References

[1] Abramowitz & Stegun (1965), *Handbook of Mathematical Functions*, Dover.

[2] Bullard, E.C. & Gellman, H. (1954), "Homogenous dynamos and terrestrial magnetism", *Phil. Trans. Roy. Soc. Lond. A* **247**, 213–278.

[3] Dudley, M.L. & James, R.W. (1989), "Time-dependent kinematic dynamos with stationary flows", *Proc. R. Soc. Lond. A* **425**, 407–420.

[4] Forest, C.B., Bayliss, R.A., Kendrick, R.D., Nornberg, M.D., O'Connell, R., Spence, E.J., (2002), "Hydrodynamic and numerical modeling of a spherical homogeneous dynamo experiment", *Magnetohydrodynamics* **38**, 104–116.

[5] Gilbert, A.D. (1988), "Fast dynamo action in the Ponomarenko dynamo', *Geophys. Astrophys. Fluid Dynam.* **44**, 241–258.

[6] Gilbert, A.D. & Ponty, Y. (2000), "Dynamos on stream surfaces of a highly conducting fluid', *Geophys. Astrophys. Fluid Dynam.* **93**, 55–95.

[7] Golub, G.H. & Van Loan, C.F. (1996), *Matrix Computations*, 3rd ed., John Hopkins Press, Baltimore.

[8] Ivers, D.J. & Phillips, C.G. (2003), "A vector spherical harmonic spectral code for linearised magnetohydrodynamics", *ANZIAM J.* **44**(E), C423–C442.

[9] Ivers, D.J. & Phillips, C.G. (2006), "Scalar and vector spherical harmonic spectral equations of rotating non–linear and linearised magnetohydrodynamics', preprint.

[10] Ivers, D.J. & Phillips, C.G. (2001c), "Dynamo problems in spherical and nearly spherical geometries", in P.Chossat et al.(eds.), *Dynamo and Dynamics, a Mathematical Challenge*, 207–215, Kluwer Academic Publishers, Netherlands.

[11] James, R.W. (1973), "The Adams and Elsasser dynamo integrals", *Proc. R. Soc. Lond. A.* **331**, 460–478.

[12] James, R.W. (1974), "The spectral form of the magnetic induction equation", *Proc. R. Soc. Lond. A.* **340**, 287–299.

[13] Lortz, D. (1968), "Exact solutions of the hydromagnetic dynamo problem", *Plasma Phys.* **10**, 967–72.

[14] Ponomarenko, Yu.B. (1973), "On the theory of hydromagnetic dynamos", *Zh. Prikl. Mech. Tech. Fiz. (USSR)* **6**, 47–51.

[15] Sorensen, D.C. (1992), "Implicit application of polynomial filters in a k-step Arnoldi method", *SIAM J. Matrix Anal. Appl.* **13**, 357–385.

[16] Ruzmaikin, A.A., Sokoloff, D.D. and Shukurov, A.M. (1988), "A hydromagnetic screw dynamo', *J. Fluid Mech.*, **197**, 39–56.

Appendix A

Derivatives of Ω and $\overline{W}$

$$
\begin{aligned}
\frac{1}{Q} &= \psi_r^2 + \frac{\psi_\theta^2}{r^2} \\
Q_r &= -2Q^2\left(\psi_r\psi_{rr} + \frac{\psi_\theta\psi_{r\theta}}{r^2} - \frac{\psi_\theta^2}{r^3}\right) \\
Q_\theta &= -2Q^2\left(\psi_r\psi_{r\theta} + \frac{\psi_\theta\psi_{\theta\theta}}{r^2}\right) \\
Q_{rr} &= \frac{2Q_r^2}{Q} - 2Q^2\left(\psi_{rr}^2 + \psi_r\psi_{rrr} + \frac{\psi_{r\theta}^2}{r^2} + \frac{\psi_\theta\psi_{rr\theta}}{r^2} - \frac{4\psi_\theta\psi_{r\theta}}{r^3} + \frac{3\psi_\theta^2}{r^4}\right) \\
Q_{r\theta} &= \frac{2Q_rQ_\theta}{Q} - 2Q^2\left(\psi_{rr}\psi_{r\theta} + \psi_r\psi_{rr\theta} + \frac{\psi_{r\theta}\psi_{\theta\theta}}{r^2} + \frac{\psi_\theta\psi_{r\theta\theta}}{r^2} - \frac{2\psi_\theta\psi_{\theta\theta}}{r^3}\right) \\
Q_{\theta\theta} &= \frac{2Q_\theta^2}{Q} - 2Q^2\left(\psi_{r\theta}^2 + \psi_r\psi_{r\theta\theta} + \frac{\psi_{\theta\theta}^2}{r^2} + \frac{\psi_\theta\psi_{\theta\theta\theta}}{r^2}\right).
\end{aligned}
$$

$$
\begin{aligned}
\nabla^2\psi &= \psi_{rr} + \frac{2\psi_r}{r} + \frac{\psi_{\theta\theta}}{r^2} + \frac{\cot\theta\,\psi_\theta}{r^2} \\
(\nabla^2\psi)_r &= \psi_{rrr} + \frac{2\psi_{rr}}{r} - \frac{2\psi_r}{r^2} + \frac{\psi_{r\theta\theta}}{r^2} - \frac{2\psi_{\theta\theta}}{r^3} + \frac{\cot\theta\,\psi_{r\theta}}{r^2} - \frac{2\cot\theta\,\psi_\theta}{r^3} \\
(\nabla^2\psi)_\theta &= \psi_{rr\theta} + \frac{2\psi_{r\theta}}{r} + \frac{\psi_{\theta\theta\theta}}{r^2} + \frac{\cot\theta\,\psi_{\theta\theta}}{r^2} - \frac{\csc^2\theta\,\psi_\theta}{r^2}.
\end{aligned}
$$

$$
\nabla\nabla F = \mathbf{1}_r\mathbf{1}_rF_{rr} + (\mathbf{1}_r\mathbf{1}_\theta + \mathbf{1}_\theta\mathbf{1}_r)\left(\frac{F_{r\theta}}{r} - \frac{F_\theta}{r^2}\right) + \mathbf{1}_\theta\mathbf{1}_\theta\left(\frac{F_r}{r} + \frac{F_{\theta\theta}}{r^2}\right) + \mathbf{1}_\phi\mathbf{1}_\phi\left(\frac{F_r}{r} + \frac{\cot\theta\,F_\theta}{r^2}\right)
$$

$$
\nabla\psi\cdot\nabla\nabla F\cdot\nabla\psi = \psi_r^2F_{rr} + 2\psi_r\frac{\psi_\theta}{r}\left(\frac{F_{r\theta}}{r} - \frac{F_\theta}{r^2}\right) + \frac{\psi_\theta^2}{r^2}\left(\frac{F_r}{r} + \frac{F_{\theta\theta}}{r^2}\right)
$$

$$
\nabla\psi\cdot\nabla\nabla\psi\cdot\nabla F = \psi_r\psi_{rr}F_r + \left(\frac{\psi_{r\theta}}{r} - \frac{\psi_\theta}{r^2}\right)\left(\frac{\psi_\theta}{r}F_r + \psi_r\frac{F_\theta}{r}\right) + \frac{\psi_\theta}{r}\left(\frac{\psi_r}{r} + \frac{\psi_{\theta\theta}}{r^2}\right)\frac{F_\theta}{r} = -\tfrac{1}{2}\nabla Q\cdot\nabla F.
$$

$$
\begin{aligned}
\nabla Q\cdot\nabla\psi &= Q_r\psi_r + \frac{Q_\theta\psi_\theta}{r^2} \\
(\nabla Q\cdot\nabla\psi)_r &= Q_{rr}\psi_r + Q_r\psi_{rr} + \frac{Q_{r\theta}\psi_\theta}{r^2} + \frac{Q_\theta\psi_{r\theta}}{r^2} - \frac{2Q_\theta\psi_\theta}{r^3} \\
(\nabla Q\cdot\nabla\psi)_\theta &= Q_{r\theta}\psi_r + Q_r\psi_{r\theta} + \frac{Q_{\theta\theta}\psi_\theta}{r^2} + \frac{Q_\theta\psi_{\theta\theta}}{r^2} \\
R &= \nabla Q\cdot\nabla\psi + Q\nabla^2\psi \\
R_r &= (\nabla Q\cdot\nabla\psi)_r + Q_r\nabla^2\psi + Q(\nabla^2\psi)_r \\
R_\theta &= (\nabla Q\cdot\nabla\psi)_\theta + Q_\theta\nabla^2\psi + Q(\nabla^2\psi)_\theta \\
\nabla Q\cdot\nabla F &= Q_rF_r + \frac{Q_\theta F_\theta}{r^2} \\
\nabla\psi\cdot\nabla F &= \psi_rF_r + \frac{\psi_\theta F_\theta}{r^2} \\
\nabla\psi\cdot\nabla R &= \psi_rR_r + \frac{\psi_\theta R_\theta}{r^2}.
\end{aligned}
$$

$$
F_2 = (R^2 + Q\nabla\psi\cdot\nabla R)F + (2RQ + Q\nabla Q\cdot\nabla\psi)\nabla\psi\cdot\nabla F - \tfrac{1}{2}\nabla Q\cdot\nabla F + Q^2\nabla\psi\cdot\nabla\nabla F\cdot\nabla\psi
$$

$$
\overline{W}' = \Omega\left(\frac{\overline{W}}{\Omega}\right)' + \frac{\overline{W}\Omega'}{\Omega}, \qquad \overline{W}'' = \Omega\left(\frac{\overline{W}}{\Omega}\right)'' + \frac{2\overline{W}'\Omega'}{\Omega} + \frac{\overline{W}\Omega''}{\Omega} - \frac{2\overline{W}(\Omega')^2}{\Omega^2}.
$$

Appendix B

Recurrence Relations

The following recurrence relations follow the two fundamental recurrence relations,

$$y'_n = \tfrac{1}{2}\kappa^{-1}(ny_{n-1} - y_{n+1})\,, \qquad \Upsilon y_n = \kappa(ny_{n-1} + y_{n+1})\,.$$

$$y''_n = \tfrac{1}{4}\kappa^{-2}[n(n-1)y_{n-2} - (2n+1)y_n + y_{n+2}] \tag{B.1}$$
$$y'''_n = \tfrac{1}{8}\kappa^{-3}[n(n-1)(n-2)y_{n-3} - 3n^2y_{n-1} + 3(n+1)y_{n+1} - y_{n+3}] \tag{B.2}$$
$$\Upsilon^2 y_n = \kappa^2[n(n-1)y_{n-2} + (2n+1)y_n + y_{n+2}] \tag{B.3}$$
$$\Upsilon^3 y_n = \kappa^3[n(n-1)(n-2)y_{n-3} + 3n^2y_{n-1} + 3(n+1)y_{n+1} + y_{n+3}] \tag{B.4}$$
$$\Upsilon y''_n = \tfrac{1}{4}\kappa^{-1}[n(n-1)(n-2)y_{n-3} - n(n-2)y_{n-1} - (n+3)y_{n+1} + y_{n+3}]\,. \tag{B.5}$$

$$\Upsilon y'_n = \tfrac{1}{2}n(n-1)y_{n-2} + \tfrac{1}{2}y_n - \tfrac{1}{2}y_{n+2} \tag{B.6}$$
$$\Upsilon^2 y''_n = \tfrac{1}{4}n(n-1)(n-2)(n-3)y_{n-4} + n(n-1)y_{n-2} - \tfrac{1}{4}(2n^2+2n-1)y_n - y_{n+2} + \tfrac{1}{4}y_{n+4} \tag{B.7}$$
$$\Upsilon^4 y_n = \kappa^4\{n(n-1)(n-2)(n-3)y_{n-4} + 2n(n-1)(2n-1)y_{n-2} + 3(2n^2+2n+1)y_n + 2(2n+3)y_{n+2} + y_{n+4}\}\,. \tag{B.8}$$

$$\Upsilon^3 y_{n-3} = \kappa^3\{(n-3)(n-4)(n-5)y_{n-6} + 3(n-3)^2y_{n-4} + 3(n-2)y_{n-2} + y_n\} \tag{B.9}$$
$$\Upsilon^3 y_{n-1} = \kappa^3\{(n-1)(n-2)(n-3)y_{n-4} + 3(n-1)^2y_{n-2} + 3ny_n + y_{n+2}\} \tag{B.10}$$
$$\Upsilon^3 y_{n+1} = \kappa^3\{(n+1)n(n-1)y_{n-2} + 3(n+1)^2y_n + 3(n+2)y_{n+2} + y_{n+4}\} \tag{B.11}$$
$$\Upsilon^3 y_{n+3} = \kappa^3\{(n+3)(n+2)(n+1)y_n + 3(n+3)^2y_{n+2} + 3(n+4)y_{n+4} + y_{n+6}\}\,. \tag{B.12}$$

$$\Upsilon y''_{n-3} = \tfrac{1}{4}\kappa^{-1}\{(n-3)(n-4)(n-5)y_{n-6} - (n-3)(n-5)y_{n-4} - ny_{n-2} + y_n\} \tag{B.13}$$
$$\Upsilon y''_{n-1} = \tfrac{1}{4}\kappa^{-1}\{(n-1)(n-2)(n-3)y_{n-4} - (n-1)(n-3)y_{n-2} - (n+2)y_n + y_{n+2}\} \tag{B.14}$$
$$\Upsilon y''_{n+1} = \tfrac{1}{4}\kappa^{-1}\{(n+1)n(n-1)y_{n-2} - (n+1)(n-1)y_n - (n+4)y_{n+2} + y_{n+4}\} \tag{B.15}$$
$$\Upsilon y''_{n+3} = \tfrac{1}{4}\kappa^{-1}\{(n+3)(n+2)(n+1)y_n - (n+3)(n+1)y_{n+2} - (n+6)y_{n+4} + y_{n+6}\}\,. \tag{B.16}$$

Appendix C

Real, Imaginary and q Parts of $p_4 + i\omega_4$

We separate C_1 into real, imaginary and q parts, R_1, I_1 and Q_1. Q_1 may be real or imaginary.

$$R_1 = \overline{\chi}_{1,o} + \tfrac{1}{2}(\overline{\mu}_{l,o} + \overline{\lambda}_{d,o}) - \tfrac{1}{16}(2n^2+2n+1)\overline{\gamma}_0\Pi_o''''/\Pi_o'' - \tfrac{1}{8}(2n^2+2n-1)\overline{\gamma}_2 + \tfrac{1}{2}\overline{(\nabla^2\psi)}_o' + \tfrac{1}{2}\overline{\chi}_{4,o}'$$
$$I_1 = \overline{\chi}_{2,o} + k\overline{\mu}_{j,o} + m\overline{\mu}_{k,o} + k\overline{\lambda}_{b,o} + m\overline{\lambda}_{c,o} + m\overline{\lambda}_{g,o}\overline{W}_o'/\Omega_o' + \overline{\chi}_{0,o}'$$
$$Q_1 = \tfrac{1}{8}(2n+1)\Omega_o'\overline{\chi}_{3,o}/q - \tfrac{1}{4}(2n+1)\overline{\chi}_{5,o}''q\,.$$

Separate C_2 into real, imaginary and q parts,

$$R_2 = \{\tfrac{5}{24}(n^2+n+\tfrac{11}{30})\frac{\overline{\gamma}_0\Pi_o'''}{\Pi_o''} + \tfrac{3}{8}(n^2+n+\tfrac{7}{18})\overline{\gamma}_1 + \tfrac{1}{4}(n^2+n+\tfrac{1}{2})[(\overline{\nabla^2\psi})_o + \overline{\chi}_{4,o}]\}\frac{\Pi_o'''}{\Pi_o''}$$
$$I_2 = \tfrac{1}{2}(n^2+n+\tfrac{1}{2})\overline{\chi}_{0,o}\frac{\Pi_o'''}{\Pi_o''}$$
$$Q_2 = \tfrac{1}{4}(n+\tfrac{1}{2})\overline{\chi}_{5,o}'\frac{\Pi_o'''}{\Pi_o''}q\,.$$

Separate C_3 into real, imaginary and q parts,

$$R_3 = \{-\tfrac{1}{8}(n^2+n+\tfrac{5}{6})\overline{\gamma}_0\frac{\Pi_o'''}{\Pi_o''} + \tfrac{3}{8}(n^2+n-\tfrac{1}{6})\overline{\gamma}_1 + \tfrac{1}{4}(n^2+n-\tfrac{1}{2})[(\overline{\nabla^2\psi})_o + \overline{\chi}_{4,o}]\}\frac{\overline{\gamma}_1}{\overline{\gamma}_0}$$
$$I_3 = \tfrac{1}{2}(n^2+n-\tfrac{1}{2})\overline{\chi}_{0,o}\frac{\overline{\gamma}_1}{\overline{\gamma}_0}$$
$$Q_3 = -\tfrac{1}{4}(n+\tfrac{1}{2})\overline{\chi}_{5,o}'\frac{\overline{\gamma}_1}{\overline{\gamma}_0}q\,.$$

Separate C_4 into real, imaginary and q parts,

$$R_4 = \{-\tfrac{1}{4}(n^2+n+\tfrac{1}{2})\overline{\gamma}_0\frac{\Pi_o'''}{\Pi_o''} - \tfrac{1}{4}(n^2+n+\tfrac{3}{2})\overline{\gamma}_1 - \tfrac{1}{4}[(\overline{\nabla^2\psi})_o + \overline{\chi}_{4,o}]\}\overline{\nabla^2\psi}_o/\overline{\gamma}_0 + (\overline{\chi}_{0,o})^2/\overline{\gamma}_0\,.$$
$$I_4 = -\tfrac{1}{2}\overline{\chi}_{0,o}\overline{\nabla^2\psi}_o/\overline{\gamma}_0 + \{-\tfrac{1}{2}(n^2+n+\tfrac{1}{2})\overline{\gamma}_0\frac{\Pi_o'''}{\Pi_o''} - \tfrac{1}{2}(n^2+n+\tfrac{3}{2})\overline{\gamma}_1 - \tfrac{1}{2}[(\overline{\nabla^2\psi})_o + \overline{\chi}_{4,o}]\}\overline{\chi}_{0,o}/\overline{\gamma}_0\,.$$
$$Q_4 = -\tfrac{1}{2}(n+\tfrac{1}{2})\overline{\chi}_{5,o}'q(2i\overline{\chi}_{0,o} + \overline{\nabla^2\psi}_o)/\overline{\gamma}_0\,.$$